Mayank Shah

ON THE USE OF ELECTRICALLY STIMULATED MUSCLE AS A CONTROLLED ACTUATOR OF A LIMB

Report No. EDC 4-67-17

3919AN

by

William J. Crochetiere

June 1967

Project Director:

Dr. James B. Reswick

Cybernetic

Systems

Group

ON THE USE OF ELECTRICALLY STIMULATED

MUSCLE AS A CONTROLLED ACTUATOR

OF A LIMB

A Thesis Submitted to

Case Institute of Technology

In Partial Fulfillment of the Requirements

for the Degree of

Doctor of Philosophy

by

William J. Crochetiere

June 1967

Thesis Advisor:

Dr. James B. Reswick

ABSTRACT

The feasibility of inducing controlled movement of a paralyzed limb by means of applying electric currents is discussed. This is preceded by a functional description of muscle and its electrical excitability and the musculo-skeletal system of the human arm. Experiments are described which were performed to gain a basic understanding of the mechanical response of the lower arm due to stimulation of the biceps muscle. The dynamic model of this single degree of freedom system thus obtained is then used to synthesize suitable feedback control schemes. Two basically different systems are discussed: the control of the angular position, and the control of the angular velocity of the elbow joint. The velocity controller is found to be superior and is implemented in hardware. Three types of velocity controllers are compared: open loop, proportional closed loop, and proportional plus integral closed loop. The proportional plus integral closed loop is found to be superior. The author also indicates that a closed loop torque control may perform as well or better and also is simpler to implement.

ACKNOWLEDGEMENTS

TABLE OF CONTENTS

Page

LIST OF FIGURES

x

LIST OF SYMBOLS

A	gain in velocity controller
B	gain of integrator in velocity controller
B_B, B_F	viscosity in spindle model of stark
C	viscous coefficient, capacitance
C_T	viscous coefficient of transducer
D	current pulse duration
e	error in closed loop system, base of Naperian logarithm
F	force
f	frequency (cps)
$G(s)$	transfer function
g	conductance
$H(s)$	spindle transfer function
I	current amplitude
J	inertia
K	gain
K_p, K_s	parallel and series stiffness of muscle
K_T	transducer stiffness
K_1, K_2	spring constant
K_F, K_B	stiffness in spindle model of stark

L(s)	passive dynamics of limb
LMNL	lower motor neuron lesion
ma	milliamp
ms	millisecond
M_T	mass of transducer
P	time constant of isometric muscle model, force on muscle model
P_o	isometric force
P_T	force on transducer
Q	time constant of arm dynamics
r_1	moment arm of muscle
R	rest period between stimulus pulses, resistance
S	Laplacian operator
S - D	strength - duration curve
t	time
t_o	delay plus lag time
T	torque
T_M	muscle torque
T_L	load torque
T_D	delay time
UMNL	upper motor neuron lesion
V	voltage

v	velocity
ω	frequency (radians / sec)
x_i	internal shortening of muscle
x_e	external shortening of muscle
x_m	length of muscle spindle
x_c	length of nuclear bag spindle
α	large motor neuron
$\delta(t)$	impulse at $t = 0$
Δ	indicates a small change
Σ	mathematical summation
ϕ	angle
$\dot{\phi}$	angular velocity
$\phi_c,\ \dot{\phi}_c$	controlled angle, controlled velocity
$\phi_r,\ \dot{\phi}_r$	reference angle, reference velocity
θ	angle
ζ	damping ratio
τ	time constant

CHAPTER I

THE CONCEPT OF AN ORTHOSIS
POWERED BY STIMULATED SKELETAL MUSCLE

A. NEED FOR ORTHOTIC DEVICES

There are several million people who have potential need
for orthotic devices. Their disabilities range from the paralysis
of a single muscle to a state of total disability as in quadriplegia.
The disorder may be the result of poliomyelitis, neurological
diseases such as multiple sclerosis, Parkinson's disease, and
cerebral palsy or a spinal cord lesion. Smith[58] estimated that
there were 100,000 people living in the United States in 1959 who
had spinal cord lesions. Moreover, the number of these paralyzed
people is on the increase due to advances in medical care, in-
creased longevity, population increases, the consequences of high-
speed travel, etc.

1. Significance of Level of Spinal Cord Lesion

The degree of such a patient's loss of function of course
depends upon the level of his spinal cord lesion. The levels of
innervation of the critical muscle groups are fairly well docu-
mented[21] so that patients with spinal cord lesions can be classi-
fied according to the level of the lesion from purely objective

1

examination of remaining muscle function. Nerves enter and exit from the spinal cord at precisely determined points along its length between adjacent vertebra. There are seven cervical, twelve thoracic and five lumbar vertebra. Lesions of the spinal cord are classified as C, T, or L, followed by the number of the vertebra (increasing from head to tail). When a patient is listed as having a lesion at a given level, this is the lowest level in which all musculature remains functional. The major muscle groups added at each critical level are summarized below.[40] The table is representative of the "average" patient with sharp lesions at one particular level. An actual lesion, however, may span several levels and produce bizarre combinations of lost muscle function.

Deltoid, Biceps	C-5
Latissimus, Serratus, Pectoralis, Radial Wrist Extensors	C-6
Triceps, Finger Extensors and Flexors	C-7
Hand Intrinsics, Ulnar side of Wrist and Fingers	T-1
Upper Intercostals, Upper Back	T-6
Abdominals, Thoracic Extensors	T-12
Hip Flexors, Quadriceps	L-4

2. Upper versus Lower Motor Neuron Lesion

The neural path from brain to muscle is composed of two neurons in series: the upper motor neuron, and the lower motor neuron. The synapse (connection) between the two neurons occurs at the point of exit from the spinal cord. For this reason then a spinal cord lesion may produce either an upper motor neuron lesion (UMNL) or a lower motor neuron lesion (LMNL). In the case of an UMNL, the contractibility of the muscle is preserved for years after the accident but due to disuse of the muscle it may weaken considerably. For the muscle with a LMNL, the contractibility is also maintained, but for a much shorter time, and unless the muscle is artificially exercised, it gradually wastes away and becomes replaced by inextensible collagenous tissue. There are reports[61], however, that indicate that the rate of muscle atrophy may be decreased by a daily program of electrical stimulation.

A spinal cord lesion at a given level then: will have no effect on muscles which receive their innervation from levels above the lesion, produce UMNL and LMNL at the level of injury, and produce UMNL for all muscles which receive their inner-vation below the lesion.

B. THE HUMAN ARM

The human arm was chosen as the object of this study for many reasons. Among them are the experience with upper extremity orthotics acquired by the development of the Case Research Arm Aid, and the absence of large load bearing requirements which are important in lower extremity orthotics. This approach to the orthotic problem is concerned with the electrical activation paralyzed muscle to produce limb movements. It therefore becomes necessary to understand the functional anatomy of the limb.

1. Anatomy and Kinesiology

The skeletal system of the arm consists of five principal bones excluding the bones of the hand (Figure I-1). Beginning at the shoulder girdle we see that it consists of four joints. They are the:

> Sterno-clavicular joint - this is the only direct
> skeletal attachment of the arm to the body.
> Motion at this joint is not great, but it allows
> elevation and rotation of the clavicle with
> respect to the sternum.

> Acromio-clavicular - this joint is similar to the
> above in construction and positions the scapula.

> Gleno-humeral joint - this is what is usually thought
> of as the shoulder joint. It is of the ball and
> socket type and permits movements about three
> axes of rotation.
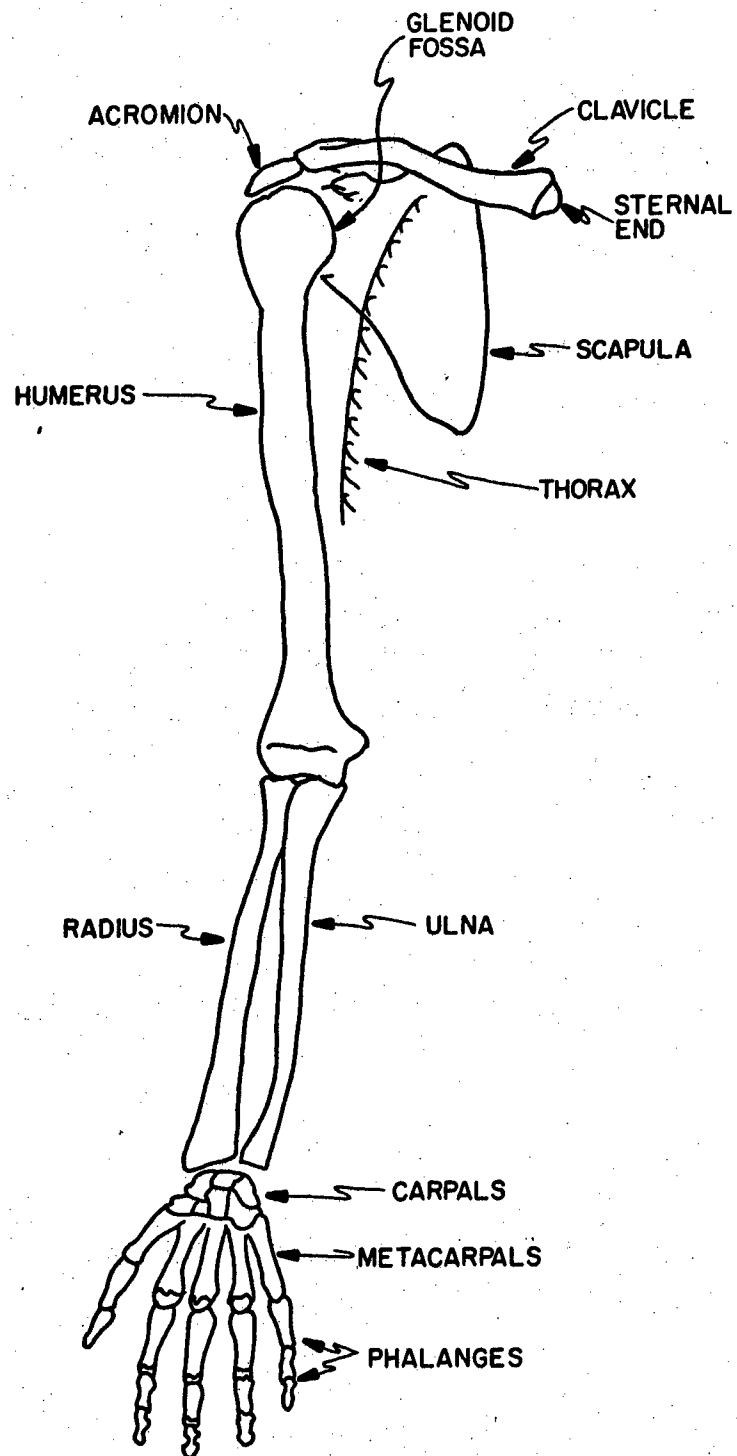
FIG. I-I, SKELETON OF THE ARM

Scapulo-thoracic joint - though not a joint in the
strictest sense, there is no ligamentous
attachment, the relative movement of the
scapula and thorax closes the kinematic loop,
so to speak, of the shoulder girdle.

Most movements of the shoulder involve articulation of all

the above joints. For this reason, the center of rotation of the

gleno-humeral joint wanders considerably during motion.

The elbow joint is the union of three bones: the humerous,

the radius and the ulna. The humero-ulnar joint is purely mono-

axial, allowing only flexion and extension of the ulna. Pronation

and supination of the forearm occurs in a distributed sense along

the radio-ulnar joint. That is, pronation and supination of the

forearm occurs when the distal end of the radius swings around the

ulna.

At the level of the wrist, the radius, ulna and carpals

merge to form the wrist joint. The metacarpals and phalanges

then form the hand.

Skeletal muscles are attached at various points among the

bones and permit the central nervous system to control the move-

ment of the limb. There are some fifty odd muscles which power

the human arm. Of these, approximately thirty can be stimulated

by means of electrodes placed on the surface of the skin. The

points of electrode application are called motor points. These

locations, for the arm, are shown in Figures I-2 and I-3.

2. Functions of the Muscles of the Arm

Skeletal muscles can be classified functionally as: prime movers, auxiliary muscles and joint stabilizers. The function of the prime mover muscle is to move a joint in the direction of its pull. The auxiliary muscles on the other hand either assist the prime movers in their function or they may be used to deflect the pull of the prime mover so that the joint will perform a more oblique movement. The joint stabilizer is used to maintain a constant joint angle in the presence of counteracting torque. This upsetting torque may be due to external loads or it may be due to the contraction of a muscle which spans more than one joint. Keep in mind that although each of the three functions is distinct, a single muscle may be called upon to perform each function at different times.

The muscles of the arm were investigated in terms of their points of attachment to the skeleton. This was done by studying anatomy texts and also participating in a cadaver dissection at the Western Reserve University Medical School. The author is indebted to Dr. Alvin Freehafer and Dr. Richard Briggs for this opportunity. The results of this study was the selection of easily stimulated muscles which could perform the function of prime
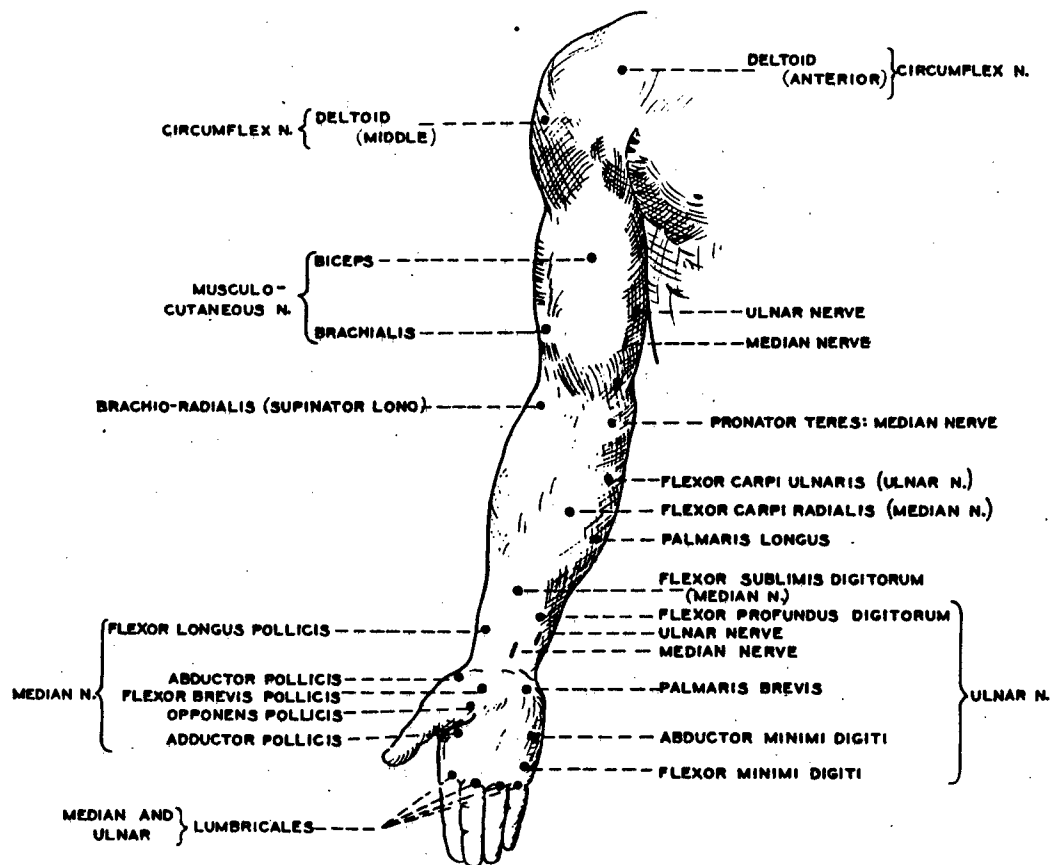
FIG. I-2. MOTOR POINTS OF ANTERIOR ASPECT OF UPPER
EXTREMITY.
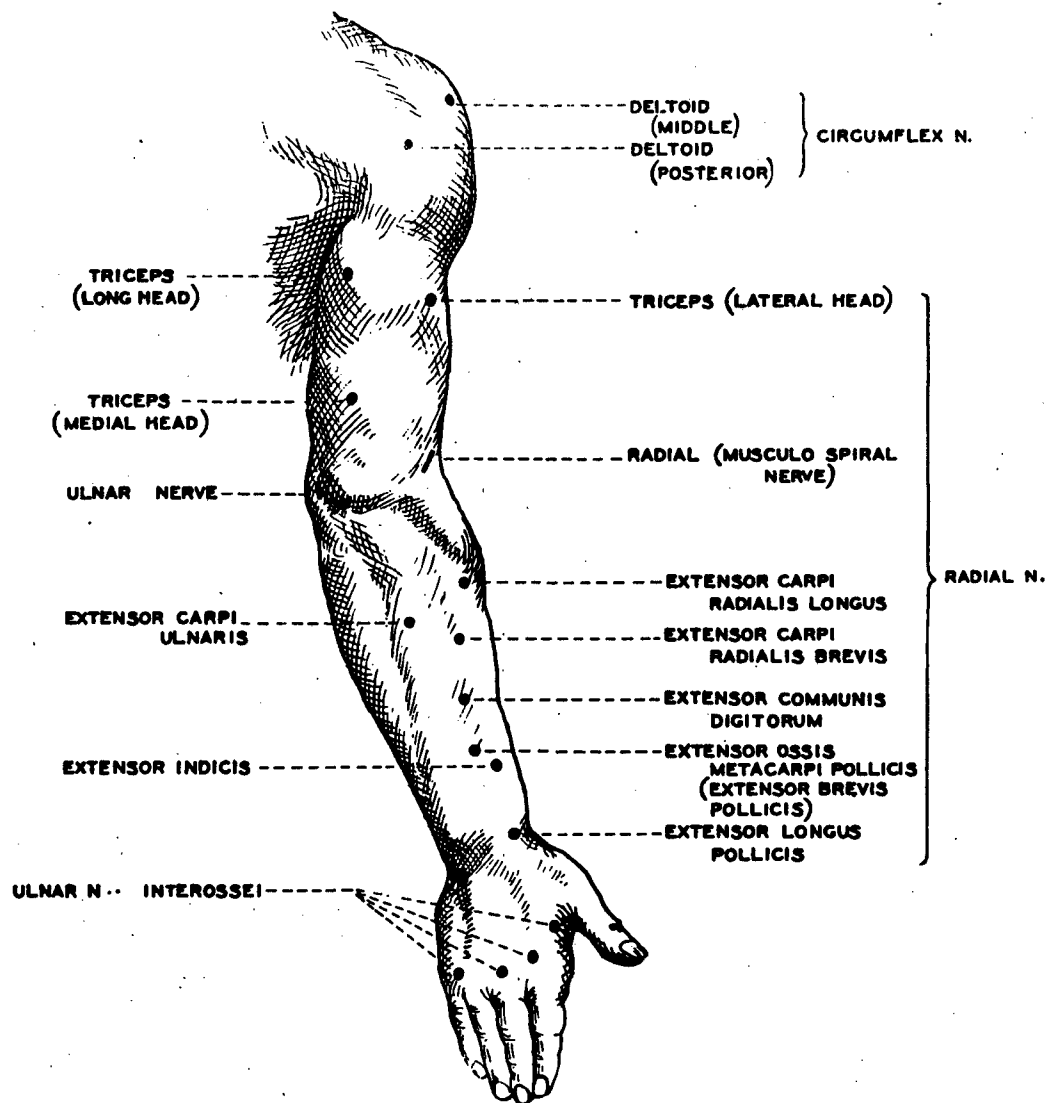
FIG. I-3. MOTOR POINTS OF POSTERIOR ASPECT OF UPPER
EXTREMITY.

movers about the major axes of rotation of the arm.   The results
are shown below.

SHOULDER JOINT

Motion		Muscles
Abduction	_____	middle deltoid supraspinatus upper trapezius serratus anterior
Adduction	_____	latissimus dorsi
Extension	_____	posterior deltoid
Flexion	_____	anterior deltoid upper trapezius serratus anterior
Internal rotation	_____	pectoralis major
External rotation	_____	infra spinatus
Elevation	_____	upper trapezius rhomboideus major
Depression	_____	gravity

ELBOW JOINT

Extension	_____	triceps
Flexion	_____	biceps

WRIST JOINT

Abduction	_____	flexor carpi radialis extensor carpi radialis longus
Adduction	_____	flexor carpi ulnaris extensor carpi ulnaris

Extension	_____	extensor carpi radialis
		  brevis
		extensor carpi radialis
		  longus

Extension (cont.)	_____	extensor carpi radial ulnaris
Flexion	_____	flexor carpi radialis flexor carpi ulnaris
Pronation	_____	pronator teres pronator quadratus
Supination	_____	supinator biceps

FINGER JOINTS

Extension	_____	extensor digitorum communis
Flexion	_____	flexor digitorum profundus flexor digitorum sublimus

C. PROPOSED LIMB ORTHOSIS POWERED BY STIMULATED MUSCLE

The above represents what are thought to be the necessary prime movers of the main joints of the arm. In a practical orthosis it is believed that the functions of the auxiliary muscles and joint stabilizers could be assumed by the mechanical structure. Since the arm will not be required to perform any strenuous movements, the assistive function of the auxiliary muscles can be neglected. The direction of movement of a bi-axial joint can be controlled by means of varying constraints placed along the axes of rotation. Such a constraint can be provided by a "joint-lock" with an electrical actuator. With such a device, the movements of the arm can possibly be guided about these individual axes in somewhat the same

manner that the auxiliary muscles perform this function. The joint locks would also serve the function of joint stabilizers when they are in the "lock" state. Notice that the arm may be held in any acceptable position with no muscle energy expenditure by passively locking all the joints. This may be quite useful, especially if the patient attempts fine finger or wrist movement about an extended terminal position.

Orthotic splints are sometimes powered by an external power source such as an electric motor or a compressed gas system. These systems are generally heavy if the actuator is actually mounted on the orthosis or complex if cables are used to transmit the force. An orthosis which utilizes the existing musculature of the paralyzed limb as a prime mover would have several advantages over the conventional devices:

1. The forces would act on the skeleton just as they do in the normal limb, thereby avoiding any subluxation forces.

2. There are as many actuators available as there are usable muscles.

3. The bulk of the orthosis should be considerably reduced.

4. The contraction and relaxation of the muscles should stimulate blood and lymph circulation as well as maintain muscle bulk.

CHAPTER II

SKELETAL MUSCLE

A. MORPHOLOGY OF MUSCLE

Before attempting to describe the functional behavior of skeletal muscle, it will be useful to examine its structure. It has been found, by means of the electron microscope, that a gross muscle is composed of thousands of bundles (fasciculi) of muscle fibers; each fiber being 10 to 100 microns in diameter and having a mean length of 5 centimeters.[15] Within each of these fibers there are several hundred thousand myofibrils, 0.5 to 10 microns in diameter, bathed in a viscous fluid which makes up about 50 percent of the bulk of the muscle. In turn, each myofibril has about 2500 filaments of polymerized proteins, called actin and myosin, arranged in an orderly fashion (Figure II-1) every 2 to 3 microns. A fibril of 5 centimeters in length therefore contains about 20,000 of these series segments which are called sarcomeres. In cross section the actin and myosin filaments are arranged in a hexagonal array.

When a muscle contracts, the actin and myosin filaments are forced to slide past one another in the longitudinal direction, thereby shortening the muscle. This force is thought to be

ACTIN
FILAMENT —
S- FILAMENT
MYOSIN
FILAMENT

Z-LINE

I SARCOMERE

2.5 μ
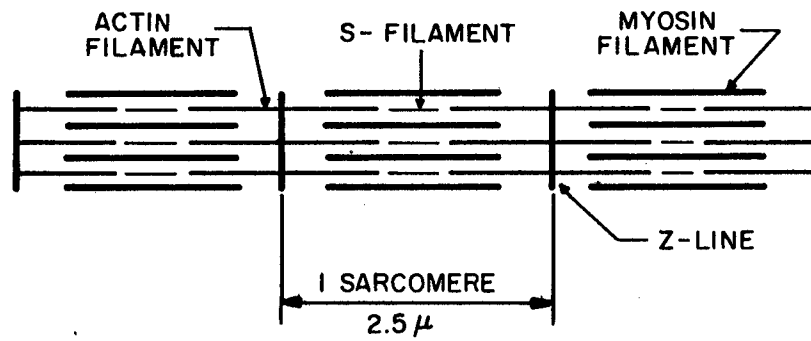
a) REST LENGTH OF SARCOMERE
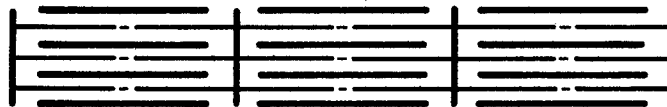
b) CONTRACTING

c) FULLY CONTRACTED
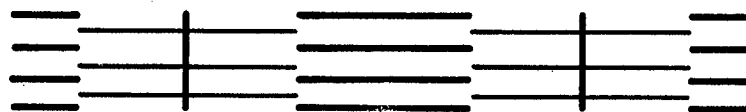
d) STRETCHED TOO FAR TO CONTRACT

FIG. II-I THE CONTRACTILE UNIT OF MUSCLE —
THE SARCOMERE

generated at a series of points in the region of overlap between the
actin and myosin filaments. These "bridges" between the two fila-
ments are believed to form spontaneously when an action potential
reaches the Z-line. When the muscle relaxes, energy is supplied
to break the bond allowing the filaments to slide freely past each
other. Figure II-1 also shows a sarcomere in relative states of
contraction. Note that only the S filament, which joins adjacent
actin filaments is stretched during lengthening. During shortening,
the actin filaments approach one another and then overlap until the
myosin filaments butt up against the Z-line. Each sarcomere
therefore constitutes a dynamic system with spontaneous force
input and an output length which is affected by a viscous drag and
the external load.

This variability of contractile force as a function of sarco-
mere length causes the gross muscle to have a similar character-
istic. Figure II-2 shows a typical length-tension diagram of a
skeletal muscle. The total tension curve was obtained by stimula-
ting the muscle at various lengths and recording the tension. The
passive tension curve was obtained by stretching the passive muscle
and recording tension. The difference between these two curves
then must be that tension which is due to the active component
alone. Just as for the single sarcomere it can produce no tension
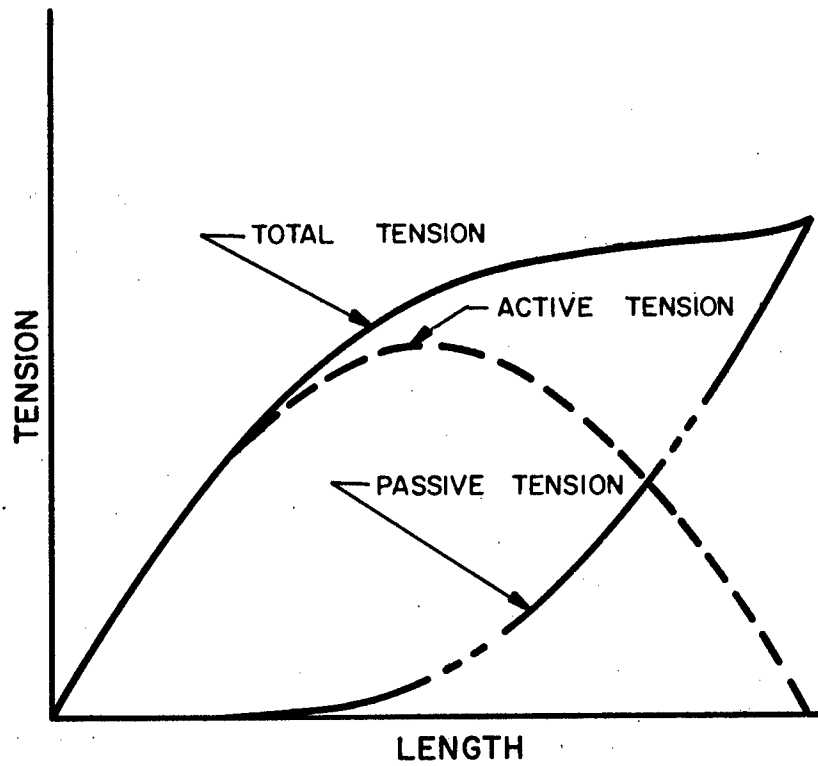
FIG. II-2   LENGTH-TENSION   RELATIONS
OF SKELETAL MUSCLE

at its extremes of length.

B. INNERVATION OF MUSCLE

Every muscle fiber has a motor end plate somewhere within the middle third of its length. It is at this point that the fiber receives its innervation from the central nervous system. A single motor neuron supplies (innervates) about 100 muscle fibers by arborizations which terminate at the motor end plate. The motor nerve and its muscle fibers constitute the "motor unit" and since muscle fibers follow the all or none principle, the contraction of the single motor unit represents the quantum of muscular contraction. To perform a motor unit contraction the motor nerve supplies an impulsive change in electrical potential (action potential) to the motor end plates. A similar action potential is generated in the muscle fiber and causes the motor unit to twitch. Let us examine this action in more detail. A nerve action potential arrives at an endplate; a muscle action potential is generated in the vicinity of the endplate and travels down the fiber in both directions at a speed of about 5 meters per second. Immediately following the muscle action potential is a "wave of contraction" which causes the muscle to twitch. This single fiber twitch is actually manifested by the successive twitches of the 20, 000 individual sarcomeres alternately contracting and relaxing.

These individual contractions summate in the tendon to produce
the fiber twitch. The motor unit twitch is then the parallel addi-
tion of single fiber twitches. Gross muscle tension is produced by
the recruitment of many motor units.

In normal muscular activities the muscle is often called
upon to produce a steady tension. The central nervous system
produces such a tension by feeding action potentials to the motor
units at a rate which is fast enough to prevent the muscle from
relaxing between twitches. This type of steady contraction is
called a tetanus.

C. MECHANICAL PROPERTIES OF MUSCLE

The mechanical properties of skeletal muscle have been
under investigation for many years. Not until the 1920's, however,
did adequate instrumentation schemes become available. It was
during this time that A. V. Hill began his lifelong work of investi-
gating the energetics of muscle contraction. Since then countless
articles have been written by him and many others concerning the
mechanical, chemical and thermodynamic properties of skeletal
muscle. It would be a mammoth undertaking indeed to attempt to
summarize these and the many other works in the field. I will
choose rather to develop a suitable model for muscle by drawing
upon the results in the literature as needed.

Muscle is classically thought of as a contractile element with its own particular properties and a series elastic element. The series elasticity acts as an energy storage device between the prime mover and the load and has a smoothing effect on limb movements. This series elasticity has been found by Hill to have a very high value of stiffness and for this reason it allows the contractile element to be easily described experimentally.

1. Isotonic Conditions

That is, if the muscle is loaded by applying a constant force (isotonic) to its tendon, and it is then stimulated, the resulting movement of the tendon is assumed to be the internal shortening of the muscle since the series elastic element does not stretch appreciably. Hill, in this way, arrived at an experimentally obtained description of the mechanical behavior of the contractile element of skeletal muscle. Figure II-3 shows the plotted results of such an experiment. The force due to the load (P) is plotted versus the speed of shortening (v). As might be expected, the velocity decreases as the load increases. The relation, however, is in general nonlinear and is given by the equation of a rectangular hyperbola:

$$(v+b)(P+a) = (P_0+a)\,b = \text{constant} \qquad \text{(III.1)}$$
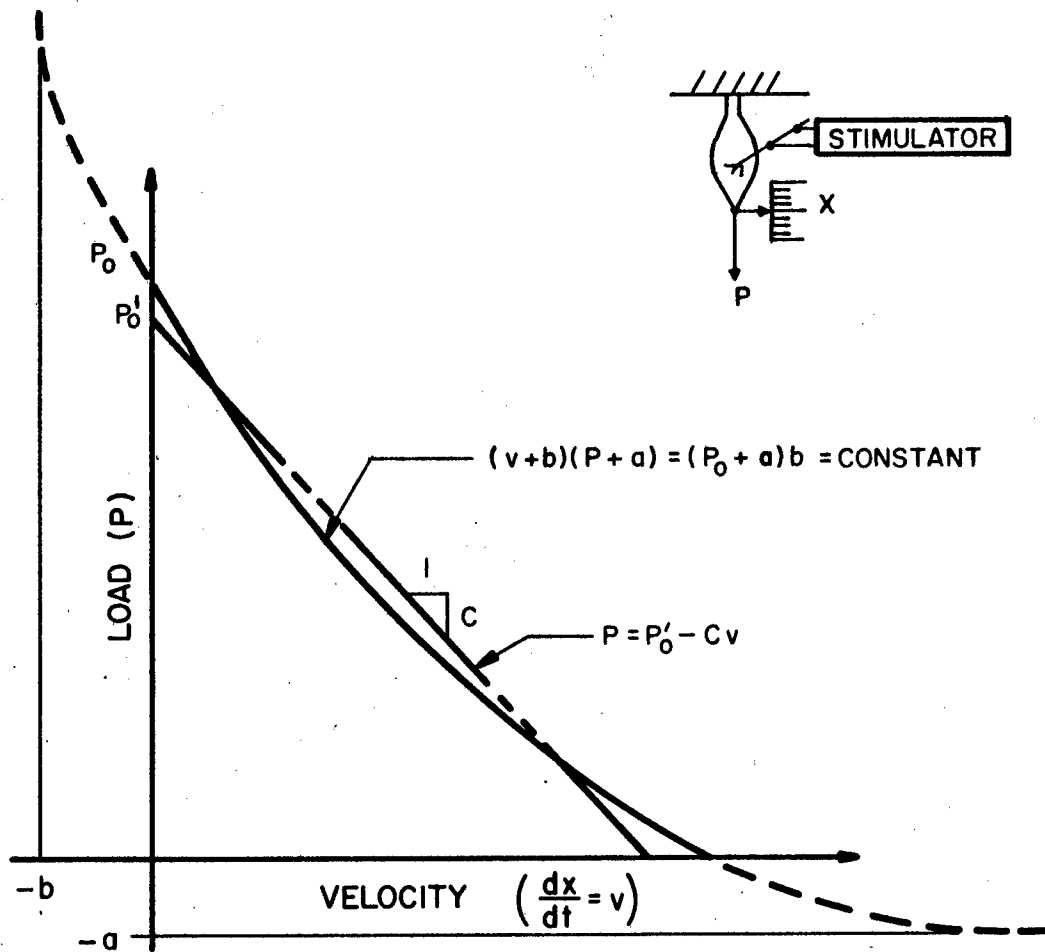
FIG. II - 3 RELATION BETWEEN LOAD AND SPEED
OF MUSCLE SHORTENING

where: P_0 is the maximum force the muscle can develop and

-b and -a are the horizontal and vertical asymptotes

of the equation.

The slope of the curve at any point has the units of a viscosity

(force/velocity) and represents the internal viscosity of the muscle.

Approximating the curve as a straight line, an average value of

muscle viscosity (C) can be obtained and Equation II. 1 becomes

$$P = P'_0 - Cv \qquad (II. 2)$$

(Refer to Figure II-3.)

A simple model which mimics the mechanical behavior of

skeletal muscle consists of a contractile element with a parallel

viscosity (C) and elasticity (K_p), and a series elasticity (K_s)

(Figure II-4). The internal and external shortenings of the muscle

are defined x_i and x_e. The load velocity curve of Figure II-3 can

be obtained by preloading or afterloading. In Figure II-4 a the

model has been preloaded by applying the load to the resting muscle

then stimulating the stretched muscle. Large loads will cause the

muscle to be at a poor mechanical advantage due to its peculiar

length-tension characteristics of Figure II-2. This difficulty can be

avoided by running the experiment in the afterloaded condition of

a) PRELOADED

b) AFTER LOADED
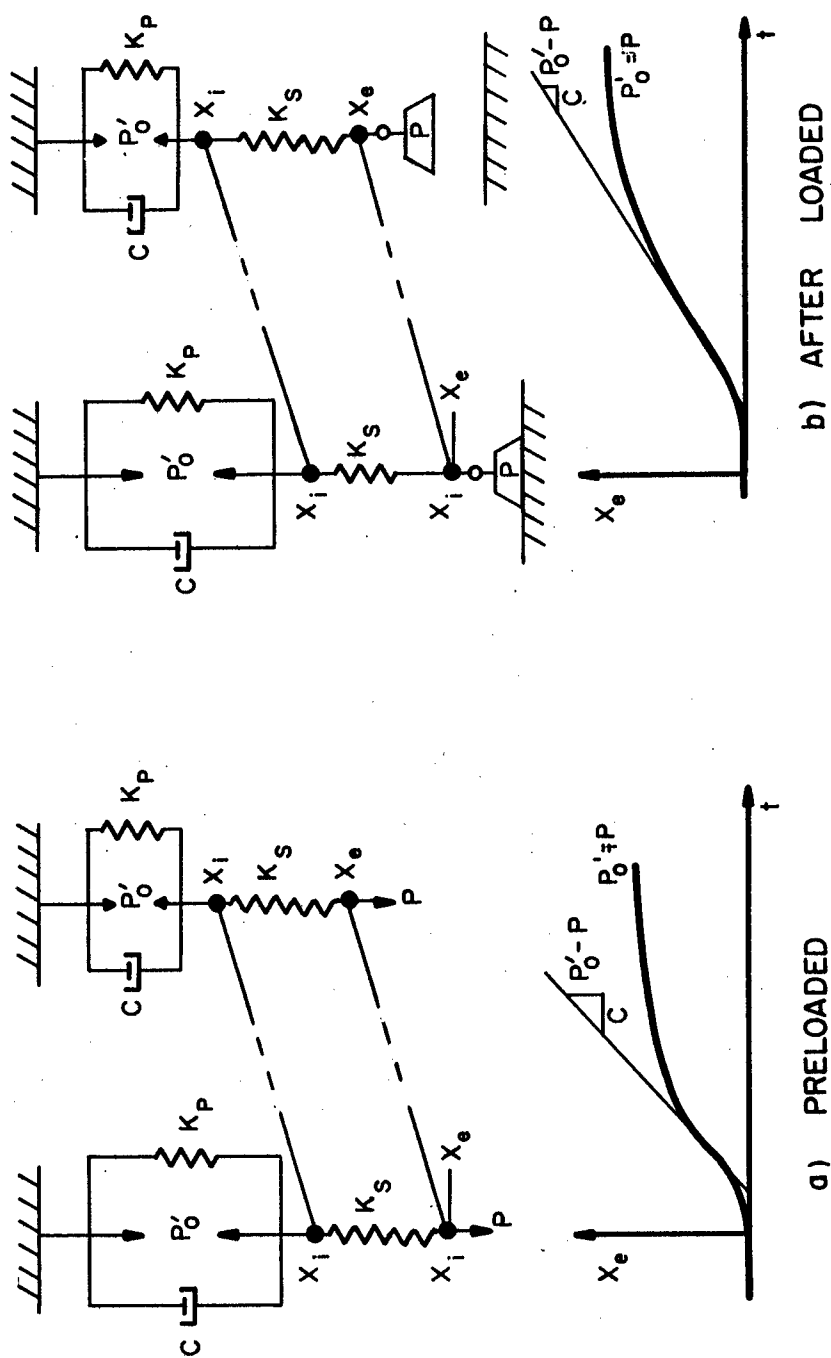
FIG. II-4 ACTIVE RESPONSE OF MUSCLE MODEL UNDER ISOTONIC CONDITIONS

Figure II- . Here the muscle at its rest length lifts a weight from

a platform. Since the muscle delivers its maximum force at rest

length, larger loads can be used and a larger portion of the force-

velocity curve can be evaluated. There is, however, a slight delay

before movement occurs which increases with the load since the

muscle must develop a tension equal to the load before movement

begins. Notice in both curves that the velocity varies during the

movement. The maximum velocity is actually used in the force-

velocity curve since this corresponds to the time at which maximum

muscle force is developed (neglecting inertial force). The equation

of motion is obtained from (II.2)[*]

$$P = P'_0 - C \frac{dx_e}{dt}$$

$$x_e = \int \frac{P'_0 - P}{C} \, dt = \frac{P'_0 - P}{C} t \qquad (II.3)$$

2. Isometric Conditions

Under isometric (constant length) conditions the overall

length of the muscle remains unchanged. However, the lengths of

the elastic and contractile elements change. The elastic element

---

[*] The parallel elasticity according to Hill produces no
    compressive force.

is stretched by an amount equal to the shortening of the contractile element (Figure II-5). Equating the force produced by the contractile element to that resisted by the elastic element.

$$K_s x_i = P'_0 - C \frac{dx_i}{dt} \qquad \text{(II.4)}$$

$$\frac{dx_i}{dt} + \frac{K_s}{C} x_i = \frac{P'_0}{C} \qquad \text{(II.5)}$$

This is a first order differential equation with solution

$$x_i = \frac{P'_0}{K_s} (1 - e^{-\frac{K_s}{C} t}) \qquad \text{(II.6)}$$

The isometric force is then given by:

$$P = K_s x_i = P'_0 (1 - e^{-\frac{K_s}{C} t}) \qquad \text{(II.7)}$$

3.   Quick Release Experiment

Quick release experiments have been performed to evaluate the stiffness of the series elastic element (Figure II-6). The muscle is first of all stimulated and preloaded and the external length (x_e) is noted. The load is then abruptly released and the muscle shortens. Since the contractile element cannot change its length instantaneously, the immediate change in length is due only
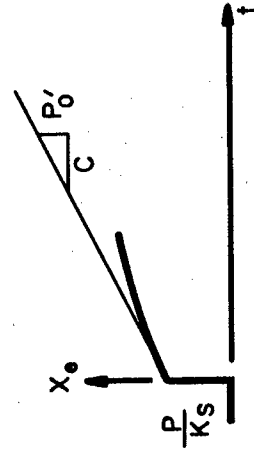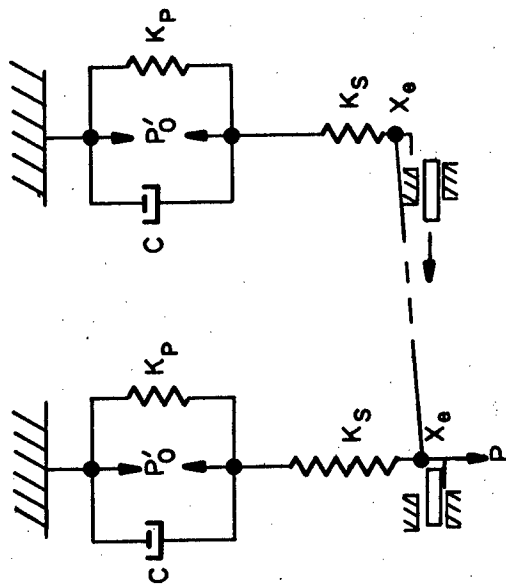
FIG. II-6 QUICK RELEASE EXPERIMENT
TO DETERMINE STIFFNESS
OF SERIES ELASTICITY
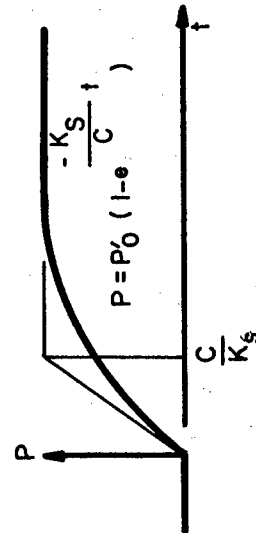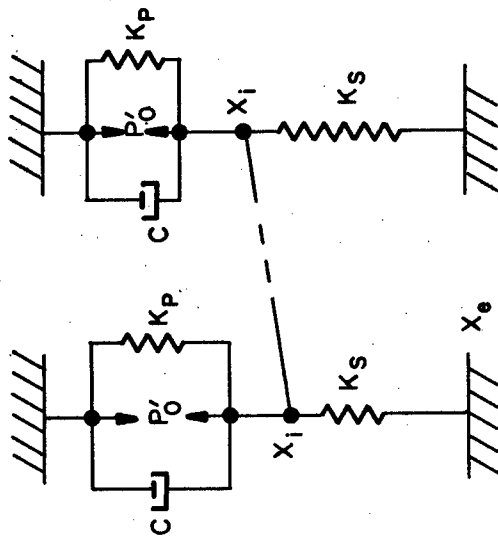
FIG. II-5 ISOMETRIC CONTRACTION
OF MUSCLE MODEL

to the shortening of the series elastic element. Then,

$$\text{at} \quad t = 0, \quad K_s = \frac{P}{\Delta x_e} \tag{II.8}$$

4. Quick Stretch Experiment

If a step change in length is applied to the resting muscle and tension is recorded, the tension will initially rise to a high value and then gradually relax to a lower level (Figure II-7). The force equations are:

$$P = K_s\left(x_e - x_i\right) \tag{II.9}$$

$$K_s\left(x_e - x_i\right) = K_p x_i - C\frac{dx_i}{dt} \tag{II.10}$$

Solving II.9 and II.10 simultaneously and applying a step change in x_e yields:

$$P = K_s x_e - \frac{K_s^2 x_e}{K_p + K_s}\left[1 - e^{-\left(\frac{K_p + K_s}{C}\right)t}\right] \tag{II.11}$$

Note that at $t = 0$, $P = K_s x_e$. Just as in the quick release experiment, the value of stiffness for the series elasticity is available. It should be noted, however, that a quick stretch produces much

27
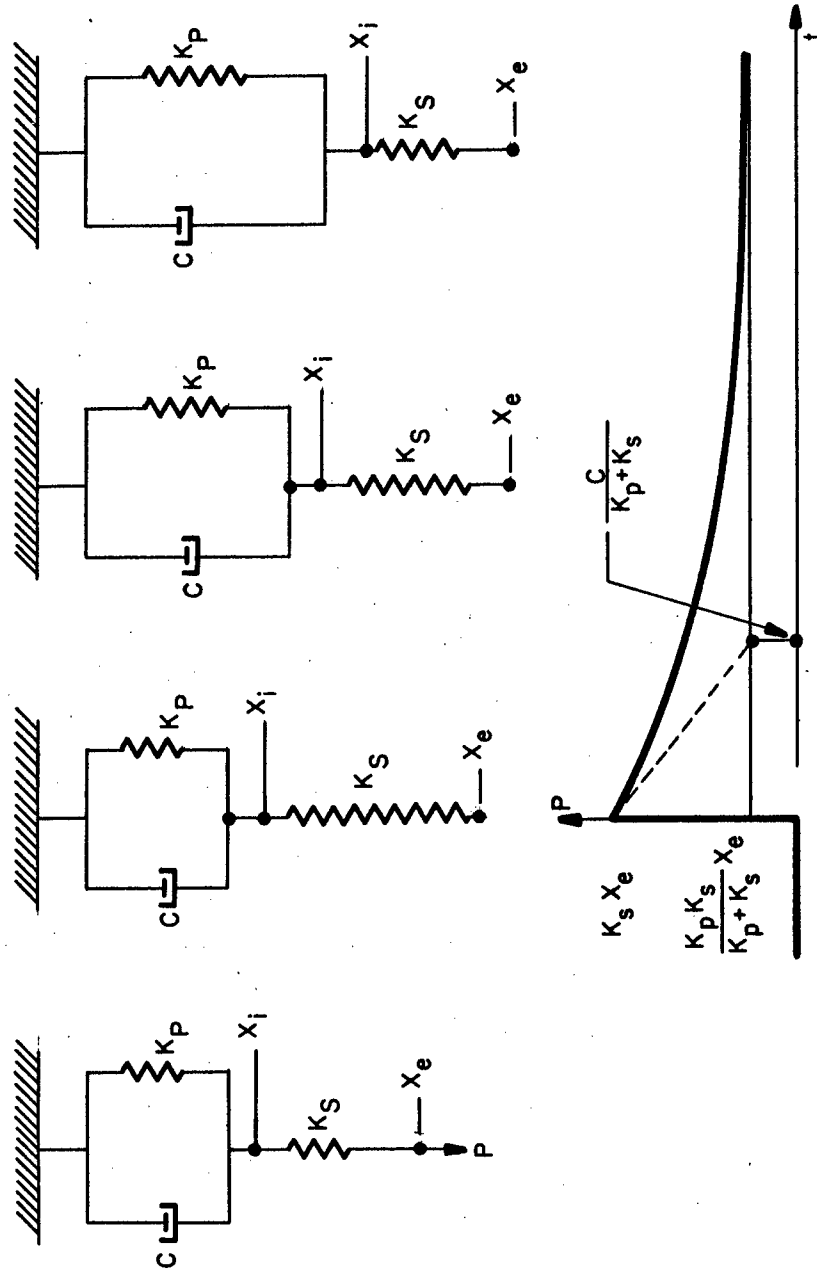
FIG. II-7 PASSIVE RESPONSE OF MUSCLE MODEL TO QUICK STRETCH

more artifact at $t = 0$ than does a quick release due to mechanical
shock to the experimental setup. Note also that for large t,

$$P = \frac{K_p K_s}{K_p + K_s} \, x_e \qquad\qquad (II.12)$$

Length-tension diagrams of muscle are plotted using these equili-
brium values. Since we are dealing with linear models, the length
tension curve of the model will not have a parabolic shape as does
muscle (Figure II-2) but will be linear of slope $\dfrac{K_p K_s}{K_p + K_s}$.

5. Twitch Contraction

Figure II-8 shows the isometric twitch response of a maxi-
mally stimulated skeletal muscle. Notice that first of all there is
a delay between the time of stimulus application until the time that
the tension begins to increase. This is called the latent period and
is usually between 1 and 10 milliseconds. The twitch curve itself
has a form which resembles the impulse response of a system
which is at least second order. The dashed curve in Figure II-8 is
the delayed impulse response of a second order system which has
been matched to the experimental curve. The equation describing
the dotted curve is:

$$\frac{P_i K_S}{C} e^{-\frac{K_S}{C} t}$$

$$(t-.01)e^{-25(t-.01)}$$

RECORDED

TENSION

0   .02   .04   .06   .08   .10   .12   .14   .16   .18   .20   T(SEC)
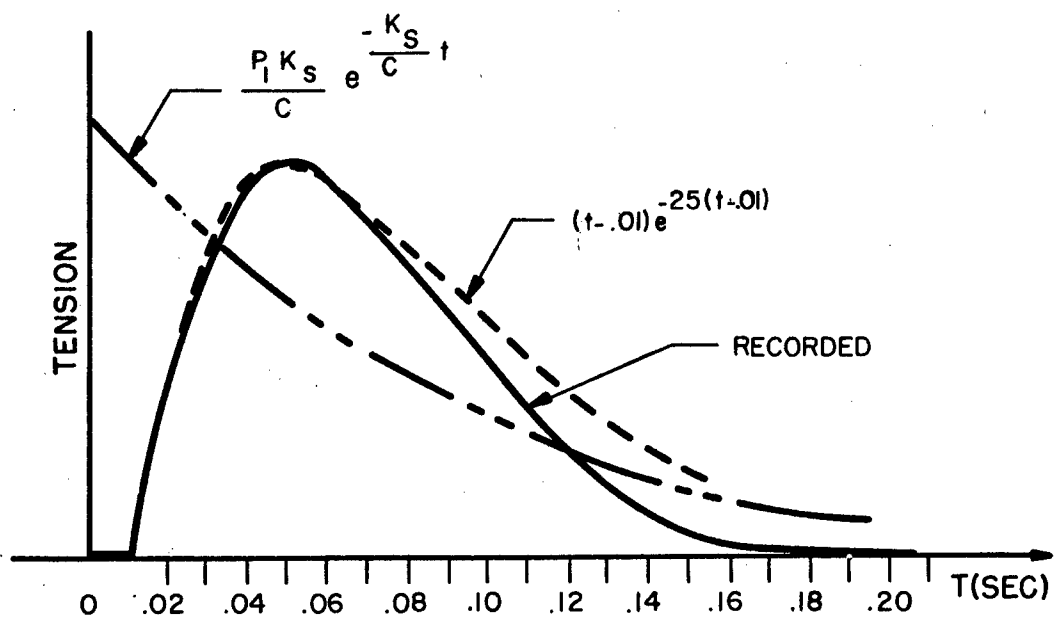
FIG.II-8. TWITCH CONTRACTION OF MUSCLE AND MUSCLE MODELS

$$\text{Twitch} = Pt'e^{-25t'} \tag{II.13}$$

where $t' = t - T_D$, and T_D is the delay time (10 ms.).

If we assume that an action potential causes an impulse of force P_1 to be applied to our model, then the isometric response of the model will be

$$\text{Twitch of model} = \frac{P_1 K_s}{C} e^{-\frac{K_s}{Ct}} \tag{II.14}$$

this is shown as a dashed curve in Figure II-8. Clearly the curve does not describe the muscle twitch. The discontinuous rise of this curve at $t = 0$ does not match the muscle twitch. A much closer fit can be obtained if another spring and dashpot are added to our inadequate model as shown in Figure II-9. Since the muscle twitch response was critically damped it is necessary that

$$\frac{C}{K_s} = \frac{C'}{K'_s} = \frac{1}{a} \tag{II.15}$$

and once again that K'_p produces no compressive force. Also it is necessary that no loading occurs between the primed and unprimed stages, i.e.,

31
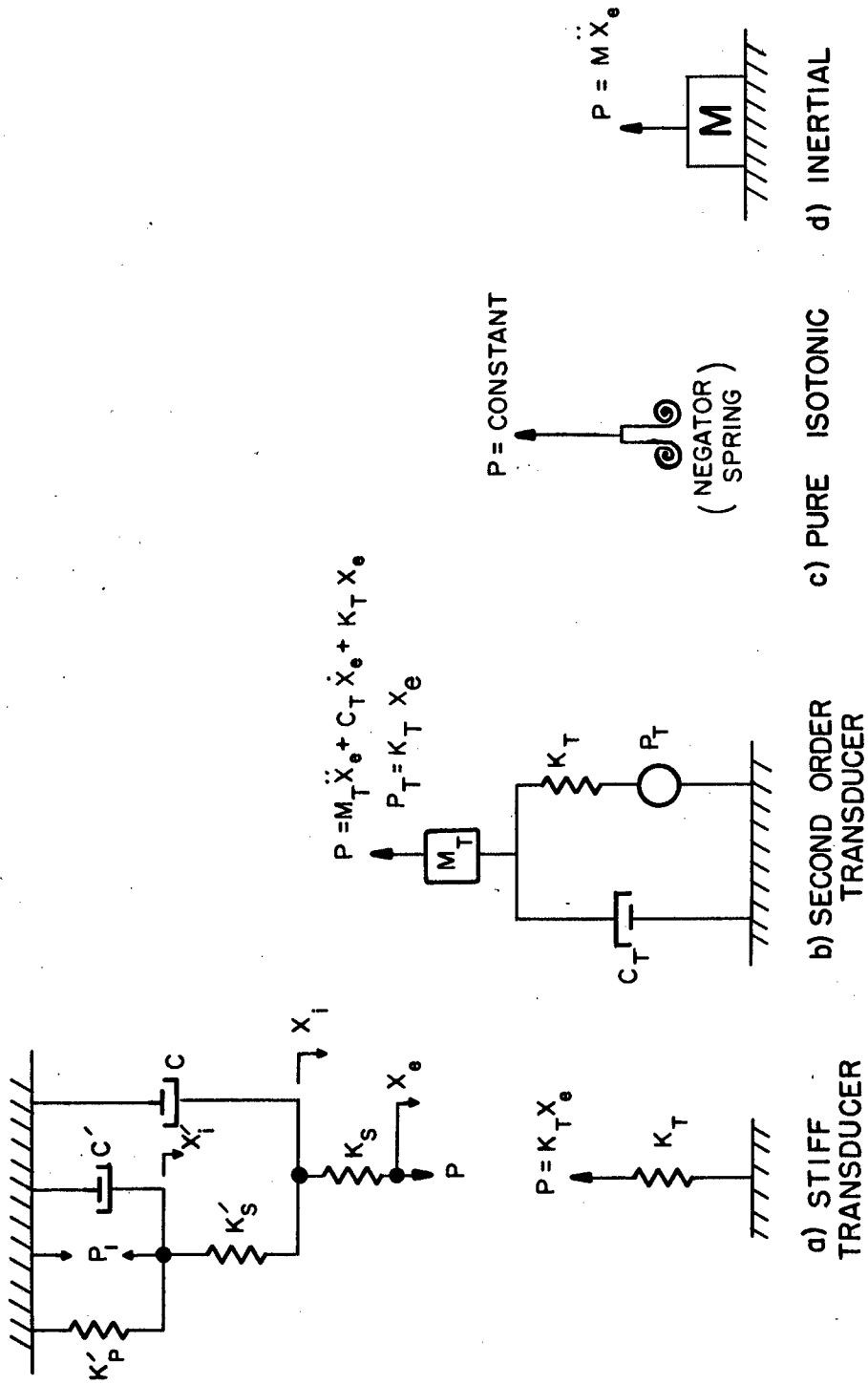
FIG. II-9 IMPROVED MUSCLE MODEL UNDER VARIOUS TEST CONDITIONS

$$\dot{x}'_i \gg \dot{x}_i \qquad\qquad (II. 16)$$

The isometric response of the model to an impulse of force P_1 is then:

$$\text{Twitch of model} = K_s x_i = P_1 a^2 t e^{-at} \qquad\qquad (II. 17)$$

which is identical to Equation II. 13.

6.   Effect of Transducer on Isometric Muscle Twitch

Equation II. 17 is the equation for a twitch contraction of the model which would be obtained using a perfect tension transducer. That is, a transducer of infinite stiffness and damping and zero mass. Any realizable transducer therefore would affect the form of the twitch contraction. Let us first of all observe the effects of a stiff transducer. Figure II-9a shows the transducer mounted in series with the model. The stiffness of the transducer (K_T) in series with K_s produces a resultant series elasticity of

$$K' = \frac{K_s K_T}{K_s + K_T} \qquad\qquad (II. 18)$$

which changes the form of twitch contraction to

$$\text{Measured twitch} = K_t x_e = A \left[e^{-\frac{K'}{C}t} - e^{-\frac{K'_s}{C'}t} \right] \tag{II.19}$$

where

$$A = \frac{K'_s K_s K_T P_1}{(K_s + K_T)(K'_s C - K'C')} \tag{}$$

If the muscle acts against a transducer with finite stiffness, damping and mass (Figure II-9b), the measured twitch will also be affected. The equations of motion for the transducer are:

$$P = M_T \ddot{x}_e + C'_T \dot{x}_e + K_T x_e \tag{II.20}$$

$$P_T = K_T x_e \tag{II.21}$$

where P_T is the force measured by the transducer. For mathematical simplicity, the dynamic operator $S = \frac{d}{dt}$ will be used in the following equations. Equation II.20 then becomes

$$P = (M_T s^2 + C_T s + K_T) x_e \tag{II.22}$$

The force which the muscle produces is from Equation II. 17

(assuming x_e is small, i.e., K_T large)

$$P = \frac{P_1 a^2}{(s+a)^2} \qquad (II.23)$$

Equating II. 22 and II. 23,

$$\frac{x_e}{P_1} = \frac{a^2}{(M_T s^2 + C_T s + K_T)(s+a)^2} \qquad (II.24)$$

$$P_T = \frac{P_1 K_T a^2}{(M_T s^2 + C_T s + K_T)(s+a)^2} = \frac{P K_T}{(M_T s^2 + C_T s + K_T)} \qquad (II.25)$$

The tension as measured by the transducer (P_T) then is affected

by an attenuation and a second order lag. We will have recourse to

use this expression in the experimental section of the thesis.

7.   E f f e c t o f Transducer on Isotonic Muscle Twitch

Let us first of all calculate the isotonic response of the

model to a constant inertialess, undamped load (Figure II-9c).

Again we make the assumption that the series elasticity has a large

stiffness such that $x_e = x_i$. The equations of motion for the muscle

model are:

$$P_1 = C'\dot{x}'_i + K'_s(x'_i - x_i) \tag{II.26}$$

$$P = K'_s(x_i - x'_i) + C'\dot{x}_i \tag{II.27}$$

Solving these two equations simultaneously and making use of the "s" notation:

$$x_i = \frac{K'_s P_1 - P(C's + K'_s)}{(Cs + K'_s)(C's + K'_s) - K'^2_s} \tag{II.28}$$

Many so-called isotonic experiments are performed using weights as the load. What are the effects of this added inertia on the isotonic contraction of the muscle model? (Figure II-9d). The equations of motion are:

$$P_1 = C'\dot{x}'_i + K'_s(x'_i - x_i) \tag{II.29}$$

$$O = K'_s(x_i - x'_i) + C\dot{x}_i + M\ddot{x}_i \tag{II.30}$$

Solving these equations simultaneously yields:

$$x_i = \frac{P_1 K'_s}{s[MC's^2 + (MK'_s + CC')s + K(C + C')]} \tag{II.31}$$

Equation II.31 has a much different form from Equation II.28 which represents a true isotonic contraction. It should be mentioned, however, that muscles in the body usually act against inertial loads, especially the proximal joints of the extremities. The results of the experiments with inertial load should therefore have more relevance to actual muscle function than do the isotonic experiments. It should also be remembered that although the muscle force P_1 is shown as a constant in the equations, it is a function of the number of motor units active and the length of the muscle.

In summary then, a viscoelastic muscle model, including the dynamics of contraction is given in Figure II-9. The twitch contraction of this model due to a single action potential (impulse) is

$$\text{twitch} = P_1 a^2 t e^{-at} \tag{II.17}$$

where

$$a = \frac{C}{K_s} = \frac{C'}{K'_s}$$

During the steady state contraction of the muscle model to a rapid stimulus rate (tetanus), the response may be characterized by:

$$\text{isotonic} \qquad x_e = \frac{P'_0 - P}{C} t \qquad\qquad (II.3)$$

$$\text{isometric} \qquad P = P'_0 (1 - e^{-\frac{K_s}{C} t}) \qquad\qquad (II.7)$$

If the transient response of the model to a tetanic stimulus is also desired even in the presence of transducer effects then the dynamic equations of motion of the particular configuration can be written and solved.

D. THE SERVOMECHANISM OF MUSCLE CONTRACTION

We have seen that each muscle fiber behaves much like an nth order system with a delay time. These muscle fibers are divided functionally into two classes: The extrafusal and intra fusal fibers. The extrafusal fibers, which are much more numerous, act as prime movers; whereas the intrafusal fibers, interspersed throughout the muscle, act as regulators of gross muscle length. Groups of these intrafusal fibers make up the muscle spindles. These usually run the whole length of the muscle and act as length sensors. It has been shown experimentally that the muscle spindle emits a string of action potentials to the central nervous system, the rate of which is proportional to the change of muscle length. In addition to these afferent signals, it also

receives an efferent signal from the central nervous system which
biases the operating point of the transducer. Figure II-10 shows,
in simplified form, the neural connections to an extrafusal and
intrafusal fiber. A command signal is generated in the motor
cortex which is then transmitted down the spinal cord via an upper
motor neuron. According to Granit the signal is then transmitted
out of the spinal cord on an α or γ lower motor neuron. In the
case of γ innervation, the signal travels to the spindle fiber and
causes it to contract. This biases the spindle and is interpreted
by the transducer portion of the spindle as a length change. This
error information flows back to the spinal cord along the groups II
(length change) and Ia (rate of change length) afferent fibers.
After synapsing with interneurons the signals reach the α motor
neurons which then cause the extrafusal fibers to contract until
the desired length is assumed. This feedback path is known as the
reflex loop and is responsible for the "knee-jerk" commonly
observed in a clinical examination. That is, when the tendon is
tapped the muscle spindles are stretched briefly and vigorously.
A burst of action potentials then traverses the reflex loop and
causes the muscle to contract a short time later. The γ innerva-
tion is thought to be used by the central-nervous system in the
execution of precise motions. For quick, less accurate motions
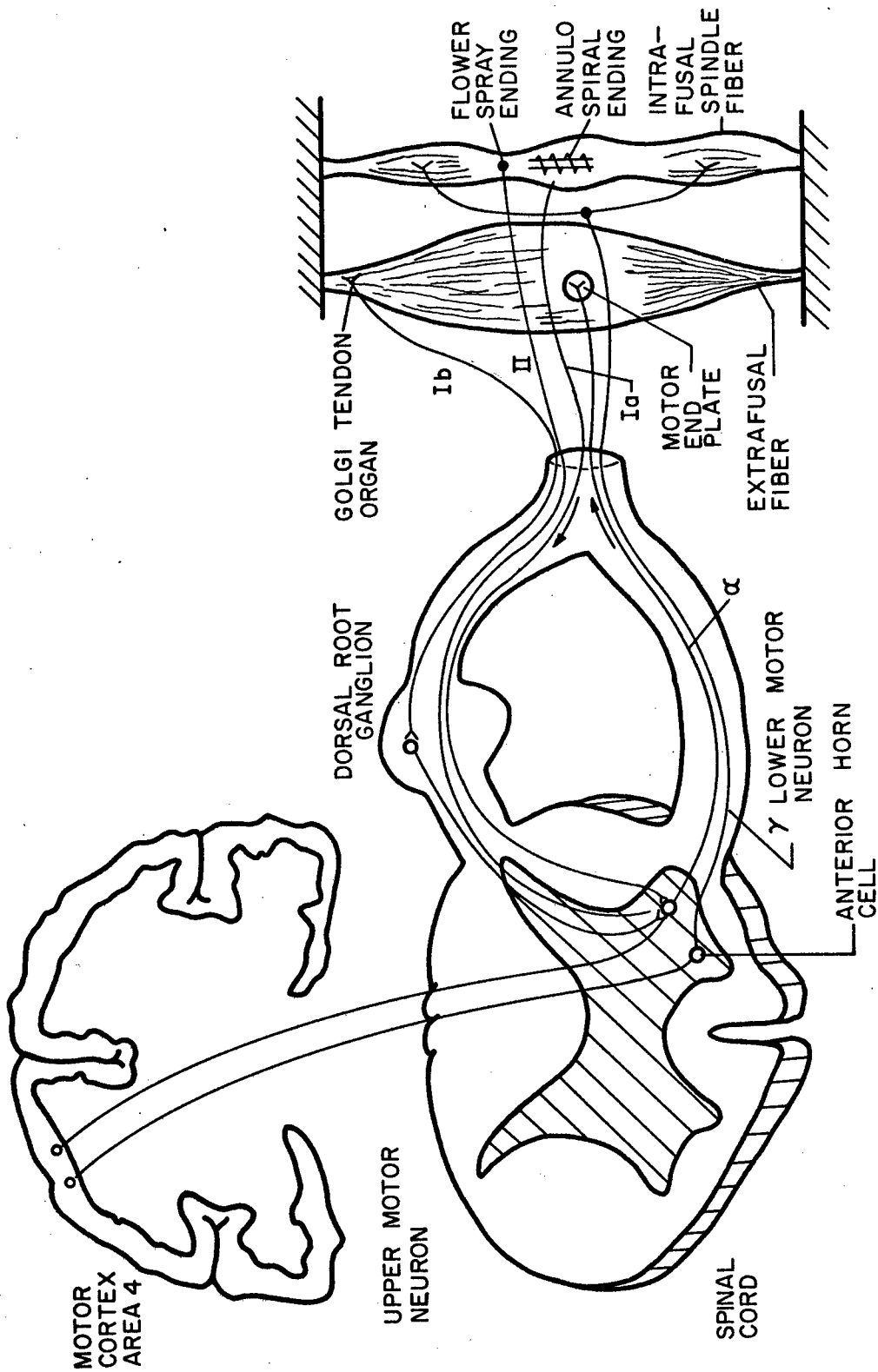
FIG. II-10 NORMALLY INNERVATED SKELETAL MUSCLE

the α motor neurons are thought to be innervated directly, in open loop fashion.

1. Muscle Spindle, Function and Models

There have been at least three different models of the muscle spindles proposed in the literature. Each was derived in part by consideration of the length and rate sensitivity of the spindle. Houk[29] proposes a transfer function between spindle firing rate and muscle length of the form:

$$\frac{f_s}{x_m} = C \left(\frac{n\tau s + 1}{\tau s + 1} \right) \tag{II.32}$$

The response to a step change in length gives the desired response:

$$f_s(t) = x_m C \left[1 + (n-1) e^{t/\tau} \right] \tag{II.33}$$

Vossius[75] proposes a similar transfer function of the form:

$$\frac{f_s}{x_m} = K_1 + \frac{K_2 \tau s}{\tau s + 1} \tag{II.34}$$

The step response of this model also shows the same type of response.

$$f_s(t) = X_m(K_1 + K_2 e^{-t/\tau})$$ (II. 35)

Stark[59] based his model for the muscle spindle on the visco-elastic properties of the fiber. The viscoelastic model is shown in Figure II-11. It consists of three elements in series: the tendon stiffness, the lumped stiffness and viscosity of the intrafusal fibers, and the stiffness and viscosity of the nuclear bag of the spindle. If the equations of motion for the model are written, a transfer function is obtained.

$$\frac{f_s}{x_m} = \frac{\Delta x_c}{x_m} = \frac{G_m(\tau_1 s+1)}{(\tau_2 s+1)(\tau_3 s+1)}$$ (II. 36)

where Δx_c is the change in length of the nuclear bag which determines the firing rate. If the proper assumptions are made, the time constants and gain are given by:

$$\tau_1 = \frac{B_F}{K_F}$$ (II. 37)
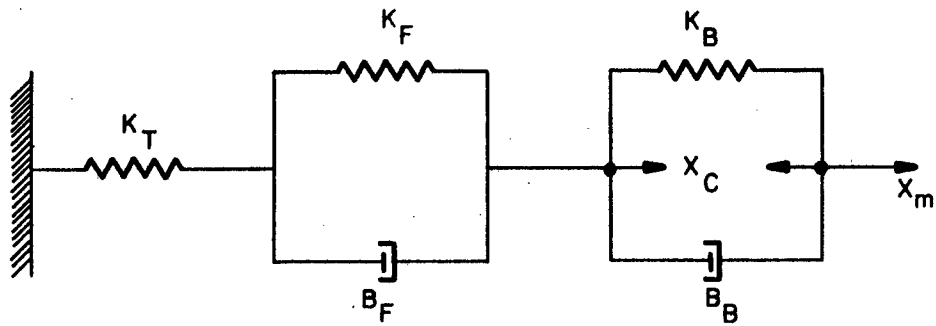
FIG. II - II   SPINDLE MODEL OF STARK

$$\tau_2 = \frac{B_F + B_B}{K_F + K_B} \qquad \text{(II. 38)}$$

$$\tau_3 = \frac{B_F B_B}{K_T (B_F + B_B)} \qquad \text{(II. 39)}$$

$$G_m = \frac{K_T}{K_F K_B} \qquad \text{(II. 40)}$$

This transfer function represents a lead-lag network. Stark found from his frequency response experiments that the spindle also has this lead-lag behavior. The step response of this transfer function is given by:

$$f_s = X_m G_m \left\{ 1 + \frac{1}{\tau_3 \tau_2} \left[(\tau_3 - \tau_1) e^{-t/\tau_3} - (\tau_2 - \tau_1) e^{-t/\tau_2} \right] \right\} \qquad \text{(II. 41)}$$

Again it is of the same form as equations II. 33 and II. 35 except that it has two decaying exponentials.

Another element which is important in the control of muscular contraction is the Golgi tendon of the muscle. If the tension in the muscle exceeds a preset level, the tendon organ informs the central nervous system. It has no efferent input.

There are other functional elements involved in the control of muscle such as joint receptors, pressure receptors, etc.

Unfortunately, not as much is known about these receptors or exactly how they influence muscular contraction at the present time. We will therefore limit the discussion to the above-mentioned elements.

2.   System Operation

The simplest skeletal joint is the mono-axial joint bridge by two antagonistic muscles. A block diagram showing the agonistic action of one of these muscles is shown in Figure II-12. The central nervous system innervation enters the motor neuron pool and synapses with a γ or a α motor neuron. For γ innervation the train of action potentials is transformed to a length signal by the D/A converter. This reference input (-Xr) then is summed with the muscle length:

$$X_m = r_1 \Phi \qquad\qquad (\text{II}.42)$$

where r_1 is the moment arm of the muscle and Φ is the joint angle. The error signal,

$$X_e = X_m - X_r \qquad\qquad (\text{II}.43)$$

45
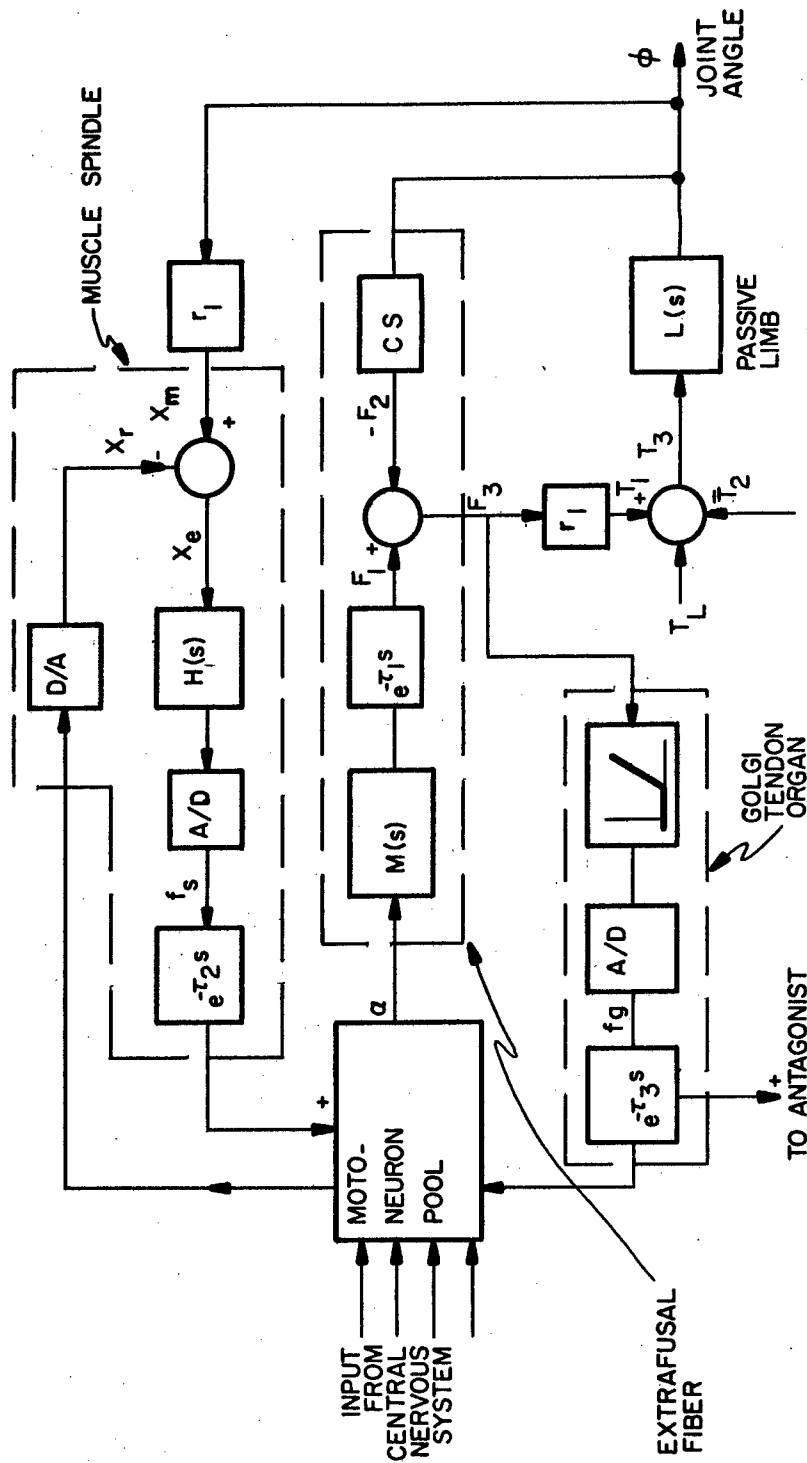
FIG. II – 12. BLOCK DIAGRAM OF NORMALLY INNERVATED MUSCLE

is then sensed by the spindle and transformed into a train of action potentials (f_s) by H(s). H(s) can be represented by either of the Equations (II. 32), (II. 34) or (II. 36). After a delay (τ_2) this signal then enters the motor neuron pool and synapses with several a motor neurons which in turn cause the extrafusal fibers to contract. After a delay (τ_1) an isometric force (F_1) is developed which acts against the viscous drag of the muscle (F_2). A resultant force (F_3) then causes a torque

$$T_1 = r_1 F_3 \qquad\qquad (II.44)$$

to be transmitted to the limb. This is opposed by any load torque that is present (T_L), the torque caused by the antagonistic muscle (T_2) and the dynamics of the limb (T_3). The joint angle then assumes a value equal to

$$\Phi = T_3 L(s) \qquad\qquad (II.45)$$

the reflex loop acts until the muscle length

$$X_m = r_1 \Phi \qquad\qquad (II.46)$$

is equal to the reference input.

In the event that the required muscle force (F_3) becomes large enough to cause damage to the tendon, the Golgi tendon organ fires and, after a delay (τ_3) has an inhibitory effect on the α innervation of the agonist and a facilitory effect on the antagonist. This protective role is the only known function of the Golgi tendon organ.

The above paragraphs are by no means the last word in this highly complex business of understanding the neurologic control of muscle. This area is currently under the investigation of many researchers, and new developments and new theories are forming at a rapid pace. The purpose of this section is only to review briefly the general nature of muscular control. Some of the material will have relevance in Chapter III where the behavior of electrically stimulated muscle will be discussed.

CHAPTER III

THE ELECTRICAL EXCITABILITY
OF MUSCLE

A. THE STRENGTH-DURATION CURVE

1. Mathematical Modeling

The strength-duration (S-D) curve is a graphical representa-
tion of the excitability of a single axon, whole nerve, or muscle in
response to a pulsed DC electrical stimulus. The strength-
frequency (S-F) curve, similarly, is a measure of the excitability
of nervous tissue to an AC electrical stimulus. We will be con-
cerned here only with the S-D curve. Figure III-1 shows the form
of a typical S-D curve which we will assume is for a single axon.
The ordinate can either be stimulus voltage (V) or current (I)
depending upon which variable is controlled, and the abscissa is the
time duration (D) of the pulse. The S-D curve represents the
smallest values of the parameters which will cause nerve excita-
tion as determined by the presence of an action potential or the
slightest perceptible muscle contraction.

For pulses of very large duration we notice that the current
approaches a fixed level called the rheobase. As a relative
measure of excitability, the chronaxie has been defined as that
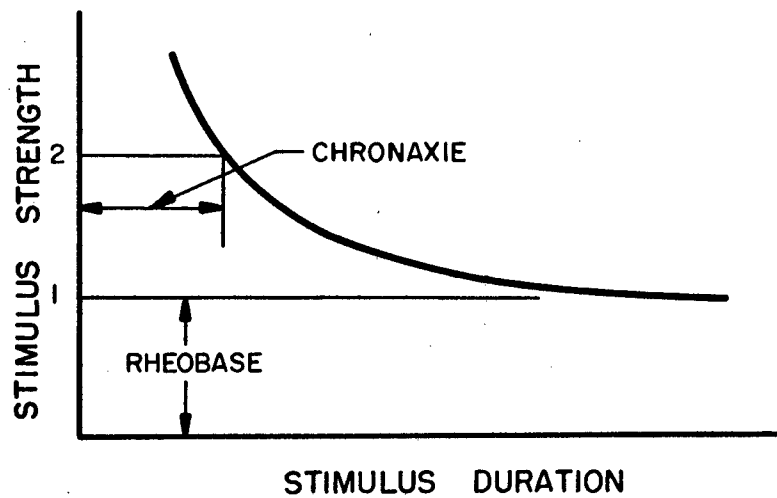
FIG. III-1   STRENGTH-DURATION   CURVE   OF
             EXCITATION
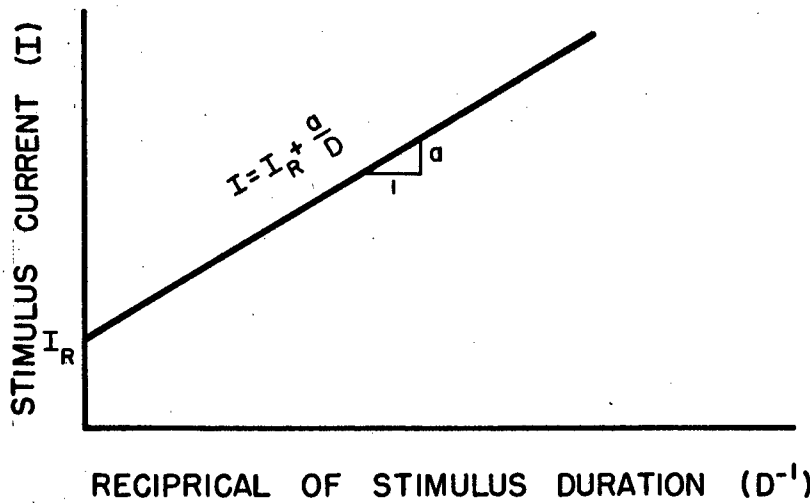
FIG. III-2 STRENGTH - DURATION   CURVE
           PLOTTED   ON   COORDINATES   I   VS. D^{-1}

pulse duration which corresponds to a current of twice rheobase

as shown.

$$\text{chronaxie} = D \Big|_{I \text{ or } V = 2 \times \text{Rheobase}} \qquad \text{(III. 1)}$$

Slightly different values for chronaxie are obtained depend-

ing upon whether voltage or current stimulation is employed. The

first attempt to mathematically model the S-D curve was to

assume that the curve was a hyperbola in the first quadrant given

by the equation:

$$(I \text{ or } V) \, D = \text{constant} \qquad \text{(III. 2)}$$

If we consider the current stimulus, this is equivalent to assuming

that the axon behaves as a pure capacitance and that excitation is

purely a function of the impressed electrical charge, i.e.,

$$Q = \int_0^D I \, dt = ID = \text{constant} \qquad \text{(III. 3)}$$

It is clear, however, that this equation which may represent the

experimental curve within certain ranges does not hold for large D

since the experimental curve is asymptotic to the rheobase, not

the zero stimulus axis.   A better approximation therefore is the

equation:

$$(I-I_R) \, D \; = \; constant \qquad\qquad (III.4)$$

where I_R = rheobase current.

This equation was first proposed by Weiss in 1901 in the

form:

$$I \; = \; I_R + \frac{a}{D} \qquad\qquad (III.5)$$

Obtaining the value of "I_R" from the experimental results is quite

straightforward.   The value of "a" may also be obtained quite

easily from the S-D curve by noting that when the stimulating

current is set equal to $2I_R$, the pulse duration (chronaxie) is given

by:

$$D \; = \; \frac{a}{I_R} \qquad\qquad (III.6)$$

This procedure for evaluating the constants in Equation

(III.6), however, gives no indication of the goodness of fit of this

equation to the data points unless some theoretical points are also

plotted and compared. A simpler way of evaluating the constants and observing the goodness of fit is to plot the data on the coordinates I vs 1/D (Figure III-2). On these coordinates the data points should fall on a straight line with vertical intercept "I_R" and slope "a".

In some instances the data points may be adequately described by Equation (III.6), but many times the data points do not fall on a straight line. A closer fit in these instances can be obtained by a more general equation of the form:

$$I = I_R + \frac{a}{D^b} \qquad \text{(III. 7)}$$

The three parameters (I_R, a, and b) may be evaluated by first of all manipulating the equation:

$$I - I_R = \frac{a}{D^b} \qquad \text{(III. 8)}$$

$$\log (I - I_R) = \log a - b \log D \qquad \text{(III. 9)}$$

This is the equation of a straight line on a log-log plot (Figure III-3). The value "b" is the slope of the line.
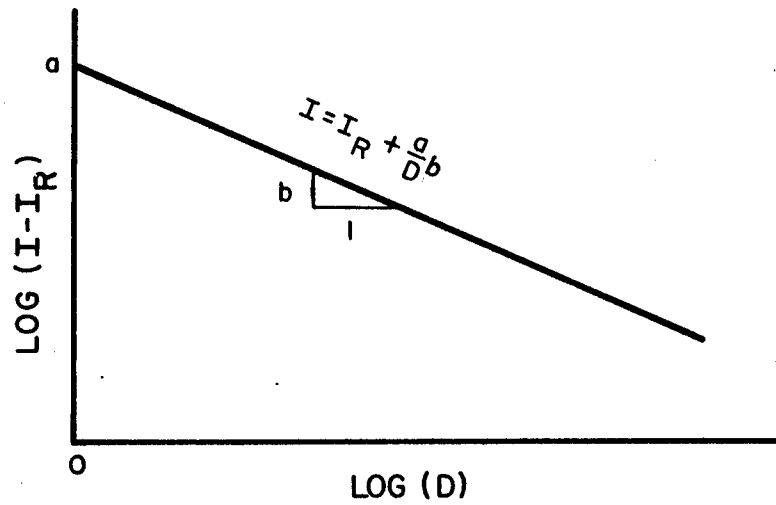
FIG. III-3. STRENGTH-DURATION CURVE PLOTTED ON
LOG-LOG COORDINATES.
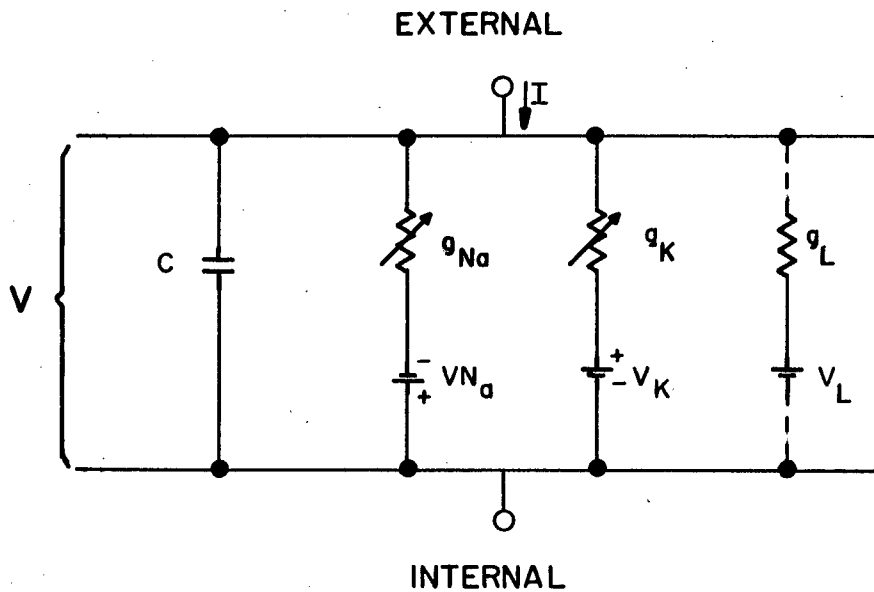
FIG. III-4. HODGKIN-HUXLEY MODEL OF SQUID
AXON MEMBRANE.

$$b = \frac{\Delta y}{\Delta x} \cdot \frac{m_x}{m_y} \qquad \text{(III.10)}$$

why Δy and Δx are linear dimensions, and m_x and m_y are the scale moduli of the log scales (i.e., linear dimension of one cycle).

The parameter "a" is evaluated by noting that at $D = 1$, $\log D = 0$, and

$$\log (I - I_R) = \log a \qquad \text{(III.11)}$$

$$I - I_R = a \qquad \text{(III.12)}$$

A better fit can be obtained to the experimental data using this equation since it is more general. What this approach lacks, however, is any physiological basis. It is a pure curve fitting technique with some vague relation to electric charge.

A different approach to describing the S-D curve was attempted first of all by Blair and later refined by Rashevsky.[50] In this approach the S-D curve was synthesized by considerations of ion migrations. They assumed that there was some leakage of ions from the area of stimulation as well as ion buildup.

Continuing with our electrical analogy this is equivalent to a

parallel combination of a resistance and capacitance. We can de-

scribe the physiological basis for this assumed model if we ex-

amine the single axon. The functional model for the squid axon

developed by Hodgkin and Huxley[48] is shown in Figure III-4.

The model is characterized by a transmembrane capacitance (C)

in parallel with variable conductances for the ions sodium,

potassium (g_{Na}, g_K) and a leakage conductance (g_L). In addition

the conductances are biased as indicated by the sources $(V_{Na}, V_K,$

$V_L)$. When the axon is stimulated, several electrochemical events

transpire which result in the production of an action potential.

That is, when the transmembrane voltage exceeds a threshold

value, the membrane depolarizes, thereby raising the conductances

of the sodium and potassium ions. There is then a rapid influx of

sodium ions followed by an efflux of potassium ions which pro-

duces an action potential. The action potential then propagates

down the axon as ions are exchanged along its total length.

An action potential will be generated if the transmembrane

voltage V reaches a threshold value V_T. If a step change in

current is applied to the model, the transmembrane voltage will

change in the manner shown in Figure III-5. For this positive

change in current, stimulation will occur at the cathode. The time
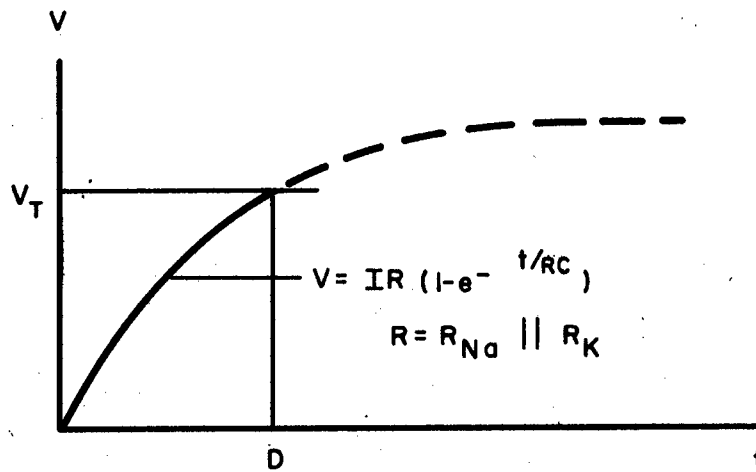
FIG. III - 5 TRANSMEMBRANE VOLTAGE DUE TO
CURRENT STIMULUS
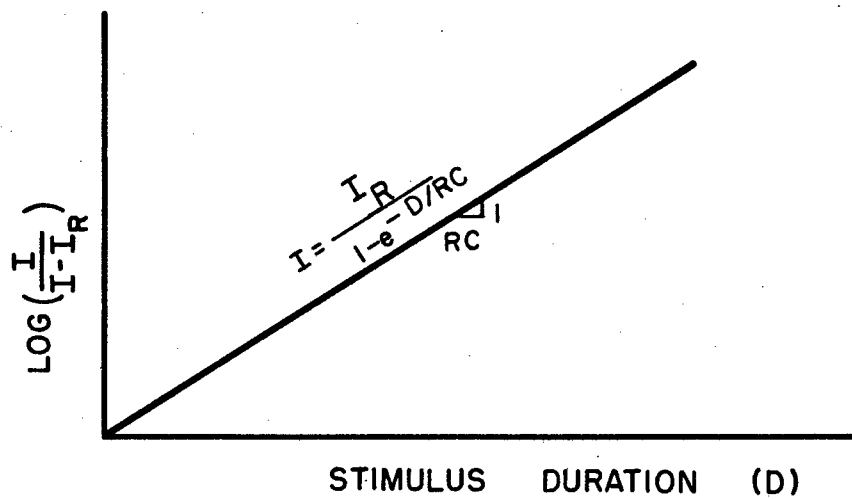
FIG. III - 6 STRENGTH DURATION CURVE PLOTTED
ON SEMI-LOG COORDINATES

at which this occurs (D) is the shortest time that the stimulus must be on for an action potential to be generated. These values of I and D therefore are a point on the S-D curve for the model. We now have all the information we need to synthesize the S-D curve of the model. To find the rheobase current (I_R) we note that for very large D the requirement for stimulation is

$$I_R R - V = V_T \tag{III.13}$$

$$I_R = \frac{V_T + V}{R} \tag{III.14}$$

where

$$R = \frac{1}{g_{Na} \times g_K}$$

the remaining portion of the curve is given by:

$$V_T = IR(1-e^{-D/RC}) - V \tag{III.15}$$

$$I(1-e^{-D/RC}) = \frac{V_T + V}{R} = I_R \tag{III.16}$$

$$\frac{I}{I_R} = \frac{1}{1-e^{-D/RC}} \tag{III.17}$$

It would be rather difficult to fit experimental data points to conform to this equation in its present form.

Rearranging:

$$\frac{I_R}{I} = 1 - e^{-D/RC} \qquad\qquad (III.18)$$

$$\frac{I - I_R}{I} = e^{-D/RC} \qquad\qquad (III.19)$$

$$\frac{I}{I - I_R} = e^{D/RC} \qquad\qquad (III.20)$$

$$\log\left(\frac{I}{I - I_R}\right) = D/RC \qquad\qquad (III.21)$$

If the data points are now plotted on a semi-logarithmic plot (Figure III-6), they should lie on a straight line with a slope $1/RC = 1/\tau$ where τ is the time constant of the membrane. This equation for the S-D curve fits the experimental data as well as, or better than, the previously derived expressions and is to be preferred since it has some physiological significance.

1. Effect of Using Surface Electrodes

The discussion thus far has been limited to transmembrane stimulation of a single axon. This thesis, however, is concerned with the gross mechanical response of muscle due to an electrical stimulus applied to the surface of the skin. Exactly how such a stimulus causes membrane depolarization is unknown. Lane and Zebo[35] have investigated the electric field distribution in a stimulated cat limb in an effort to determine if this quality of the stimulus is responsible for the induced contraction. Among their findings is the fact that most of the voltage drop occurs within the skin just beneath the stimulating "cathode" electrode. Furthermore, this cathodal field distribution is relatively unaffected by variations in the placement of a larger "anode" electrode. They are currently investigating the theory that the gradient of the electric field along the length of a fiber is responsible for its depolarization. Precise knowledge of the complex electrophysiologic events which transpire within a stimulated limb would indeed be of interest. Such knowledge, although it may be of great value in determining optimal stimulation schemes, especially with implanted electrodes, is not completely necessary in order to control the contraction of skeletal muscle by means of surface electrodes.

There are certain critical questions concerning surface electrical stimulation which were answered by means of simple experiments. It is generally known that muscle fibers have a much larger chronaxie than do nerve fibers. Lane and Zebo, by injecting curare, were able to block motor end plate transmission and thereby obtain strength duration curves for muscle. Muscle was found to have a chronaxie of about 2.0 ms. whereas the chronaxie of nerve is about 0.2 ms. When a strength-duration curve is plotted for a normal muscle, the chronaxie value conforms to that of nerve. For this reason then we can assume that surface electrical stimulation produces contraction primarily by depolarizing nerve, although some muscle fibers are probably also stimulated directly.

As we have seen in Chapter II, the motor nerve is composed of many sizes of fibers both afferent and efferent which have different functions. Most numerous among these fibers are the α motor neurons. Is it not possible, however, that the γ fibers are also innervated by the electrical stimulus thereby activating the reflex loop? This is believed not to be the case for several reasons. First of all, the threshold of the larger α fiber is much lower than that of the γ fiber. The γ fiber therefore requires a stronger stimulus in order to fire. Even if a γ fiber

were activated along with several α fibers, what would be the consequences? Let us first of all consider a twitch contraction. Since the muscle spindle produces negligible tension, the peak of the twitch will remain unchanged due to spindle contraction, but the spindle may emit a burst of action potentials since the γ innervation is interpreted as a command to shorten. This burst would then follow the reflex loop and cause a second twitch of lesser magnitude. An experiment under the author's direction was performed by J. Anderson, master's student, on a cat to determine whether the reflex loop was acting during stimulation. He measured tension of the gastrocnemius muscle of the cat during stimulation of its motor nerve. A twitch contraction was recorded with the nerve intact. The experiment was repeated after the motor nerve was cut proximal from the stimulating electrodes. There was no observable difference between the two records. The conclusion was drawn from the above experiments that surface stimulation innervates primarily the α motor neurons of the stimulated muscle.

3.   Clinical Significance of Strength-duration Curve

A standard diagnostic measure of the physical condition of a skeletal muscle is the strength-duration curve as obtained by surface electrical stimulation. In practice, the clinician places a

small, saline-soaked cathode over the "motor point" of the muscle.
The motor point is here defined as that area on the surface of the
skin which, when stimulated, produces the greatest contraction.
Of course, the location of this point depends on the position of the
limb. A large reference "anode" is placed elsewhere on the body
to complete the electrical circuit. The clinician then systemati-
cally increases the stimulus amplitude (voltage or current) and
duration until he observes the least perceptible muscle twitch and
records points on an S-D curve. From this curve he can then tell
whether the muscle is normally innervated or has an upper or lower
motor neuron lesion. Also, if he continues to record S-D curves
for a period of time he can tell if the muscle is undergoing the
"reaction of degeneration". The criterion used for these judgments
is the fact that muscle has a much larger chronaxie than nerve.
Since nerve has a lower threshold to electrical stimulation than
does muscle; when stimulation is applied to the limb the intact
nerve will fire and cause the muscle to contract. The S-D curve in
this case is that of nerve. If, on the other hand, the muscle has a
lower motor neuron lesion, the motor nerve cannot be excited and
the S-D curve obtained in this case is that of muscle. During the
reaction of degeneration the S-D curve is observed to shift to the
right and upwards, and many times takes on bizarre forms which

indicate that it is not wholly due to nerve or muscle, but a combination of both.[38]

B. THE ELECTRICAL STIMULUS

1. Discomfort Due to Stimulation

Many electrical waveforms repetitively applied to a motor nerve or muscle will cause the muscle to contract. An early phase of our research was to determine which of the many possible waveforms was "the best." There were two criteria to be satisfied; patient comfort, trauma was to be kept to a minimum, and minimum expended energy especially if a portable stimulator is ever to be realized. The response to the four different waveforms shown in Figure III-7 were investigated by Vodovnik, et al.[72] Waveforms a (sine wave) and b (alternating pulses) are alternating currents whereas c (rectangular pulses) and d (exponential pulses) have a single polarity, i.e., direct currents. Four normal female and six normal male subjects were stimulated by placing a reference electrode, size 3 x 5 inches, over the biceps and an "active" cathode electrode, size 3/4 x 1-1/4 inches, over the motor point of the extensor digitorum communries. The hand of the subject was placed in a relaxed position on a table and the stimulus was increased until the finger tips were lifted two inches above the surface of the table. Then the stimulus which caused this movement was
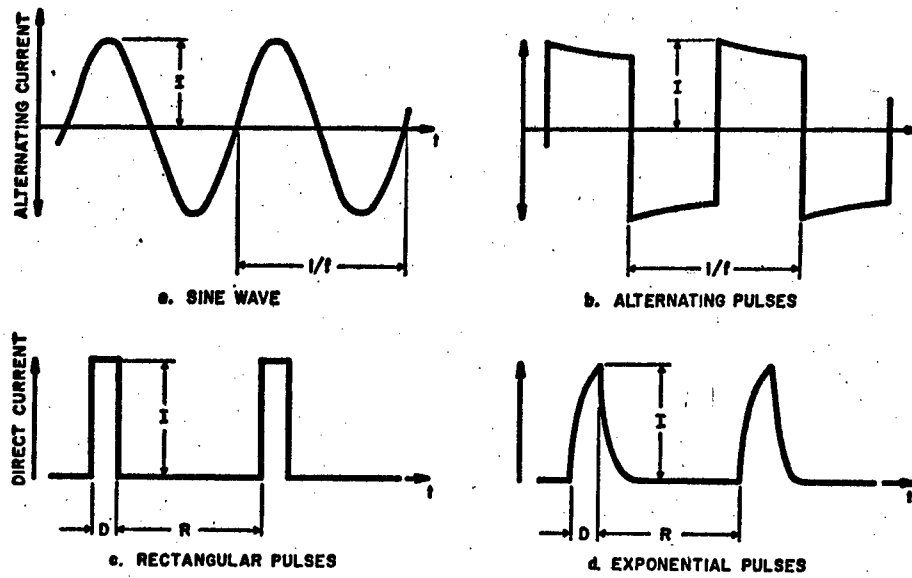
FIG. III-7. WAVEFORMS OF STIMULATION.
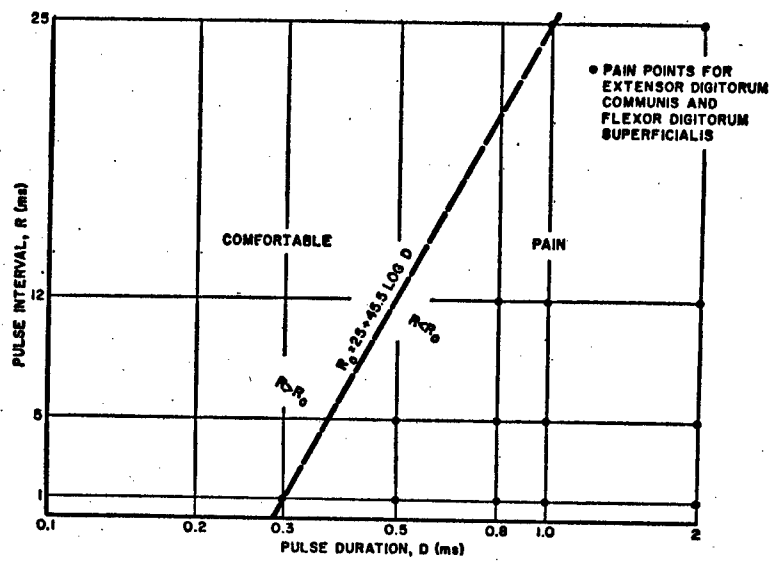
FIG. III-8. PAIN BOUNDARY FOR PULSED DC STIMULI.

recorded.　When the subject expressed a feeling of pain or much discomfort, the experiment was stopped and the values of the stimulus were labeled "pain point."

For the AC stimuli, the range of frequencies investigated was 20 to 3000 cps.　It was found that for frequencies above 300 cps, the AC square pulses were comfortable whereas for frequencies below 300 cps the stimulus was painful.　For the sinusoidal stimulus, the pain point occurred at 500 cps.

For the DC stimuli, there was no difference observed between the rectangular and exponential pulses.　Unlike the AC stimuli which can be characterized by two parameters (amplitude and frequency), the DC pulses require three parameters to describe them (amplitude, pulse duration, and pulse interval).　The dotted line in Figure III-8 represents the locus of pain points for the DC pulses.　The area to the left of the dotted line represents the combination of acceptable parameters.

$$R \; < \; 25 + 45.5 \log D \qquad\qquad (III.22)$$

Comparing the AC and DC stimuli, it seems that one is no more painful than the other; however, the DC pulses require about one percent of the power required for the AC stimuli for the same

contraction. It was, therefore, decided to investigate more completely the DC rectangular pulse type of stimulus. That is, we were interested in determining the effects of changing the pulsed DC stimulus parameters on the muscle contraction.

2. Constant Current versus Constant
Voltage Stimulation

There are two classes of stimulators in general use; the so-called constant voltage stimulator and the constant current stimulator. Before an intelligent choice can be made, the impedance of the load must be considered; the load being two electrodes in contact with the body. Figure III-9a shows a typical record of the voltage between two surface electrodes in the presence of a constant current rectangular pulse of 10 ma. and 0.2 msec. duration. The voltage trace is characterized by an exponential rise and fall. An electrical circuit model which has the same response consists of a resistor (R_1) in series with a parallel combination of a resistor (R_2) and a capacitor (C). This lumped parameter model, of course, includes the interface impedance between electrode and skin. By curve fitting techniques the following values were determined from Figure III-9.

$$R_1 = 200 \; \Omega$$

$$R_2 = 2 \, K$$

$$C = .05 \, uf$$
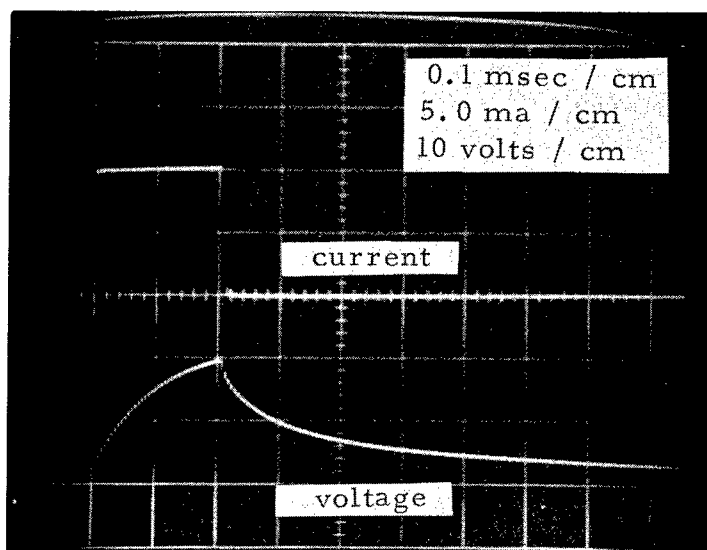
a) constant current
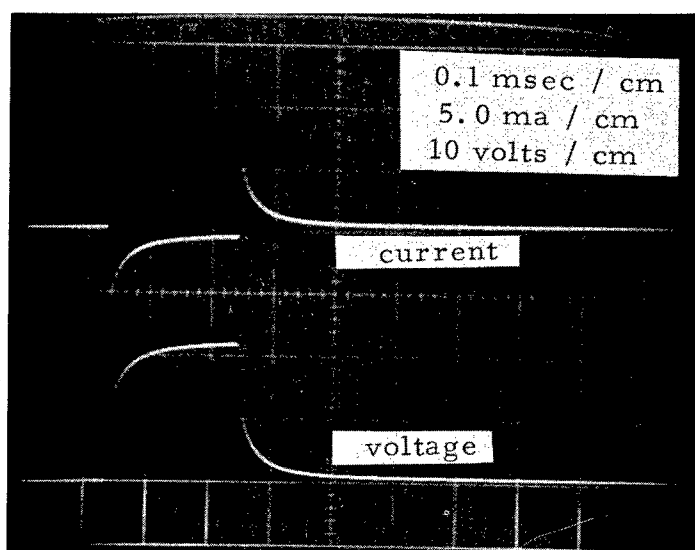
b) pseudo-constant voltage

FIG. III-9. ELECTRODE VOLTAGE AND CURRENT
DUE TO RECTANGULAR PULSE.

In the above case the maximum value of the applied voltage was 20 volts. In order for a constant voltage stimulator to apply a constant voltage pulse of 20 volts to the same electrodes requires that the initial current be:

$$I\Big|_{t=0} = \frac{V}{R_I} = \frac{20}{200} = .1 \text{ amp} \qquad (\text{III}.23)$$

Clearly then a constant voltage stimulator will not deliver a square voltage pulse to the surface electrodes unless prohibitive currents are used. Figure III-9b shows the voltage and current traces of a so-called constant voltage stimulator. This does not mean to imply that voltage stimulation is not as effective as current stimulation. An advantage of constant current stimulation is simply that it is realizable using surface electrodes whereas true constant voltage stimulation is not unless excessively large currents are supplied. A further advantage of constant current stimulation is the fact that changes in electrode impedance do not affect the current through the electrodes. In voltage stimulation, changing electrode impedance, whether due to electrodes drying out or shifting, affects the amount of voltage that is actually applied to the skin. All the following experiments were therefore performed using a constant current stimulator.

A current driver circuit was added to the output of a commercial voltage stimulator. This unit was designed to operate as a source of constant current rectangular pulses whose frequency and duration is determined by the voltage stimulator. Provision was also made so that the amplitude of the pulse train could be modulated by an externally applied signal. Figure III-10 is a schematic diagram of the current driver. For constant amplitude pulses the modulation input is shorted and the current level is set by the cathode variable resistor. The voltage stimulus input can swing from 0 to 250 volts, it is capable of turning the tube completely on or off. When on, the current is determined by the cathode variable resistor and/or the bias supply and the modulation input. The static output characteristics of the current driver are shown in Figure III-11. With this apparatus then it is possible to deliver to the stimulating electrodes: a constant current pulse with variable repetition rate, and a pulse train which can be amplitude modulated by a square, triangle or sine wave (Figure III-12a, b, c).

C. THE MOTOR POINT

The motor point has previously been described as a point on the surface of the skin overlying a muscle which, when stimulated, produces a greater contraction than any other point. This is admittedly a vague definition. Work was therefore undertaken to
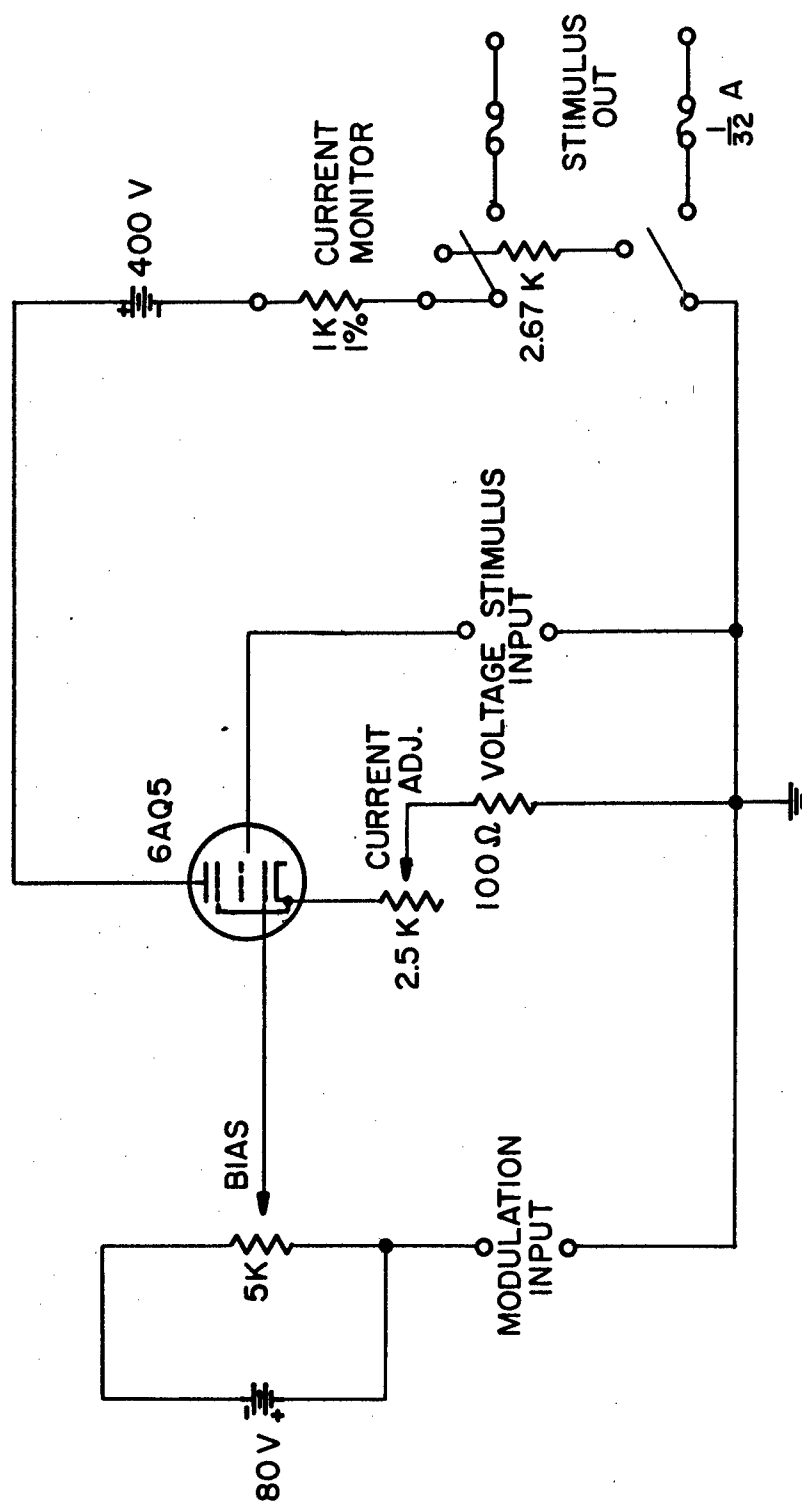
FIG. III-IO SCHEMATIC DIAGRAM OF CURRENT DRIVER

FIG. III-II. OUTPUT CURVES OF CURRENT DRIVER

JUNE 24, 1965

LOAD RESISTANCE

LOAD CURRENT
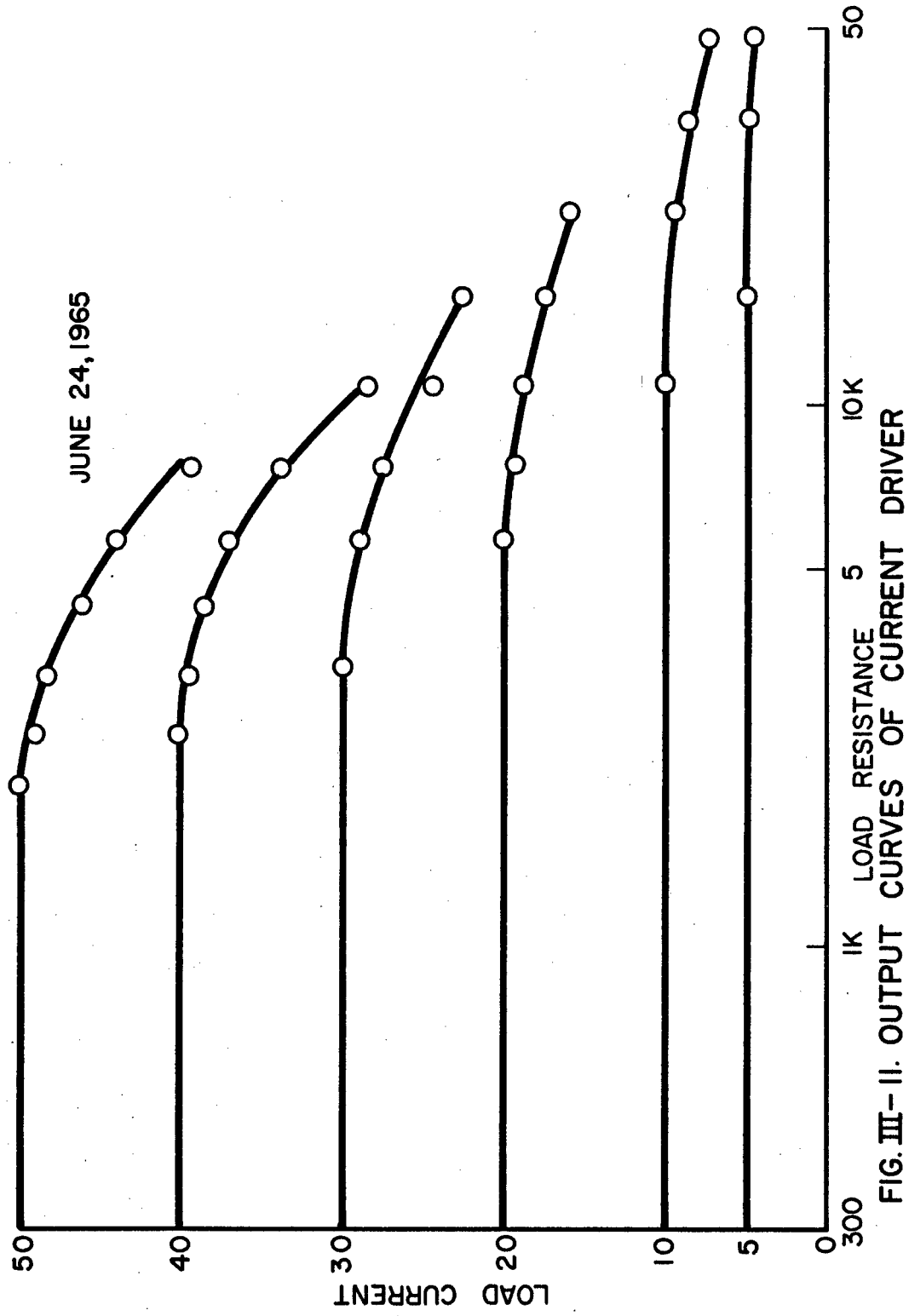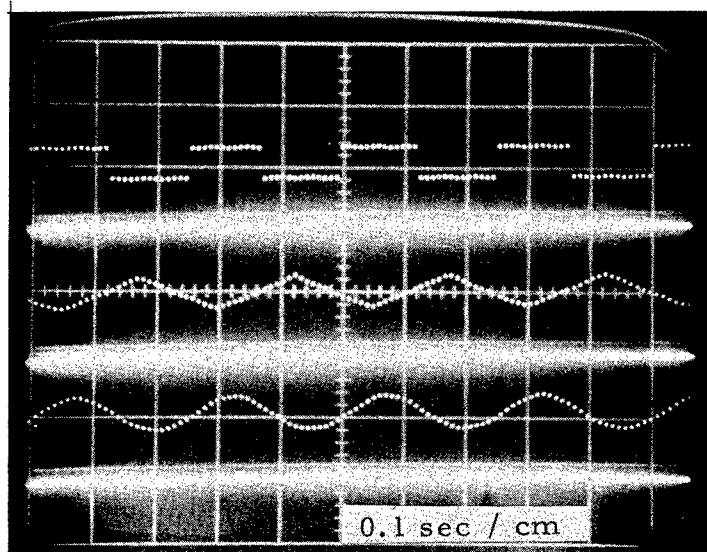
FIG. III-12. AMPLITUDE MODULATED CONSTANT CURRENT
STIMULI.

more precisely define the characteristics of a motor point.

1.   Experimental Equipment

An experimental apparatus was developed to investigate the motor points of the biceps and triceps of the arm.   This equipment, shown in Figure III-13 is actually more versatile and is more fully exploited in a later section of the thesis.   It was designed to hold the arm immobile in the horizontal plane at shoulder height.   The stimulus is applied via an electrode which is spring mounted on horizontal and vertical tracks allowing the stimulus to be precisely located over the surfaces of the upper arm.   The electrical path is completed by a neutral electrode held by the hand.   The elbow angle may be indexed in 5° increments by means of a rack and gear.   The torque developed by the stimulated muscle may then be recorded by means of strain gages placed on the cantiliver beam holding the rack.   If the rack is disengaged, the elbow is free to rotate and this angular movement may be recorded by means of a potentiometer on the end of the vertical shaft.   The first electrodes used on the project were the band-aid-snap type.   This electrode consists of a band-aid, a piece of aluminum foil, and a snap which joins the two and provides an electrical connector for application of a stimulus.   From experience it was found that this electrode could not be used directly on the skin for fear of burning the skin.

74
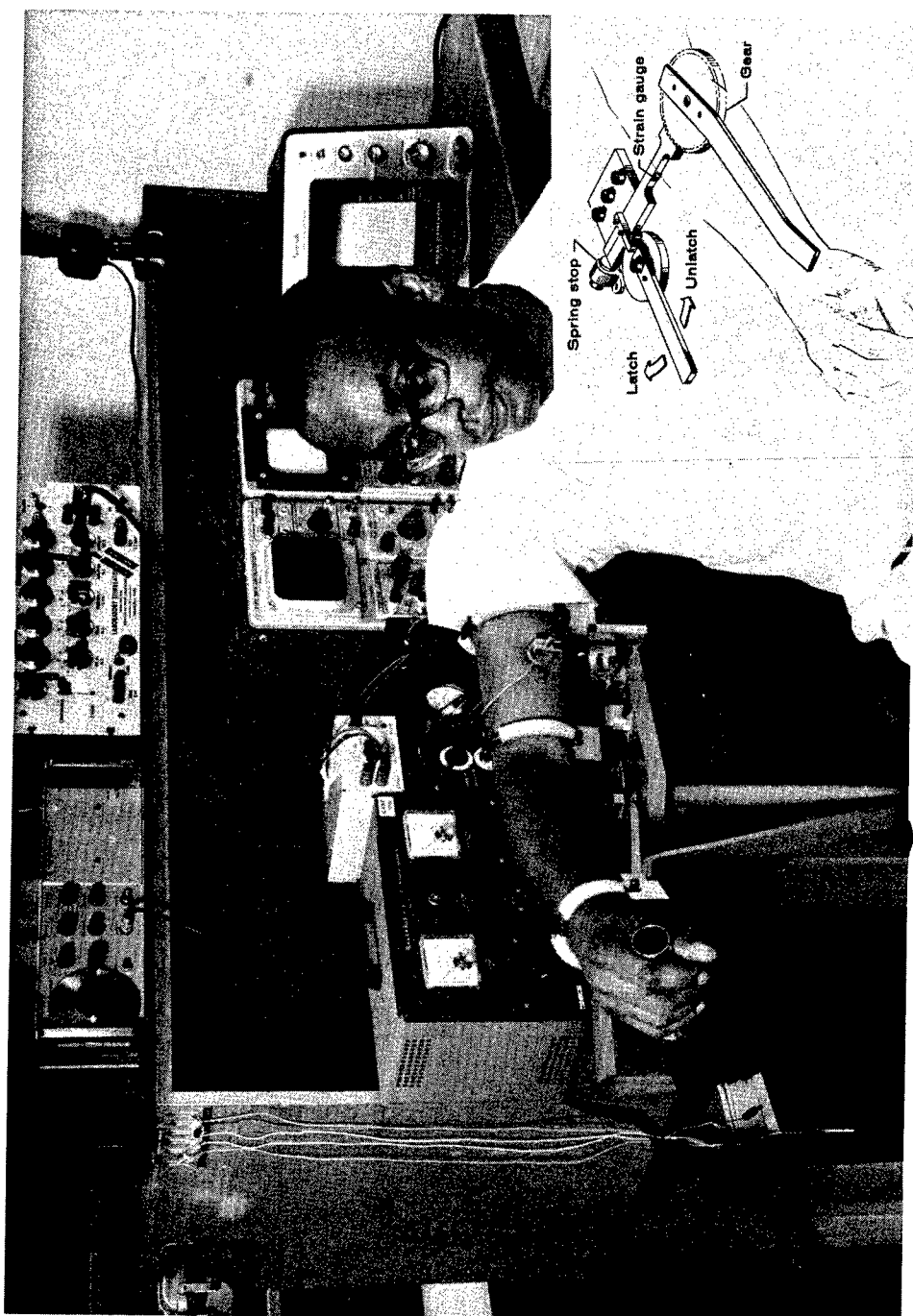
FIG. III-13. EXPERIMENTAL SETUP.

That is, unless the aluminum foil is coated with electrode paste and pressed dirmly on the skin maintaining a relatively constant impedance between the foil and the skin over the area of the foil, large current densities in isolated areas are possible which can actually burn the skin. An interface was provided between the foil and the skin by inserting a saline soaked gauze pad of the same size as the foil. This worked well except that sometimes during move-ment, the gauze pad would slip and cause the foil to come in con-tact with the skin and produce a burn. Also, the band-aid proved to be less than ideal for keeping a constant pressure between elec-trode and skin. A better electrode is shown in Figure III-14. The electrical lead is soldered to a copper disc and a felt pad (saturated in saline) is placed between the copper disc and the skin. Several electrodes of this type were made ranging in size from 3/8" dia-meter to 1" diameter in increments of 1/8". As greater accuracy became desirable the segmented electrode shown in Figure III-15 was developed. This consists of 9 electrically and mechanically isolated electrodes. The electrodes are made of felt strips 1/4" by 1 1/4" long and fit into teflon holders against conducting strips. Individual clock springs apply approximately equal pressure to each electrode segment thereby maintaining good electrode to skin contact even during muscle bulge.
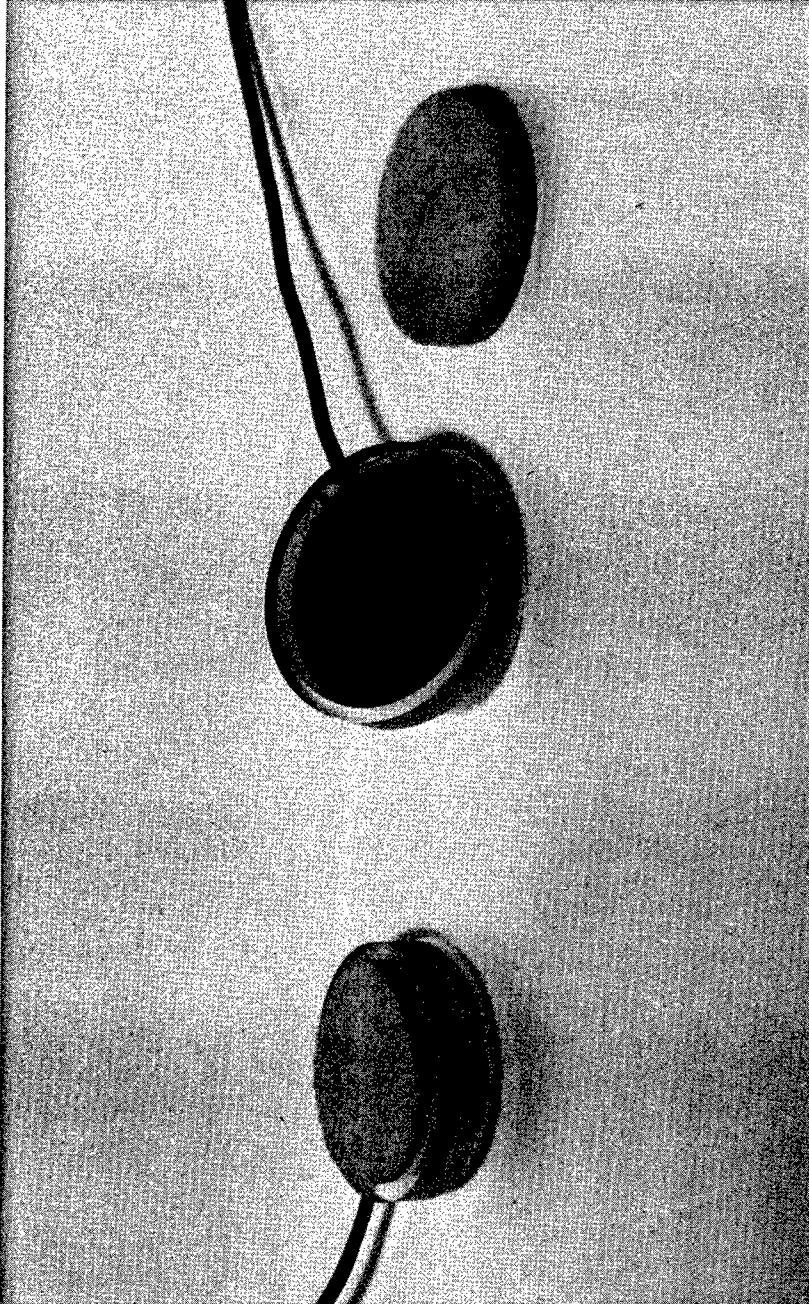
FIG. III-14. CIRCULAR STIMULATING ELECTRODE.
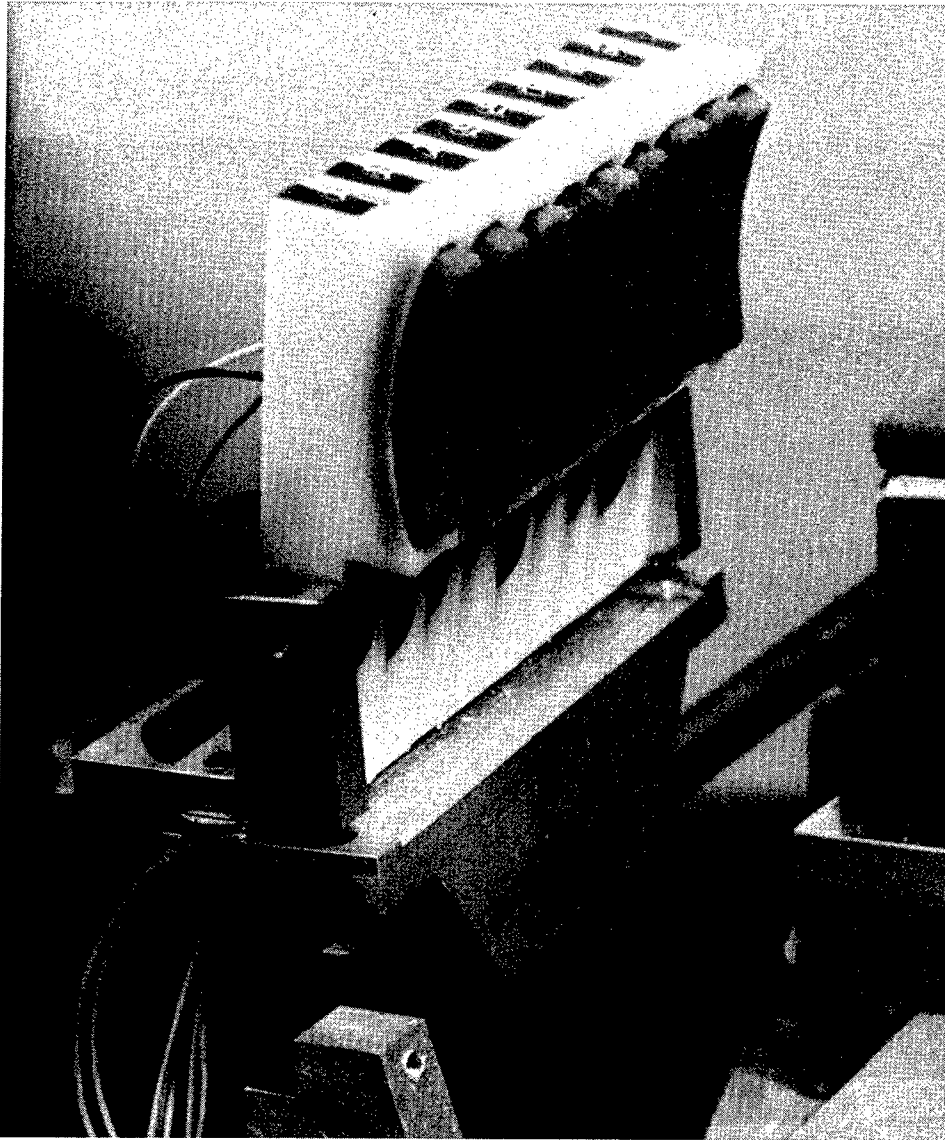
FIG. III-15. SEGMENTED ELECTRODE.

2. Size of a Motor Point

Will moving an electrode away from a motor point cause the torque to fall precipitiously or will it only decrease the torque a slight amount? The following experiment was designed to answer this question at least for biceps and triceps muscles. A 3/4" diameter electrode was placed over the muscle along a midline of the arm in increments of one centimeter, and a stimulus was applied at each location. During the experiment, the arm was held at 75° included angle and the torque about the elbow joint was recorded. The results of an experiment with the biceps muscle are shown in Figure III-16. Here three curves are shown representing three different current levels. Notice that the torque does not change greatly as the electrode is moved indicating that for the biceps muscle the motor point is not an easily defined point. The triceps, on the other hand, exhibits a very localized motor point. The lateral and medial heads of the triceps were investigated and it was found that electrode movement of less than a centimeter caused the torque to fall drastically. Typical torque values for stimulation at the motor points were: 2 ft-lbs for the medial head and 1.5 ft-lbs for the lateral head for a stimulus of 15 ma. 0.2 ms pulse duration and repetition rate of 50/sec.
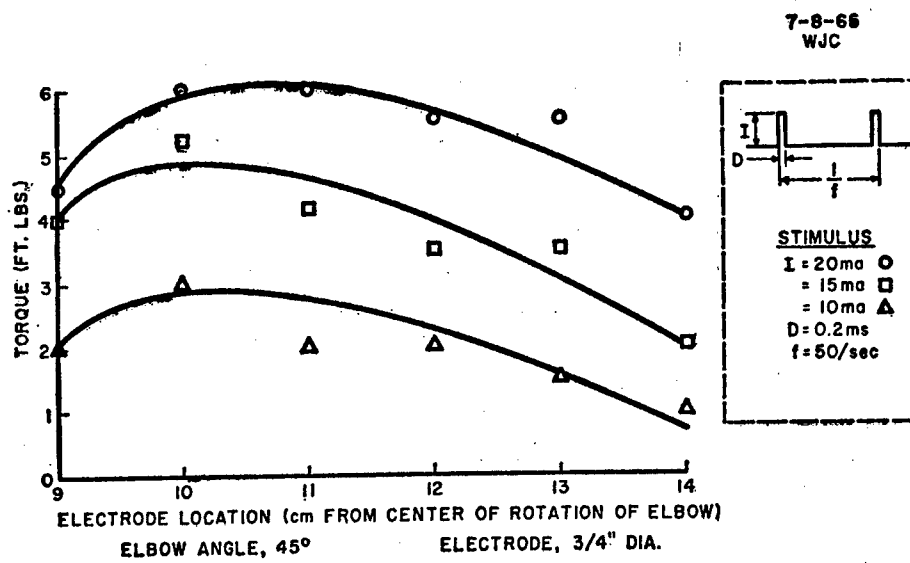
FIG. III-16. ELBOW TORQUE VS. ELECTRODE LOCATION.

3. Does the Motor Point Move?

Since the motor points of the triceps were so well defined, we were able to determine whether it remained in the same location or whether it moved as the elbow was flexed and extended. Figure III-17a, b show the results of experiments with each of the heads. The elbow angle was varied in fifteen degree increments while the motor points were stimulated at each angle and the location of the motor point was recorded. In Figure III-12a, we see that the motor point of the medial head has moved two centimeters as the elbow angle was varied between 45° and 90°. This excursion corresponds roughly to the $r\theta$ movement of the muscle as a function of elbow angle. That is, assuming that the muscle has a moment arm of 2.5 cm about the elbow joint, the excursion of the muscle would be:

$$r\theta = 2.5 \times \frac{\pi}{4} = 2 \text{cm} \qquad \text{(III.24)}$$

With the development of the segmented electrode, this experiment was performed more accurately on the biceps muscle of ten individuals. This was accomplished by indexing the arm every ten degrees. At each of these twelve positions the electrode segments were sequentially energized by operating the stimulator

8/20/65
SUBJ. W.C.
TRICEPS, MEDIAL HEAD
$I = 15$ ma
$D = 0.2$ ms
$f = 50/SEC$
$I'' = $ ELECTRODE
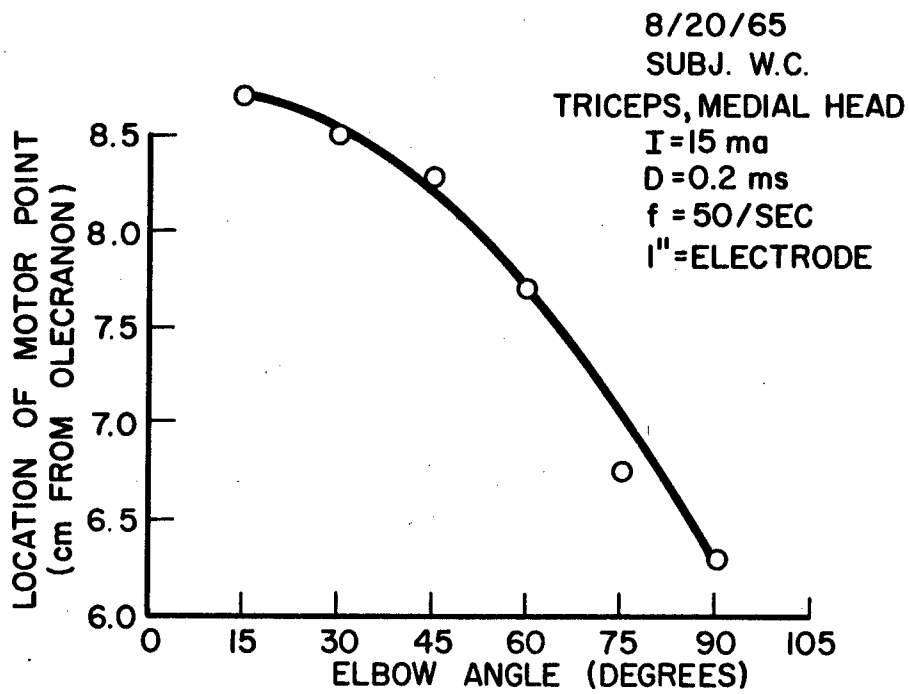
a) TRICEPS, MEDIAL HEAD
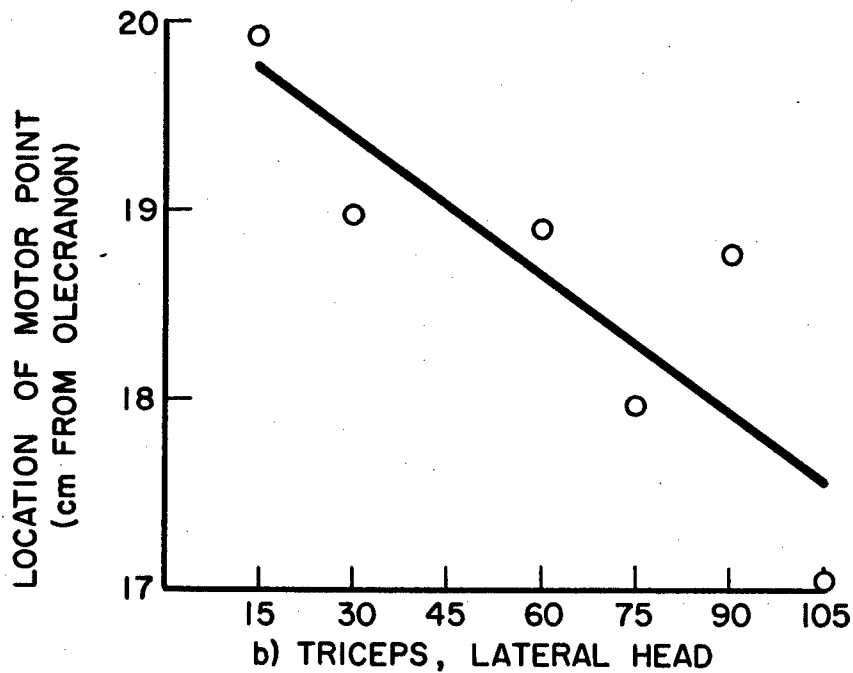
b) TRICEPS, LATERAL HEAD

FIG. III-17 LOCATION OF MOTOR POINT VS. ELBOW ANGLE

in the "trains" mode. Every second a train of six pulses (0.2 msec duration, 50/sec) was delivered by the stimulator. A manual switch was then operated between trains to direct the stimulus to the different electrode segments. Torque, stimulus and elbow angle were recorded continuously at each elbow angle. A typical record is shown in Figure III-18. The electrode which produces the largest twitch is said to be over the motor point. The maximum excursion of the motor point for the 110° of rotation was found to be .625 to 1.875 with an average value of 1.0 inch. Again this was found to correspond roughly to the $r\,\theta$ movement of the muscle.

4. Effect of Electrode Size

What is the optimal electrode size for surface stimulation? There were two criteria which can be used to determine an optimal electrode size. The first was patient comfort. A smaller electrode introduces a higher current density to the skin and causes more discomfort. On the other hand, what is the effect of electrode size on the elbow torque? With the arm held at 75°, the biceps was stimulated with electrodes varying in size from 3/8" to 1" in diameter in increments of 1/8". The results of a typical experiment are shown in Figure III-19a. The same experiment was repeated using the segmented electrodes. Here a much greater range in electrode areas was available: 5/16 in^2 to 2-13/16 in^2 as opposed
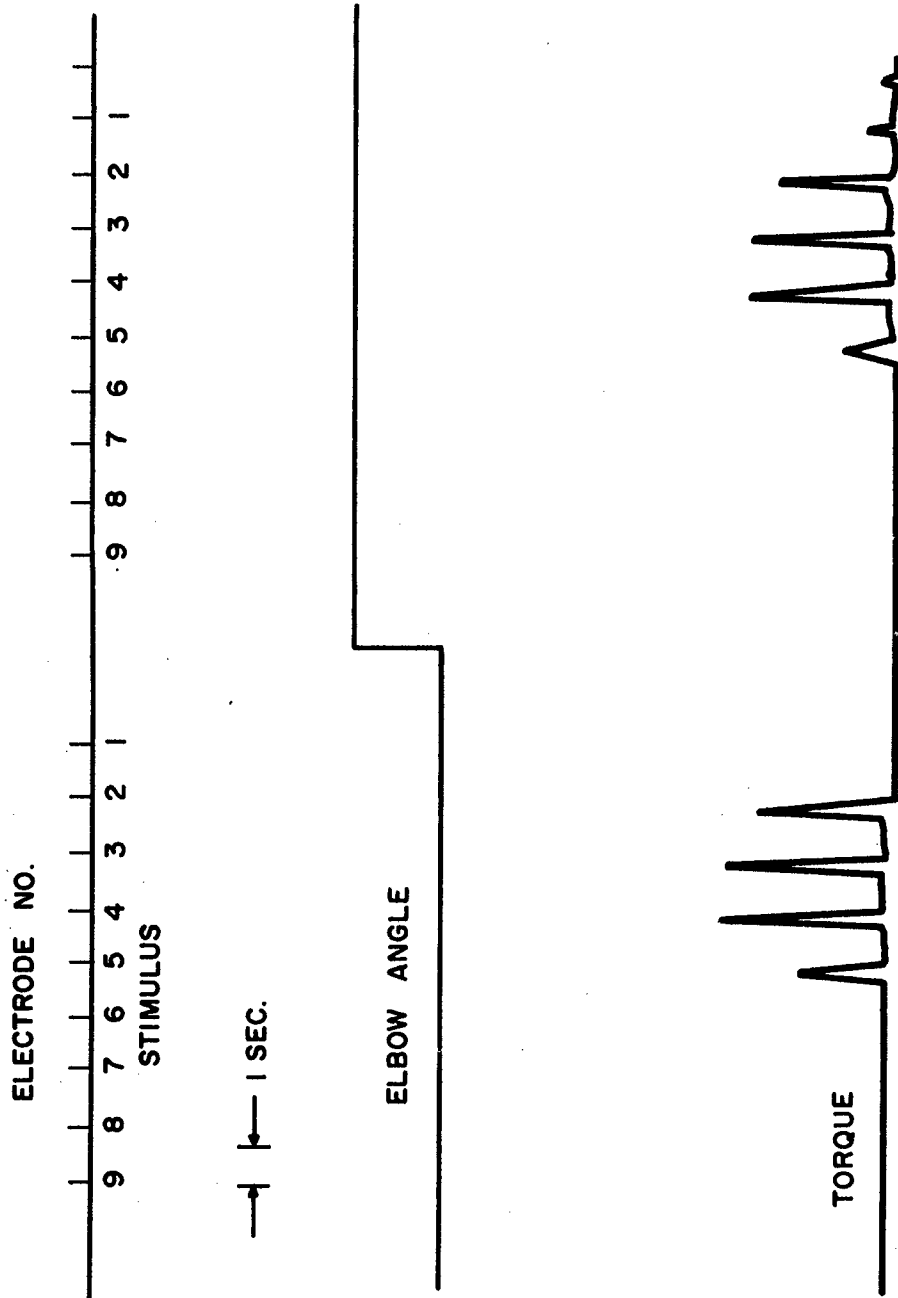
FIG. III-18 RELATIVE TORQUES DEVELOPED BY INNERVATING DIFFERENT ELECTRODES OVER BICEPS

8/12/65, P.C.
BICEPS
D=0.2 ms, f=50/SEC
ELBOW ANGLE=75°
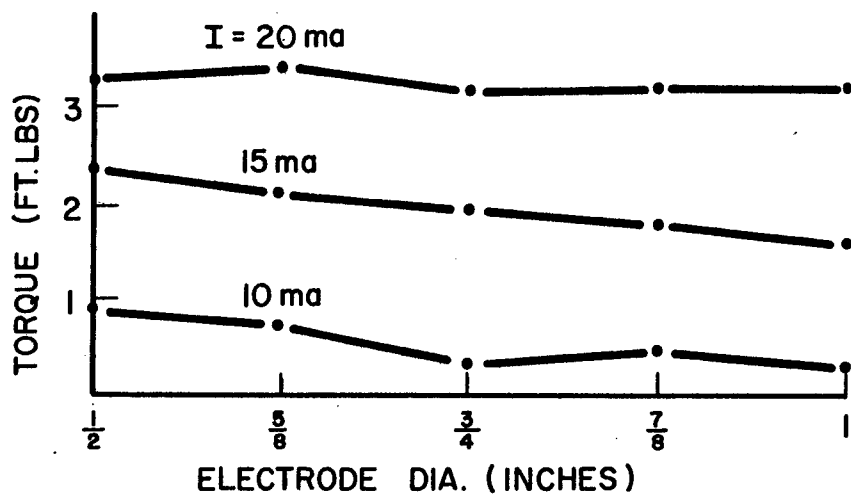
a) CIRCULAR ELECTRODES

1/3/67, J.L.
BICEPS
D=0.2ms, f=50/SEC
ELBOW ANGLE=75°
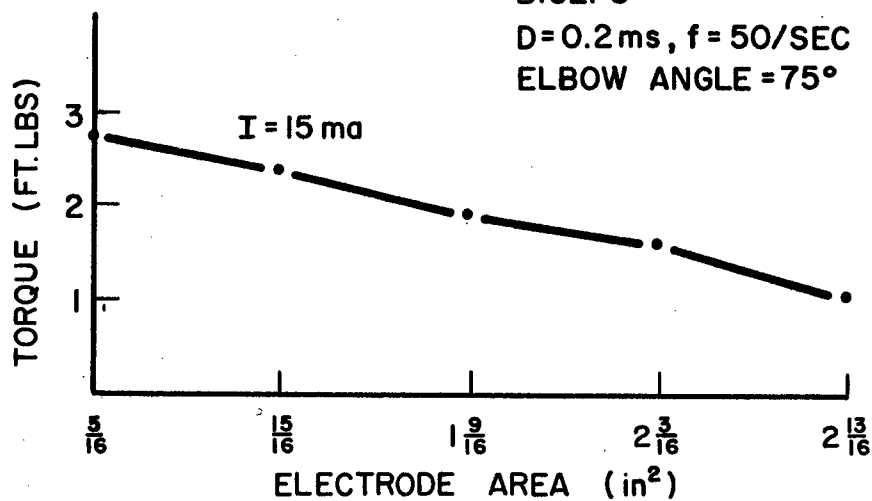
b) SEGMENTED ELECTRODE

FIG.III-19 ELECTRODE SIZE VS. TORQUE

to about 3/16 in^2 to 3/4 in^2 for the circular electrode. The result of this experiment is shown in Figure III-19b. The torque reduces by about sixty percent for a nine fold increase in electrode size.

Herein lies one of the basic problems involved in surface stimulator, viz., how to locate the stimulus over the motor point during a movement. This problem will be investigated in a later section.

D. MAGNITUDE OF ELBOW TORQUE AS A FUNCTION OF STIMULUS

1. Muscle Twitch

When a single supra-threshold pulse is applied to a motor point, the muscle contracts. If the muscle is not allowed to shorten externally the tension developed is called an isometric muscle twitch. The oscilloscope traces of Figure III-20 show a series of twitch contraction measured as torques about the elbow point. The biceps muscle was stimulated with a rectangular pulse of varying height which also triggered the oscilloscope trace. To arrive at some indication of the relative linearity of the system, several records of muscle twitch were made for different stimulus durations and amplitude. Figure III-21 shows the results of one series of such experiments where peak torque of the muscle twitch is plotted versus stimulus amplitude with pulse duration as the
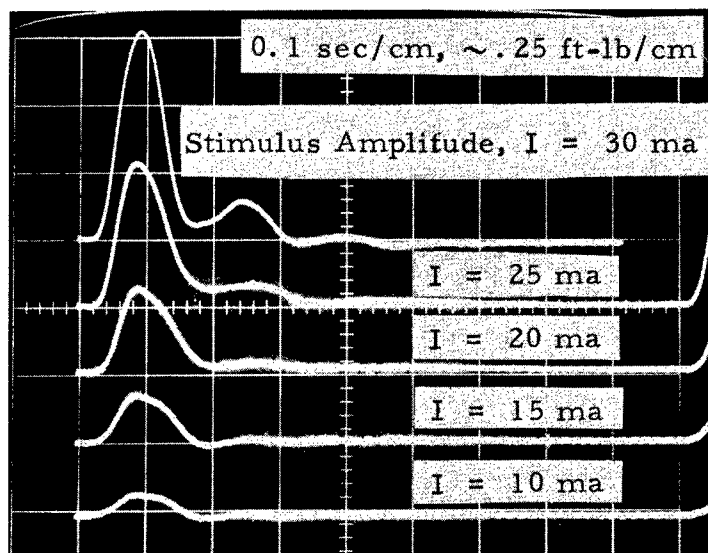
FIG. III-20. TWITCH CONTRACTIONS WITH
INCREASING CURRENT.

9/24/65
SUBJ. P. POOR
STIMULUS – SINGLE PULSE
ELECTRODE – I" DIA.

$T = (.25D + .03)(I - 10)$

□ D = 0.6 ms
○ = 0.4 ms
△ = 0.2 ms

STIMULUS AMPLITUDE, I (ma)

PEAK VALUE OF TWITCH (FT.LBS.)
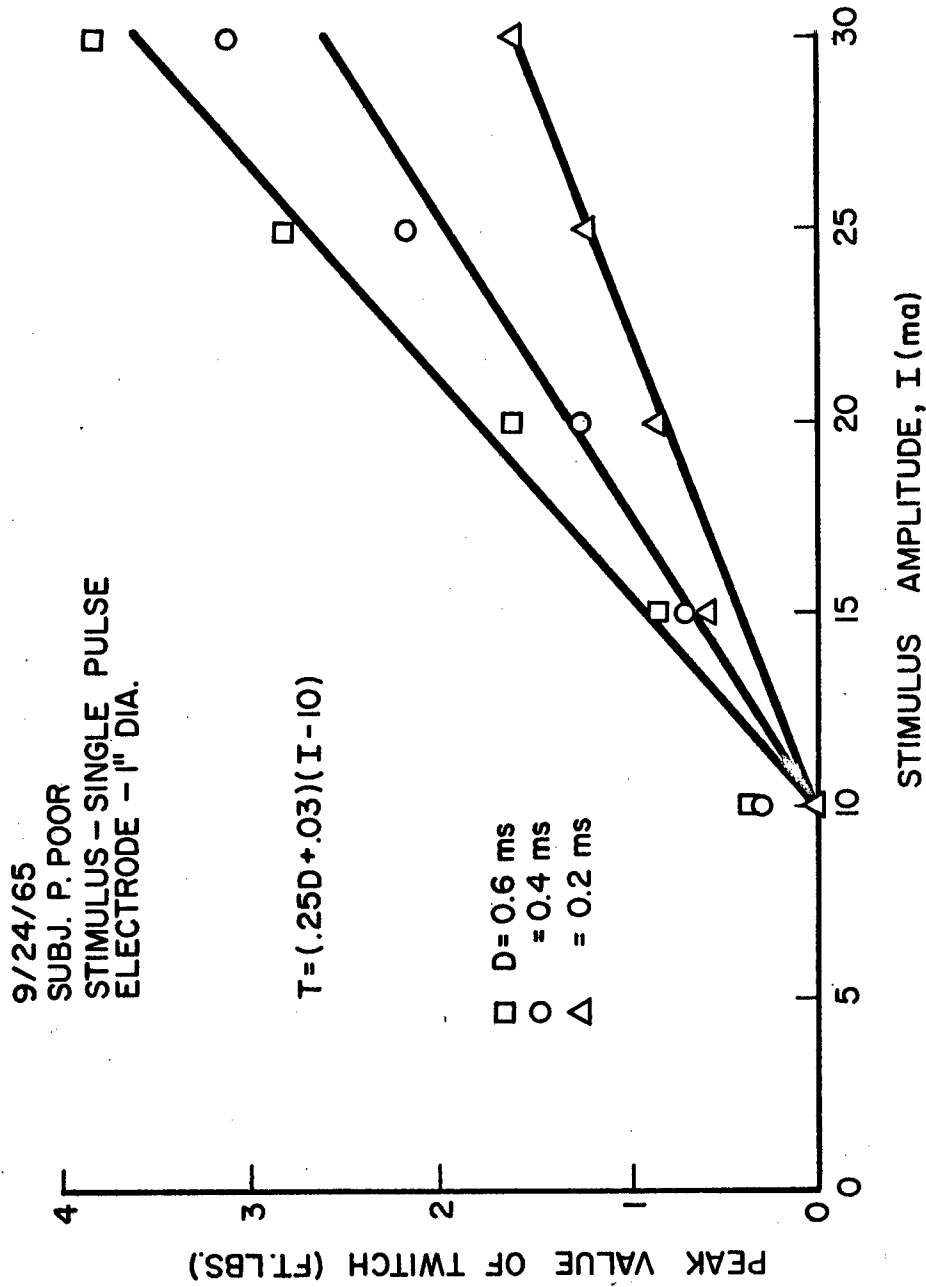
FIG III - 21 MAGNITUDE OF TWITCH VS. STIMULUS CURRENT, PARAMETER D

parameter. The curves all have a threshold nonlinearity; however, above this level the curves may be considered at least piecewise linear. A linearized approximation to these curves is also shown superimposed in Figure III-21. These straight lines are given by:

$$\text{Peak torque} = (.25D + .03)(I-10)\text{Ft-Lbs} \qquad (\text{III}.25)$$

2. Tetanic Contractions

If a muscle is stimulated by a succession of closely spaced pulses it is possible for the muscle to maintain a steady contraction. This is called a tetanic contraction. Figure III-22 shows a series of oscilloscope traces of tetanic contractions for different stimulus frequencies. The traces were triggered by the stimulus. Notice that the magnitude of the torque reaches a maximum value at a stimulus frequency of 60/sec. This can be seen more clearly in Figure III-23 which is a plot of tetanic torque versus the stimulus frequency with current as the parameter. For stimulus frequencies below 20/sec, the torque was a sequence of twitches and no readings were made. From 20 to 50/sec the average torque level increased but had some ripple of decreasing height. At about 50/sec the ripple was essentially gone and the torque reached its maximum value.
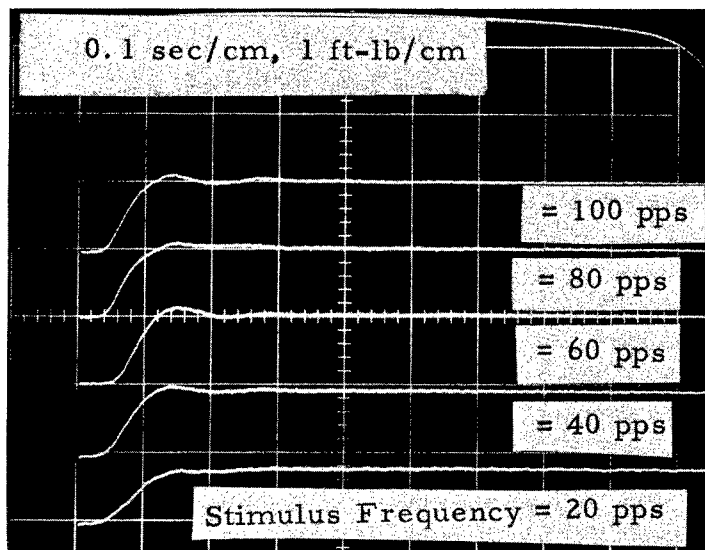
FIG. III-22. TETANIC CONTRACTION WITH
INCREASING FREQUENCY.
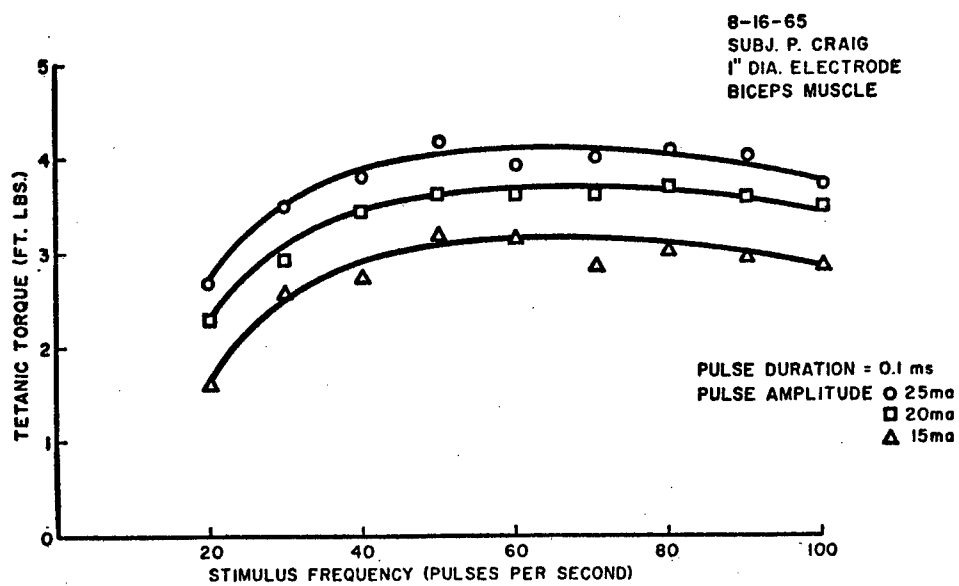
FIG. III-23. TETANIC TORQUE VS. STIMULUS FREQUENCY,
PARAMETER I.

To see exactly how the torque increased as a function of frequency between 20 and 50/sec, several more data points were obtained in this region. Typical results are shown in Figure III-24. The linearized approximations to the curves are given by:

$$\text{Torque} = (4 + \frac{f}{7}) \log \frac{I}{7.5} \qquad (\text{III}.26)$$

If muscle is stimulated at higher and higher frequencies a point is reached where the muscle cannot react to every pulse. That is, every other pulse will occur within the refractory period of the muscle and it will be unable to contract in response to this pulse. To find out at what frequency this occurs, the following experiment was performed on the biceps muscle. A train of two pulses (I = 15 ma, D = 0.4 ms) with variable spacing was applied to the muscle. Oscilloscope traces of the resulting twitches were photographed. For a pulse spacing of 200 ms (5/sec) the muscle produced two distinct twitches of equal height. As the pulse spacing was decreased the two twitches merged into a single twitch of greater than twice the magnitude of a single twitch. (Figure III-25). When the pulse spacing reached 4 msec, the torque began to decrease until at 2 msec (500/sec) the twitch was identical to that due to a single pulse. The biceps muscle therefore is unable to
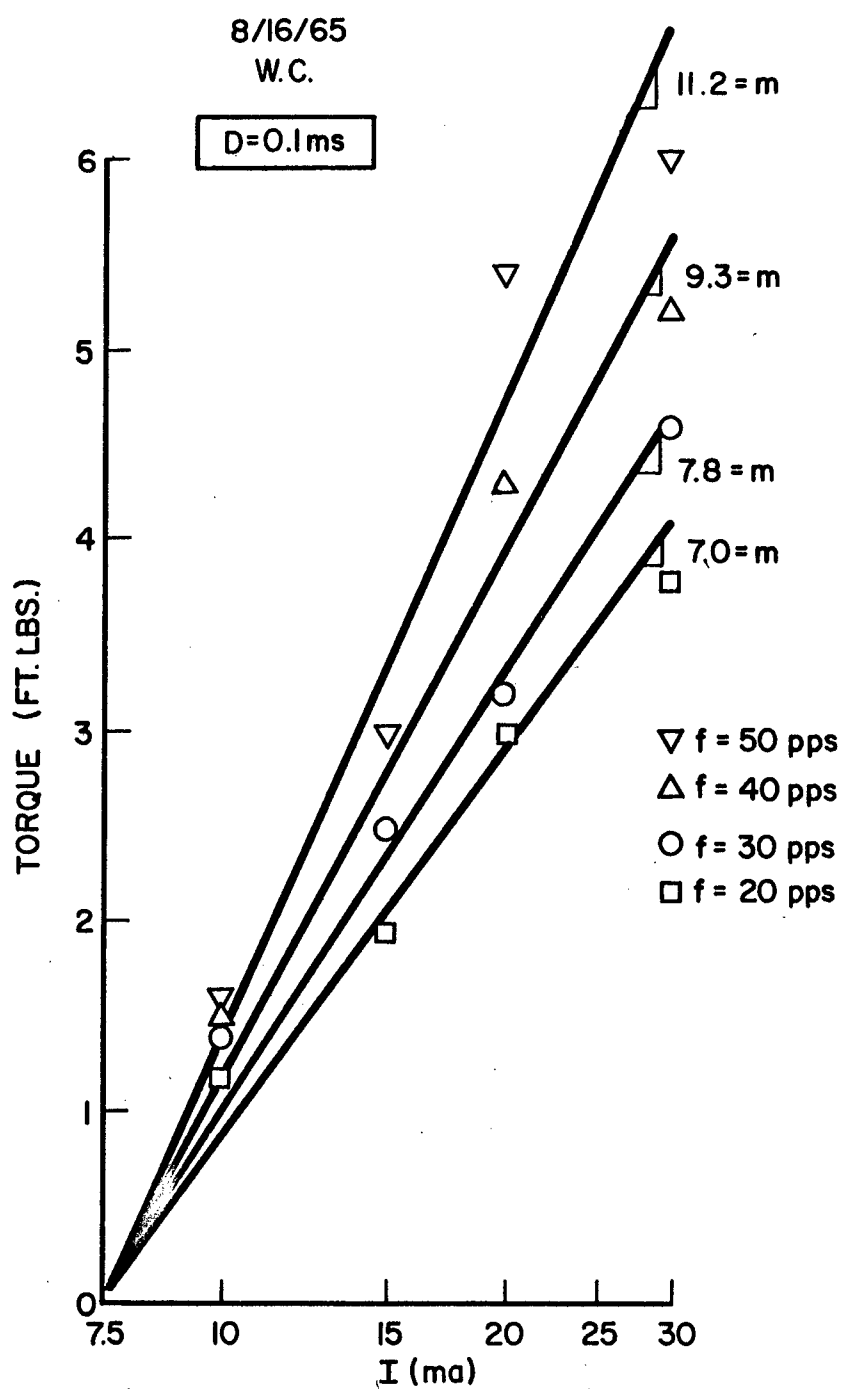
FIG. III - 24 TETANIC TORQUE VS. STIMULUS CURRENT,
PARAMETER f
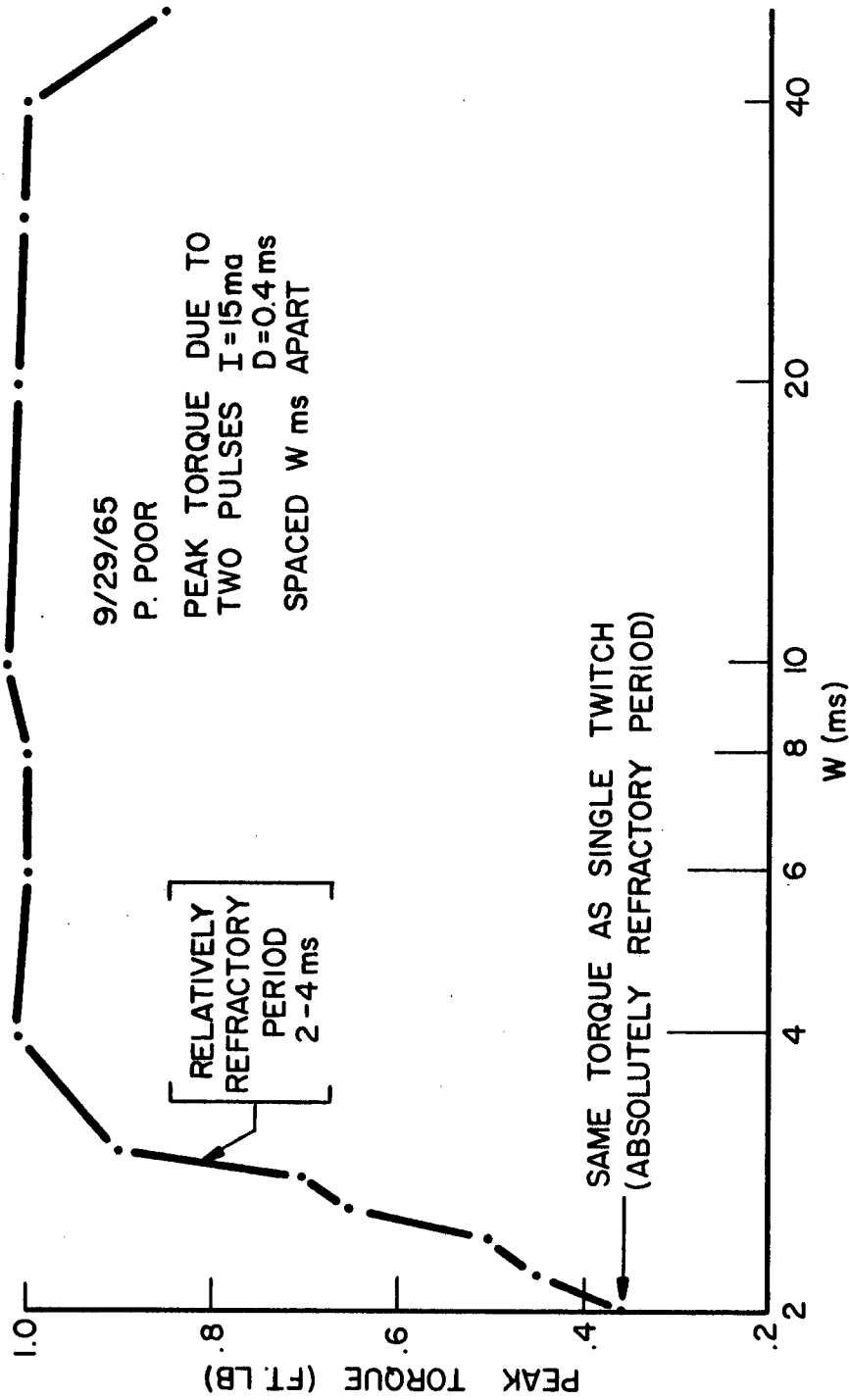
FIG. III - 25 PEAK TORQUE VS. PULSE INTERVAL

respond to a stimulus frequency of 500/sec and frequencies of this magnitude should be avoided. Also, since no greater torques are produced by frequencies above 50/sec (Figure III-23), this frequency is to be preferred at least from a functional viewpoint. Also at 50/sec the pulse interval, 20 msec, is in the comfortable range of stimulation (Figure III-8).

To see how the individual twitches at 50/sec add in a developing tetanus, the biceps was stimulated with first one pulse, then by two pulses space by 20 ms, then three, etc. The contractions were recorded each time and are shown superimposed in Figure III-26a. Figure III-26b shows the results of adding a sequence of twitches separated by 20 ms. indicating how the muscle would react if its behavior were linear. Aside from the fact that the tetanic torque levels are different, the contraction times are also different. This implies that the individual twitches add in non-linear fashion to produce a tetanic torque.

Figure III-27 is a plot of tetanic torque (at 50/sec) versus I with D as the parameter. Notice that all of the curves have a parabolic shape suggesting that the data points would plot more linearly on a semi-logarithmic graph. Figure III-28 displays the same data on the coordinates: torque versus log I. These data can be represented by:

a) MEASURED RESPONSE TO PULSES SPACED BY 20 ms

b) SUMMATION OF TWITCHES SPACED BY 20ms
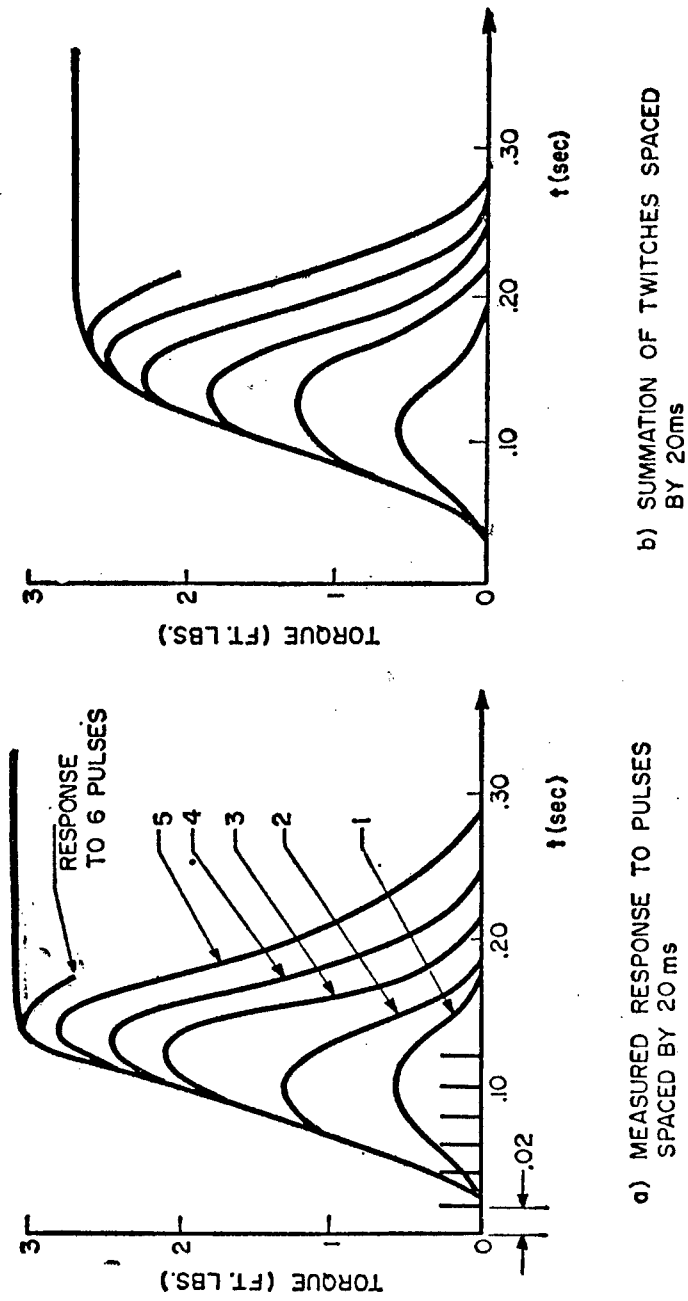
FIG. III-26. DEVELOPMENT OF TETANIC TORQUE.
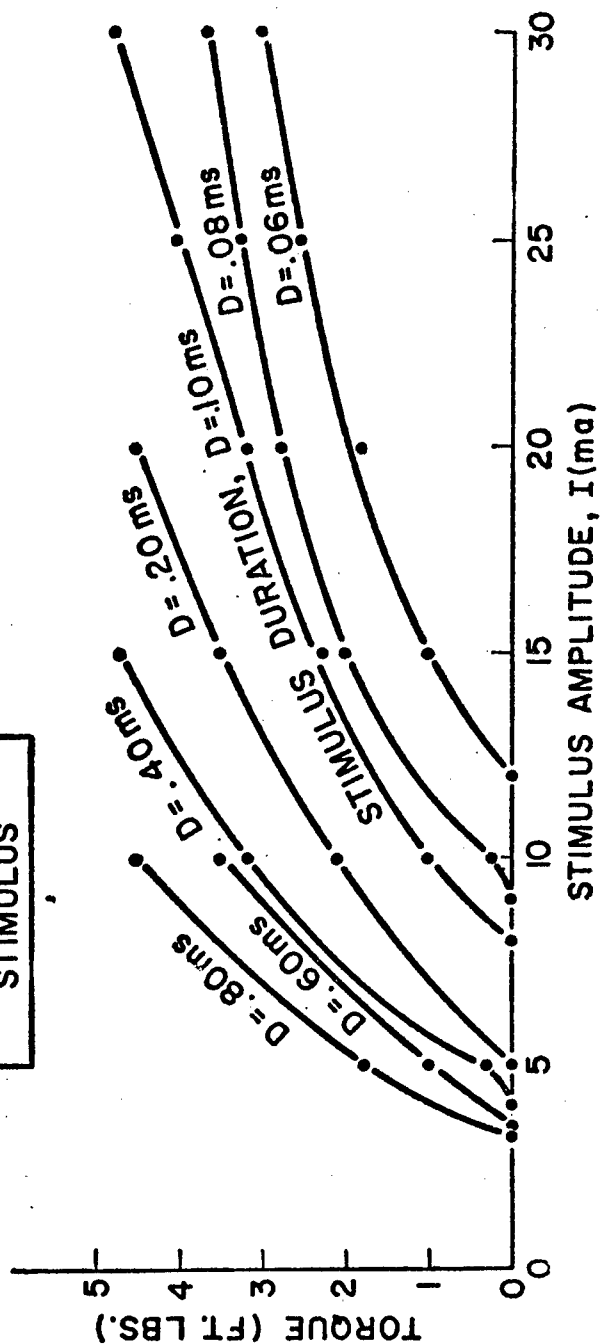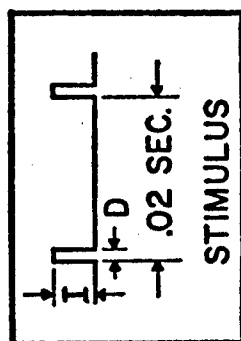
FIG. III-27. TETANIC TORQUE VS. STIMULUS CURRENT, PARAMETER D.
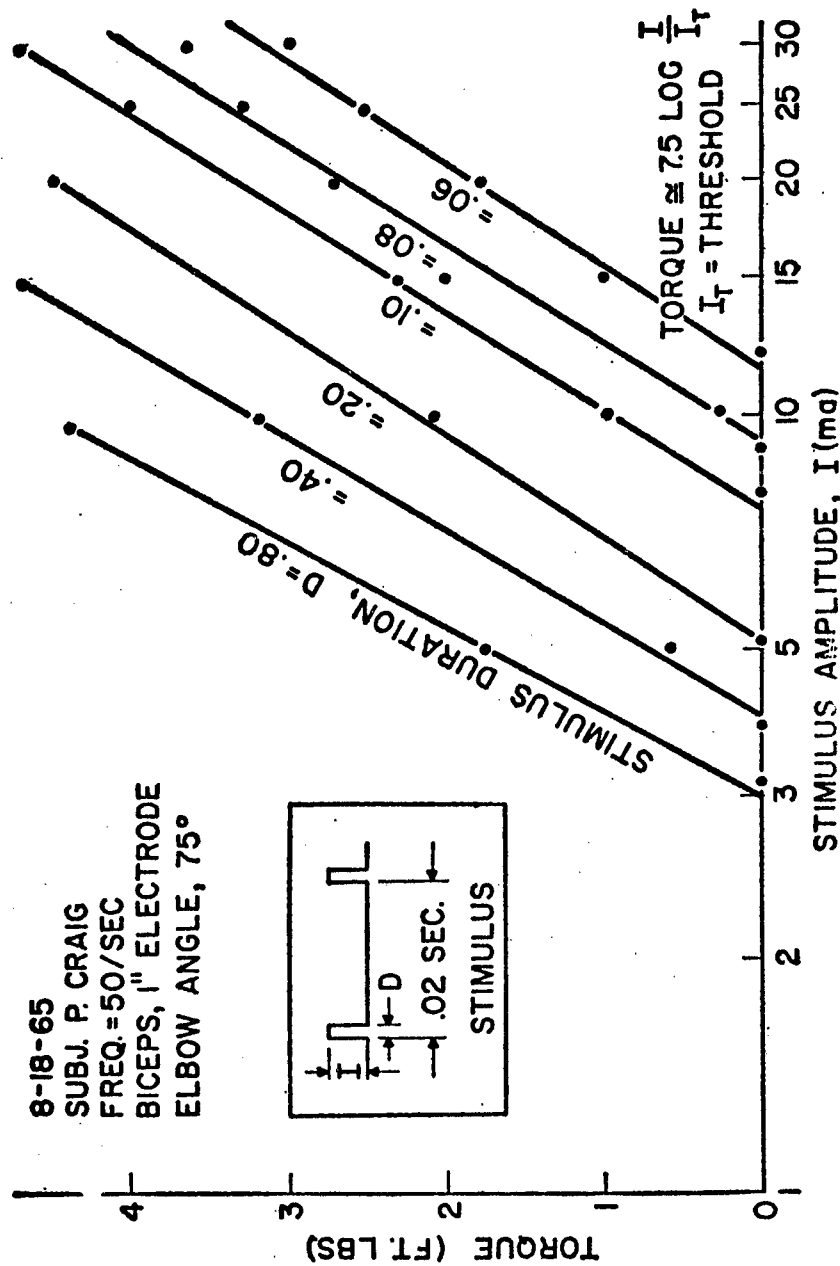
FIG. III-28. TETANIC TORQUE VS. LOG OF STIMULUS CURRENT,
PARAMETER D.

$$\text{Torque} = 7.5 \log \frac{I}{I_T} \text{ ft. lbs.} \qquad \text{(III. 27)}$$

Figure III-29 shows the same data once more with I plotted versus D and torque as the parameter. The lower curve (T = 0) is the familiar strength-duration curve which represents the threshold levels of the muscle. This curve has been fitted to Hill's equation as:

$$I = \frac{3.5}{1-e^{-6D}} \qquad \text{(III. 28)}$$

Looking at this figure in a slightly different way we see that a given torque may be achieved by setting either I or D and varying the other parameter. That is, either I or D may be used as a control signal with equal effectiveness.

In order for stimulated muscle to be useful it must also be capable of maintaining these torque levels for a period of time. It is known that the muscle fatigues during stimulation. For this reason all of the above experiments included rest periods between stimuli of at least 30 seconds. Records were obtained of torque with respect to time for a constant stimulus. The torque level remained constant for about 15 seconds before it began to
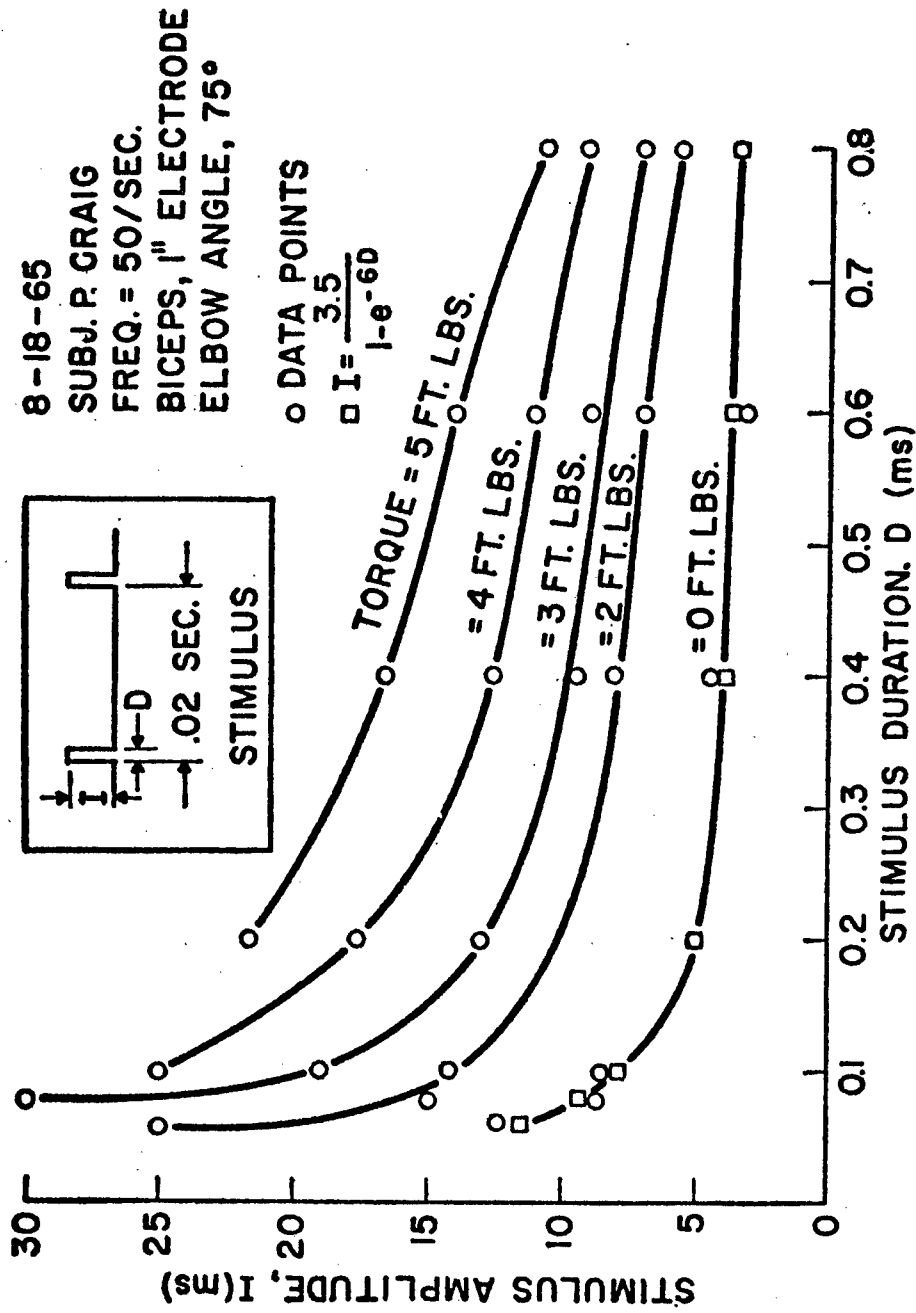
FIG. III-29. STIMULUS CURRENT VS. STIMULUS DURATION,
PARAMETER TETANIC TORQUE.

diminish. This, of course, is for normal muscle. For paralyzed
muscle the fatigue rate may be greater.

CHAPTER IV

DYNAMIC MODELING OF MUSCLE CONTRACTION

A. ISOMETRIC CONTRACTION

1. Muscle Twitch as an Impulse Response

Figures III-20 and III-22 of the preceding section show, in addition to the levels of torque, developed by the muscle, the transients involved in developing these levels. That is, the torque records are preceded by a delay and exhibit a transient behavior which is at least second order. The delay may be due to a number of causes, i.e., conduction velocity of the nerve action potential, motor end plate transmission, propagation of the muscle action potential and its wave of contraction, slackness in the resting muscle, and transducer dead zone. The transient portion of the records actually include the dynamics of the lower arm as well as the transducer. We have seen in Chapter II that transducer effects can be significant in the dynamic behavior of muscle. To deduce the actual form of the muscle twitch from these data requires the determination of the passive dynamics of the lower arm and the torque transducer. Once this is obtained a deconvolution procedure can be used to determine the actual muscle twitch.

Figure IV-1 shows, in block diagram form, the problem at hand.

Transfer function of arm support structure and torque transducer.

Figure IV-2 shows the transient response of the arm support

structure and torque transducer. This record of the deflection of

the torque transducer (θ) was obtained by releasing the arm

support from a deflected position. The response of Figure IV-2 is

similar to the step response of a second order system with transfer

function.

$$\theta(s) = \frac{1}{s^2 + 2\zeta\omega_n s + \omega_n^2} \qquad\qquad \text{(IV. 1)}$$

The values of ζ and ω_n can be evaluated directly from

Figure IV-2[65] and are:

$$\zeta = .02, \qquad \omega_n = 105 \text{ rad/sec}$$

Transfer function of arm support structure, torque transducer

and passive arm.

The same test was repeated with the arm of a subject in the

arm support. The transient response of this combination is shown

in Figure IV-3 and has a transfer function similar to equation 1

with $\zeta = .25$, $\omega_n = 40 \text{ rad/sec}$. The difference between
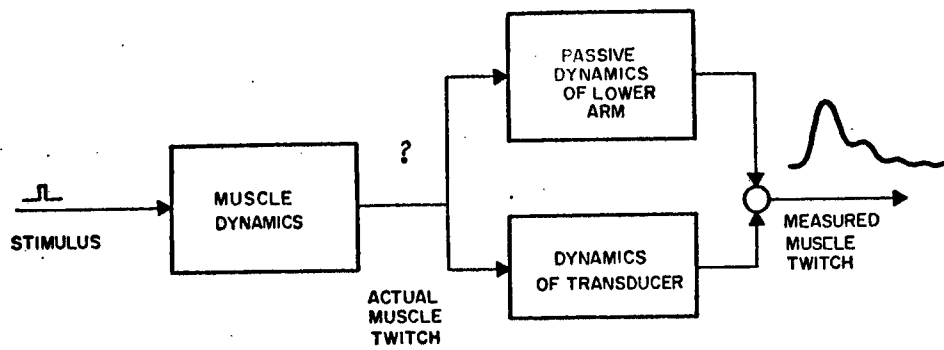
FIG. IV-1. THE DECONVOLUTION PROBLEM.
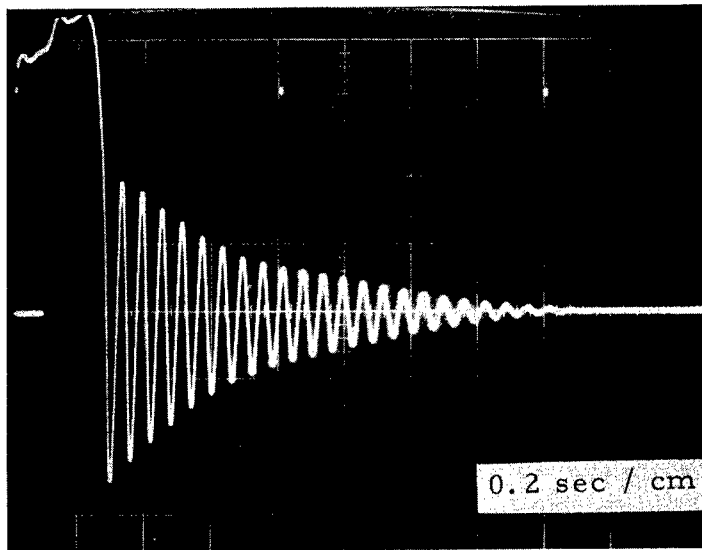
FIG. IV-2. TRANSIENT RESPONSE OF TORQUE TRANSDUCER
AND ARM SUPPORT STRUCTURE.
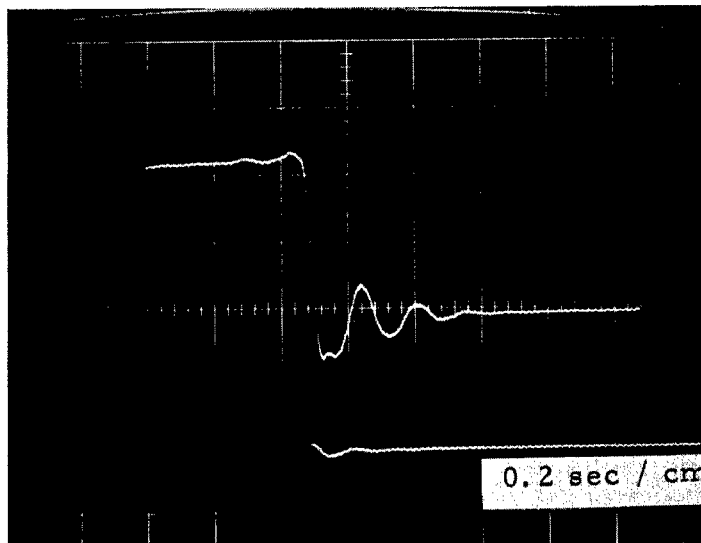
FIG. IV-3. TRANSIENT RESPONSE OF TORQUE TRANSDUCER,
ARM SUPPORT STRUCTURE AND PASSIVE ARM.

these values and those above must be solely due to the passive dynamics of the limb.

The equation of motion for either system is:

$$T(t) = J \ddot{\theta} + C \dot{\theta} + K \theta \qquad (IV.2)$$

where J is inertia, C viscous damping, and K stiffness. Evaluating the constants for the system without the arm; the inertia is given by the cumulative inertias of the parts of the arm support. This was found to be:*

$$J = .023 \ Ft \ Lb \ sec^2$$

The stiffness of the torque transducer was also calculated:*

$$K = 285 \ Ft \ Lb/rad$$

The natural frequency then is given by

$$\omega_n = \sqrt{\frac{K}{J}} \qquad (IV.3)$$
$$= \sqrt{\frac{285}{.023}} = 111.3 \ rad/sec$$

---

* See Appendix.

which checks fairly closely to the value of 105 rad/sec found

experimentally. The viscous damping coefficient is then

$$C = 2 \zeta \sqrt{K J} \tag{IV.4}$$

$$= 2(.02) \sqrt{285 \times .023}$$

$$= .102 \text{ Ft Lb sec}$$

When the arm is fastened in the arm support it will add its inertia,

some damping, but essentially no stiffness to the dynamics. The

elasticity of the elbow joint was found to be of the order of 0.5

Ft Lb/rad (Figure IV-4). The inertia of the arm is easily calcu-

lated using equation (IV.3):

$$J_{-arm} = \frac{K}{\omega_n{}^2} - .023 = \frac{255}{(40)^2} - .023$$

$$= .16 - .023 = .137 \text{ Ft Lb sec}^2 = 650 \text{ lb in}^2$$

This value is approximately twice the value given by Corell[5] of

290 lb in^2 for the average size arm. The viscous coefficient of

the arm has a calculated value:
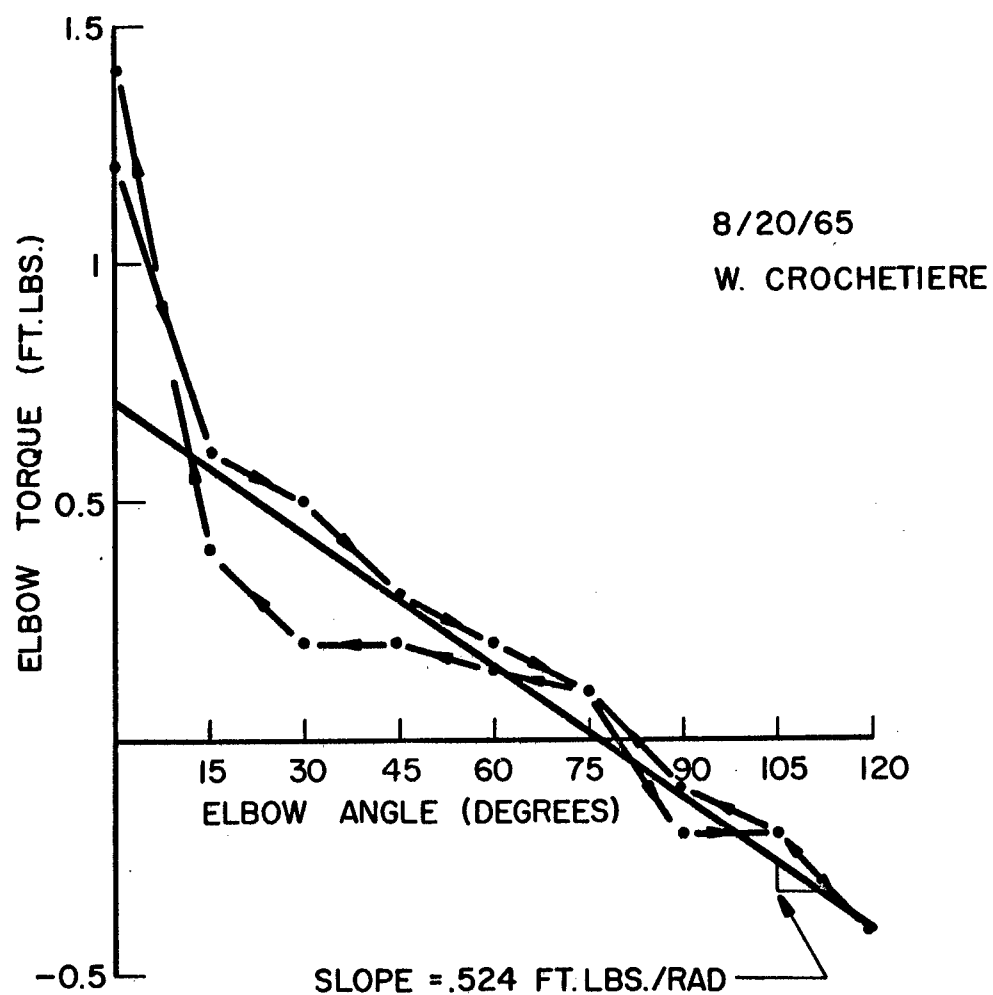
FIG. IV-4 PASSIVE TORQUE VS. ELBOW ANGLE

$$C_{arm} = 2 \,(.25) \sqrt{255 \times .16} - .102$$

$$= 3.19 - .102 = 3.088 \text{ Ft Lb sec}$$

Since we are interested in determining the dynamic behavior of muscle contraction independent of the above effects, we must account for them in our analysis. Figure IV-5 shows a muscle twitch as recorded. Knowing the combined transfer function of the transducer and passive arm and the measured muscle twitch, we can now perform the deconvolution proposed in Figure IV-1. The inverse problem is rather straightforward. That is, if the actual muscle twitch were known, the measured muscle twitch could be evaluated quite easily by convolution in the time domain. A graphical procedure for performing the inverse of convolution (deconvolution) was developed by Reswick, [51] and is described briefly in the Appendix. Using this procedure, the actual muscle twitch was determined. The solid curves in Figure IV-6a, b show a typical measured muscle twitch and the graphically determined actual muscle twitch. As a check on the accuracy of this solution a standard numerical convolution scheme was performed between the actual muscle twitch and the impulse response of the torque
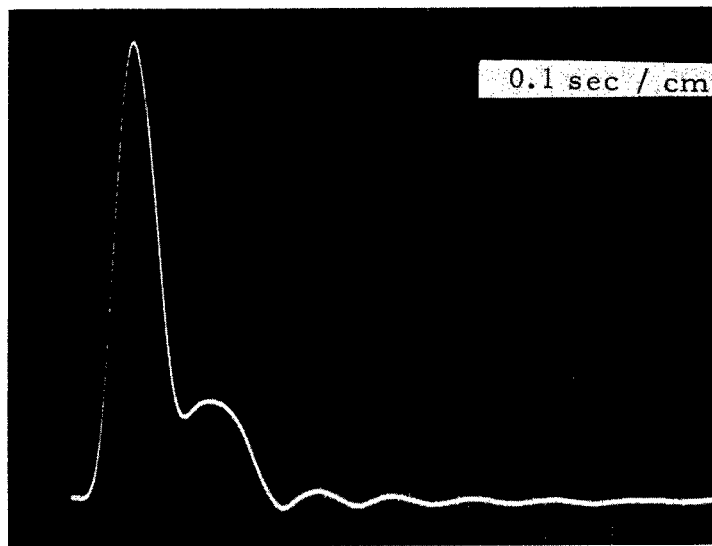
FIG. IV-5. TWITCH RESPONSE OF BICEPS.
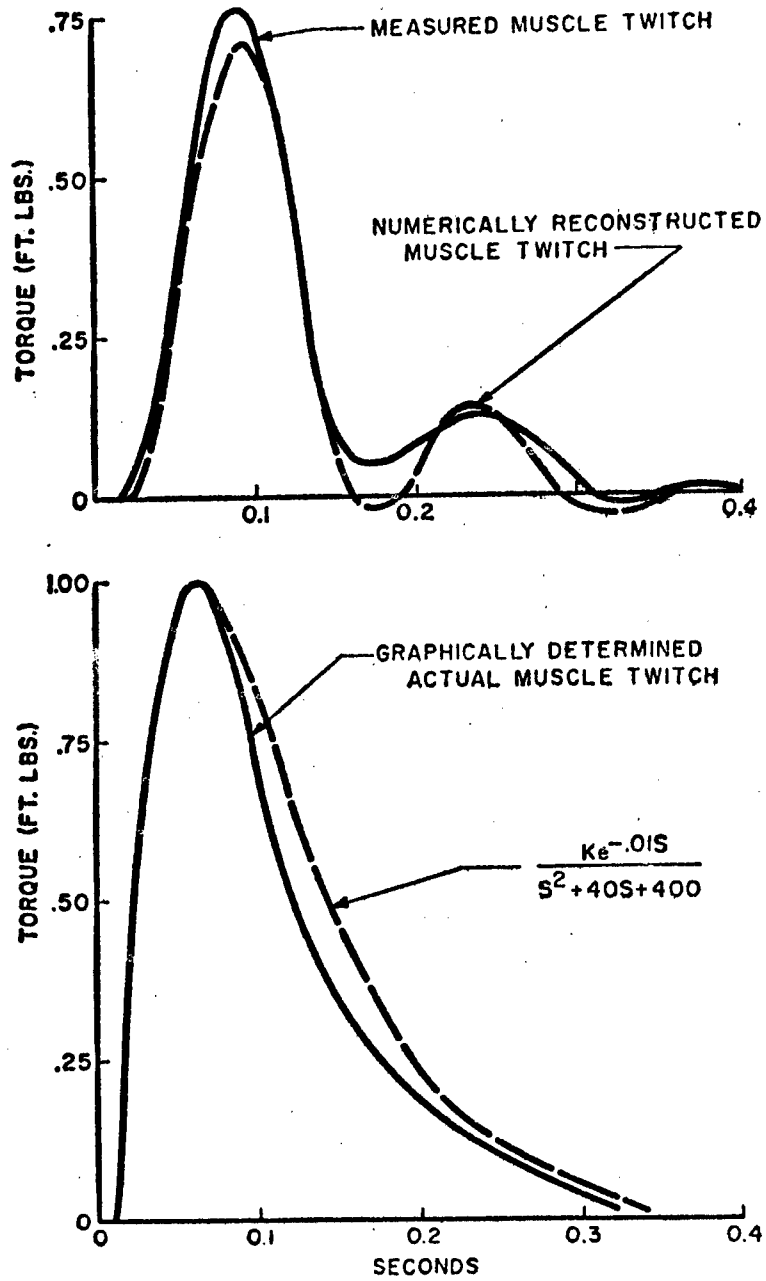
FIG. IV-6. RESULTS OF GRAPHICAL DECONVOLUTION.

111

transducer-passive arm combination. The resulting curve is shown

superimposed (dotted) on the measured muscle twitch. The curves

match quite well and the impulse response of a second order system

was then matched to the actual muscle twitch. This produced a

transfer function for stimulated muscle of:

$$\text{Muscle twitch} = \frac{Ke^{-.01s}}{(s+20)^2} \qquad (IV.5)$$

$$\text{Muscle twitch} = \frac{Ke^{-.01s}}{s^2 + 40s + 400} \text{ ft-lbs} \qquad (IV.6)$$

which is also shown in Figure IV-6b. Allowing for the stimulus

threshold nonlinearity,

$$\text{Muscle twitch} = \frac{K'(I-I_T)e^{-.01s}}{s^2 + 40s + 400} \text{ ft-lbs} \qquad (IV.7)$$

$$\text{for } I > I_T$$

2. Sinusoidal Modulation of Stimulus, Frequency Response

As mentioned in Section III, the output of the stimulator can

be modulated by an external signal generator. Frequency response

tests were therefore performed to check the dynamic transfer

function of Equation (IV.2). The amplitude of the pulse train

(50/sec, 0.4 ms duration) was modulated by a sine wave of variable frequency. Since the pulse duration is quite small, the stimulus can be represented as:

$$I(t) = A + B \sin 2\pi f_1 t \sum_{n=0}^{\infty} \delta(t - .02n) \qquad (IV.8)$$

From sampled data theory,[65] the frequency spectrum of this signal is the frequency spectrum of the modulation signal repeated along the frequency axis every multiple of the pulse frequency (Figure IV-7).

Assuming for the moment that the dynamics of stimulated muscle are represented by the twitch response of Equation (IV.2), we then define the linearized muscle transfer function as:

$$G(s) = \frac{Torque(s)}{I(s)} = \frac{Ke^{-.01s}}{s^2 + 40s + 400} = \frac{Ke^{-.01s}}{(s+20)^2} \qquad (IV.9)$$

In the frequency domain then the change in torque is given by:

$$T(f) = G(f)I(f) \qquad (IV.10)$$

where f is the frequency in cps.
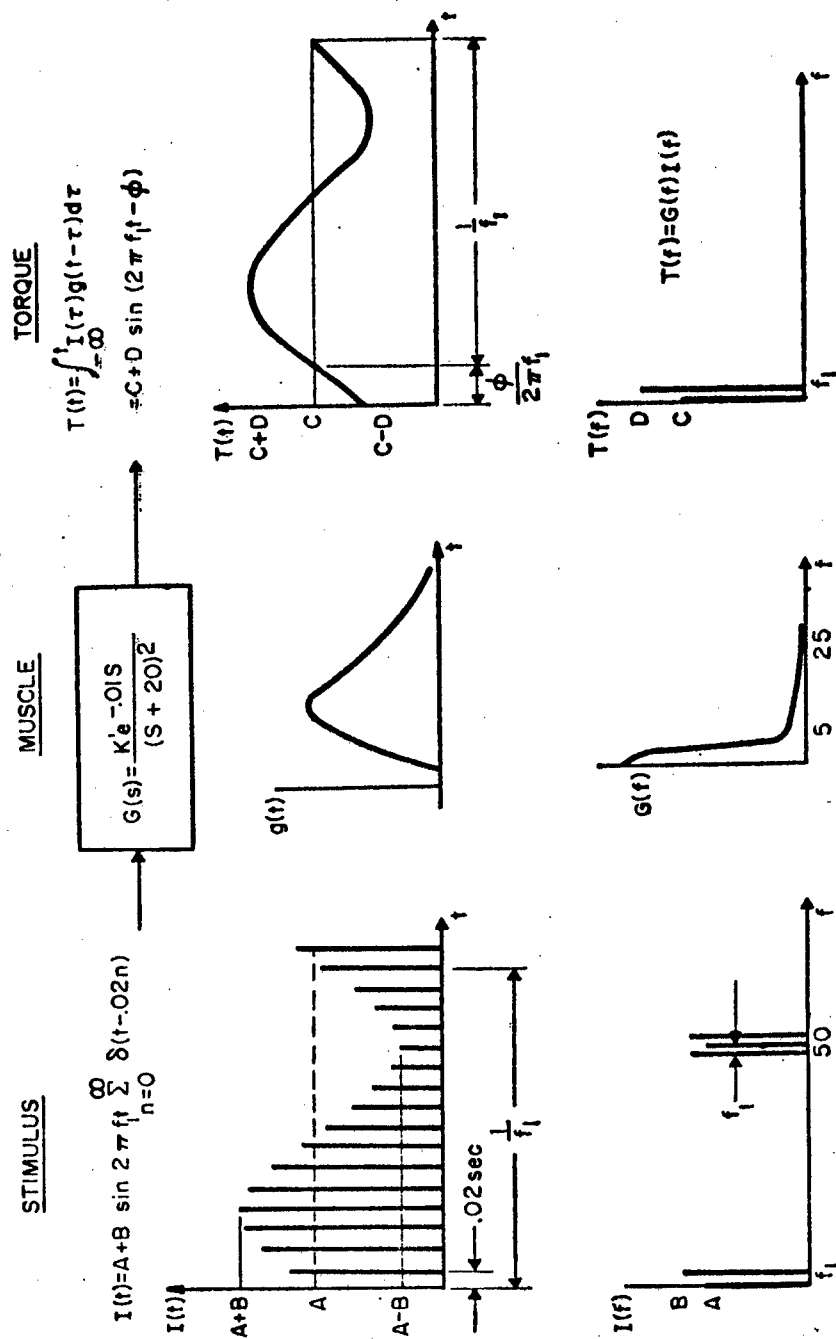
FIG. IV-7. LOW PASS FILTER CHARACTERISTICS OF STIMULATED MUSCLE.

Since the bandwidth of $G(f)$ is quite narrow, only the DC and f_1 components of the input will affect the output torque (Figure IV-7). In the time domain then the torque is given by:

$$T(t) = \int_{-\infty}^{t} I(\tau)g(t-\tau)d\tau = C+D \sin(2\pi f_1 t - \phi) \qquad (IV.11)$$

that is the frequency components of the pulse train are filtered out by the muscle and the resultant torque is a function of the modulation signal only.

The frequency response of the biceps muscle was then obtained in the following manner. The modulation was set at:

$$I(t) = 15 + 5 \sin(2\pi ft) \text{ ma} \qquad (IV.12)$$

and f was varied from 0.2 to 3.0 cps. The modulation signal and the elbow torque were recorded on a two-channel recorder. A typical record is shown in Figure IV-8. The normalized amplitude and phase data from two experiments are plotted versus frequency in Figure IV-9. The data points were best fitted by:

$$\frac{1}{s^2 + 80s + 400} \qquad (IV.13)$$
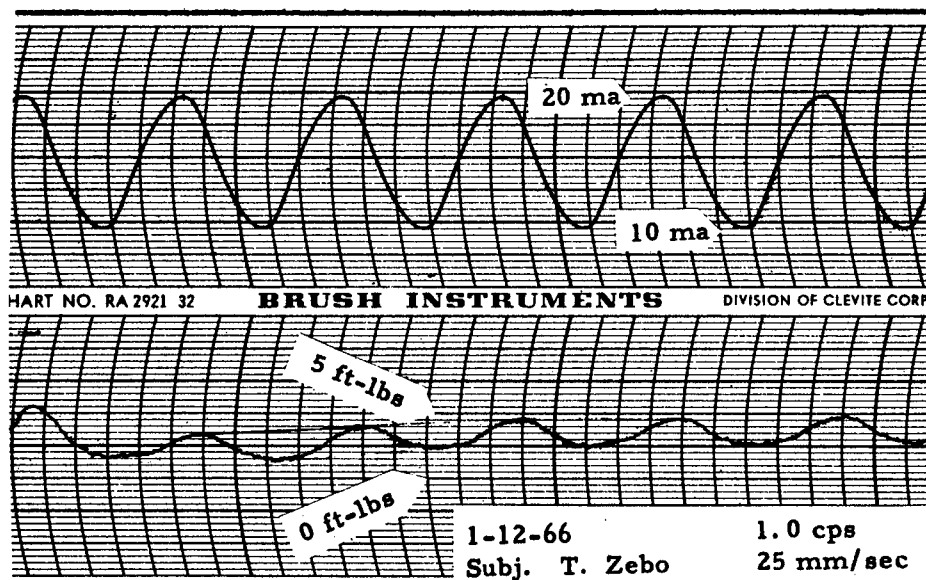
FIG. IV-8. TORQUE RESPONSE TO SINUSOIDALLY MODULATED
STIMULUS.
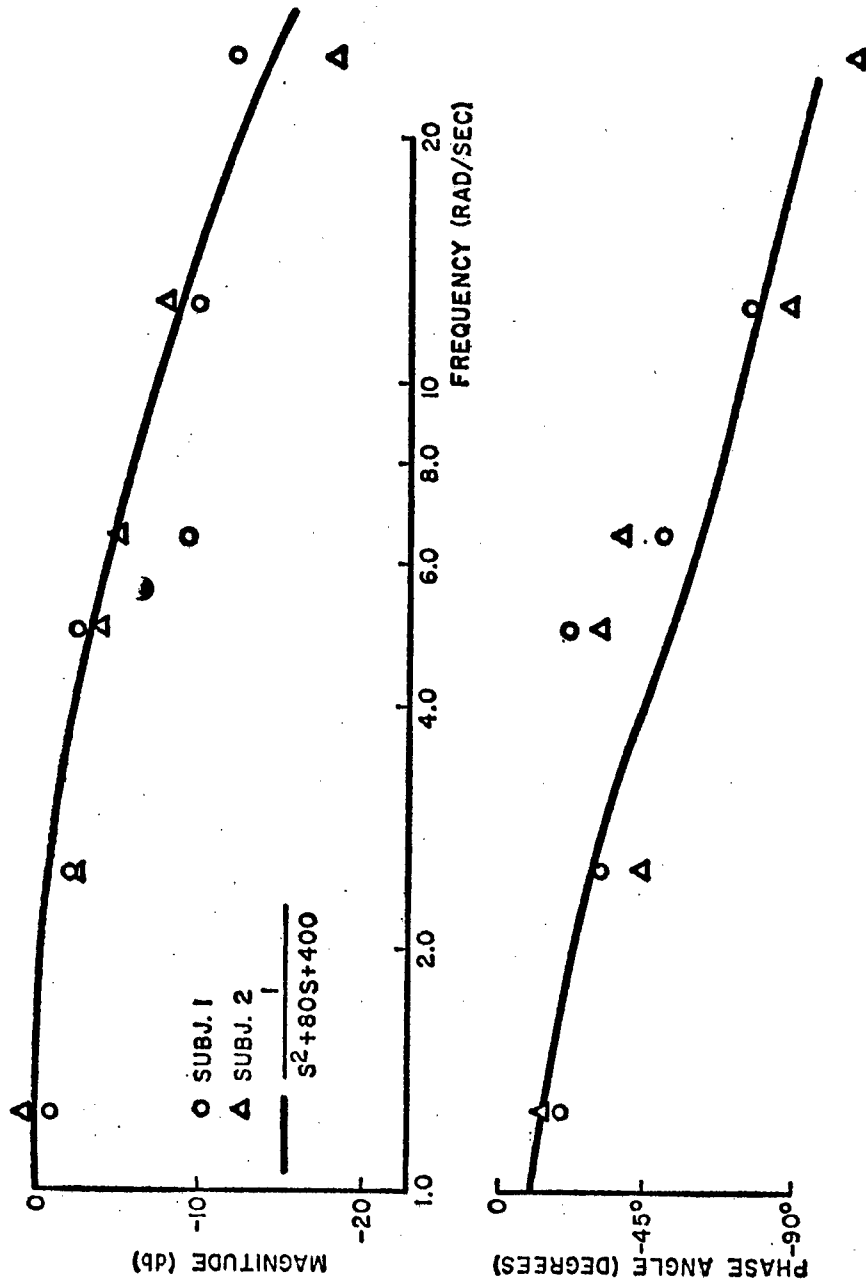
FIG. IV-9. FREQUENCY RESPONSE OF STIMULATED BICEPS MUSCLE.

This is similar to the transfer function determined from the twitch response (See Equation IV. 7) except that there is no delay time and the damping is greater. It should be noted, however, that a delay time would have no effect on the magnitude curve and a delay of .01 sec. would produce a maximum additional phase shift of only -11° at a frequency of 3.0 cps. One would also expect that the viscous damping in a contracted muscle is greater than in a relaxed muscle, possibly accounting for the increased damping in the transfer function.

B. ISOTONIC CONTRACTION

1. The Loading System

The dynamic model for isometric muscle contraction will now be expanded to include the isotonic contraction of muscle. A constant load system consisting of negator springs was designed and built under the author's direction by Keith Miller, M.S. student. This unit is shown mounted on the experimental apparatus in Figure IV-10. A negator spring resists with a constant force independent of length. With this setup, constant loads with negligible inertia may be applied to the elbow joint from 0.5 to 7.5 ft lbs in increments of 0.5 ft lbs.
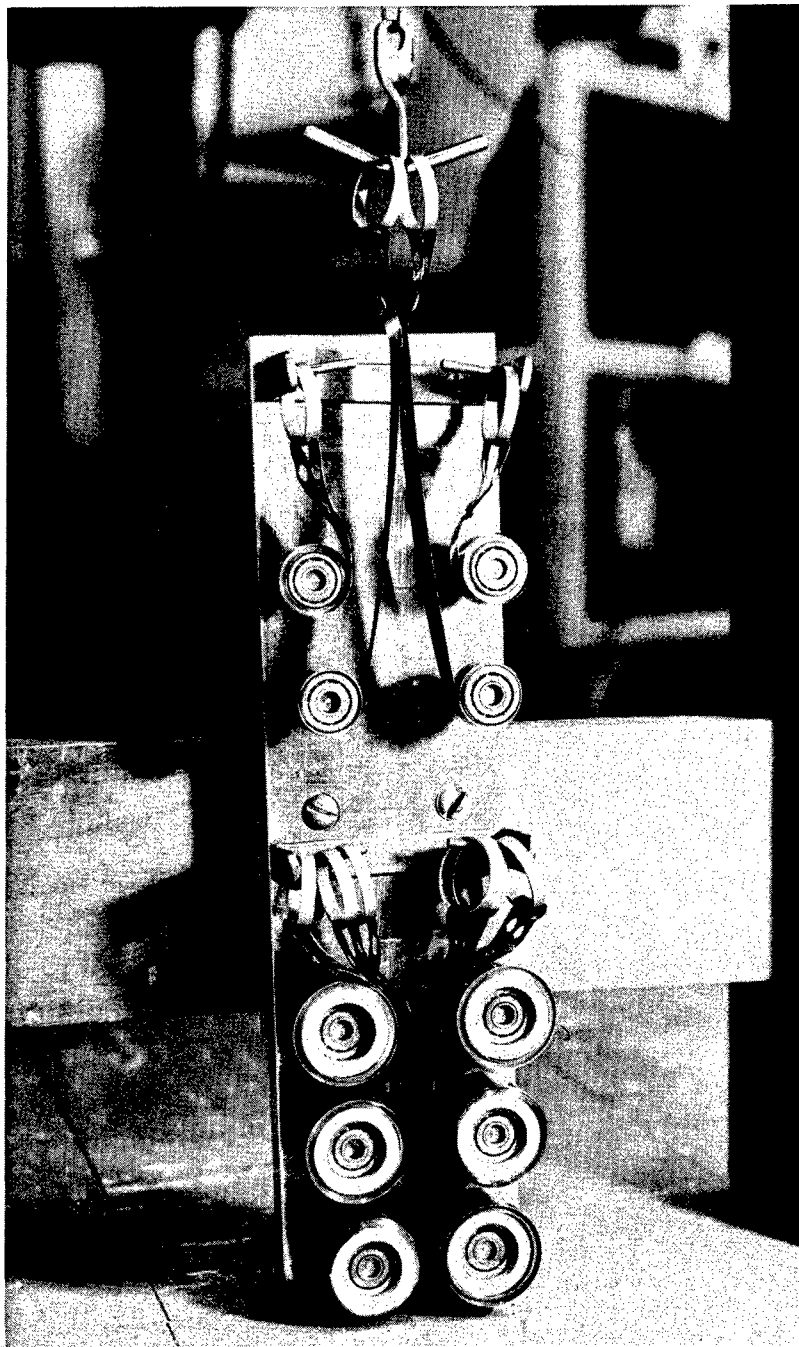
FIG. IV-10. NEGATOR SPRING LOAD SYSTEM.

2. Motor Point Tracking

As stated in Chapter III, the motor point moves during elbow rotation much as a point on the muscle would probably move. Any isotonic experiments should be performed with the stimulus always over the motor point. Before each isotonic experiment was performed therefore the movement of the motor point was recorded using the segmented electrode (Figure III-15).

It was decided to stimulate using three electrodes at a time. This gave a contact area of .94 square inches which was judged to be quite acceptable. The motor point migration data was reduced as shown in Figure IV-11 where elbow angle is tabulated versus electrode groupings. An X in a compartment indicates that at that elbow angle the motor point is beneath that group of three electrodes. We would now like to locate the stimulus at these points during elbow rotation.

A stimulation commutator was designed and constructed under the author's direction by Charles Caldwell,[4] Ph. D. student, which would ensure that the stimulus was always applied at the motor point. This consists of a printed circuit board upon which are mounted twelve normally open magnetic reed switches, spaced radially every 10° about the center of rotation of the elbow (Figure IV-12). This unit is stationary. A bracket on the arm

120

SUBJ. J. LANE
DATE. 1/3/67
STIMULUS $I = 5$ ma
$D = 0.2$ ms
$f = 50$ cps

ELECTRODE GROUPS

	123	234	345	456	567	678	789
1			X				
2			X				
3			X				
4			X				
5				X			
6				X			
7				X			
8					X		
9					X		
10					X		
11						X	
12						X	

COMMUTATOR SEGMENT

FIG. IV - 11 MOTOR POINT LOCATION VS. ELBOW
ANGLE
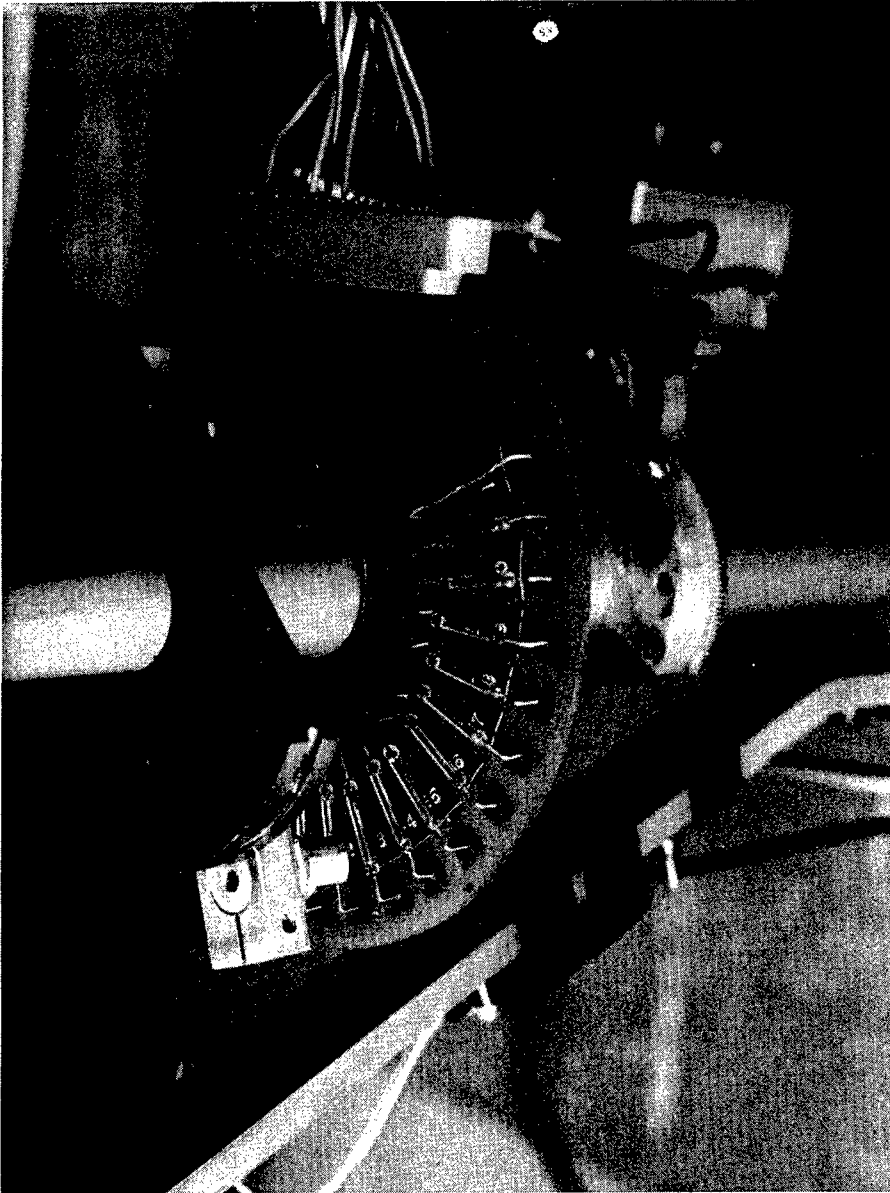
FIG. IV-12.   STIMULUS COMMUTATOR.

brace carries a permanent magnet which swings over the reed switches during elbow rotation. The magnet and switches are adjusted so that one and only one switch is closed at any time. The twelve outputs of the switches are connected to the input side of a small patchboard (Figure IV-13), and nine outputs from the patch-board are connected to the nine electrode segments. By placing shorting pins in the appropriate patchboard position, any set of electrodes can be activated at each angular position of the arm. The desired pattern previously obtained as in Figure IV-11 is then implemented on the patchboard before an isotonic experiment is performed.

3. Muscle Shortening Experiment

With the stimulator and electrodes set up as above, the ratcheting mechanism is disengaged allowing the elbow to move freely. A constant load torque is applied about the elbow joint causing it to assume the position of extreme extension. When a train of constant amplitude pulses is then applied to the biceps the elbow flexes as shown in Figure IV-14. That is, the elbow angle assumes a constant velocity of flexion after a delay and a lag. The movement, of course, is terminated when the joint reaches full flexion. In Figure IV-15 is plotted the load torque versus the steady state angular velocity of elbow flexion with stimulating

FIG. IV – I3 ELECTRODE SELECTOR

STIMULUS

FULL FLEXION

FULL EXTENSION

JOINT ANGLE VS. TIME

0.1 sec.
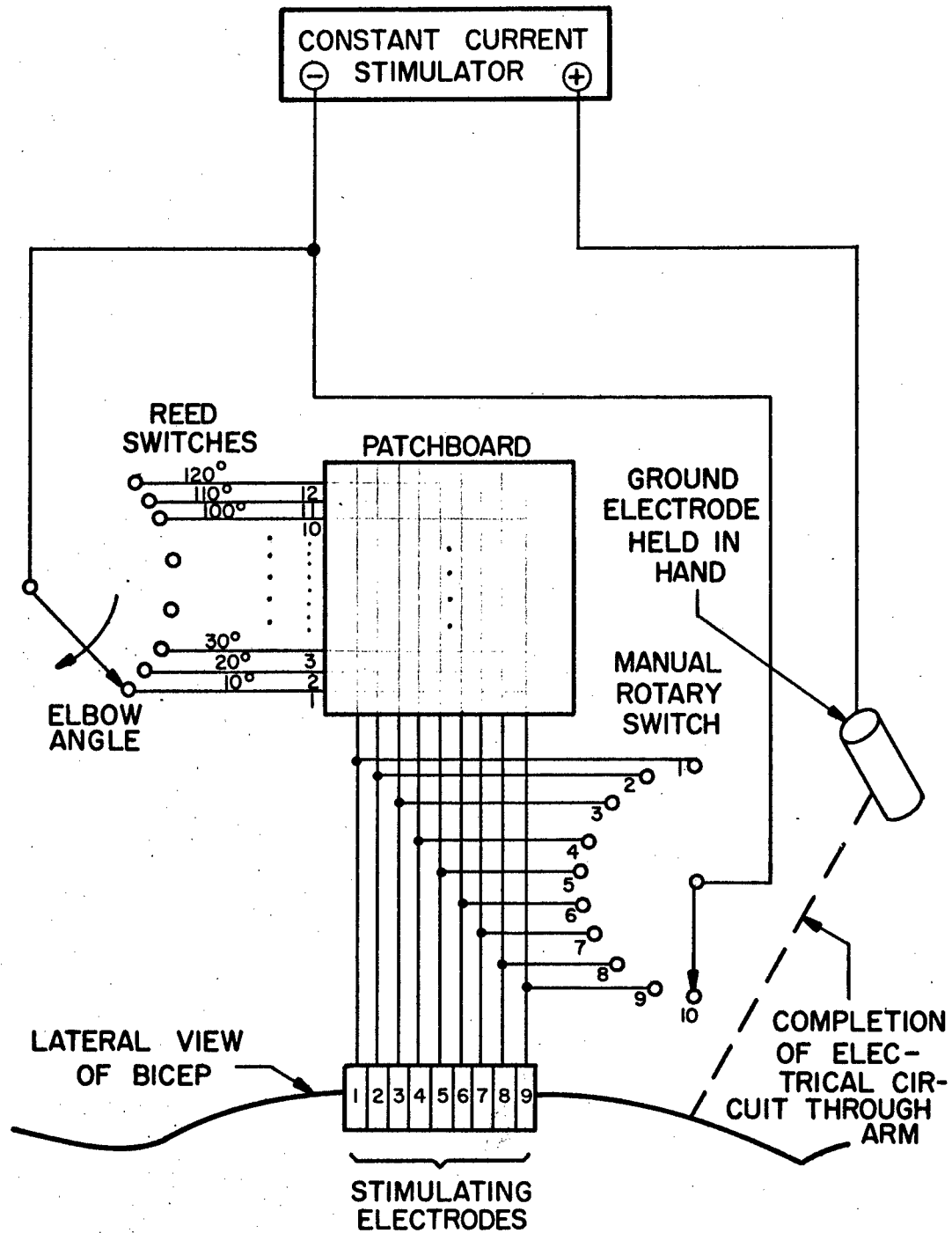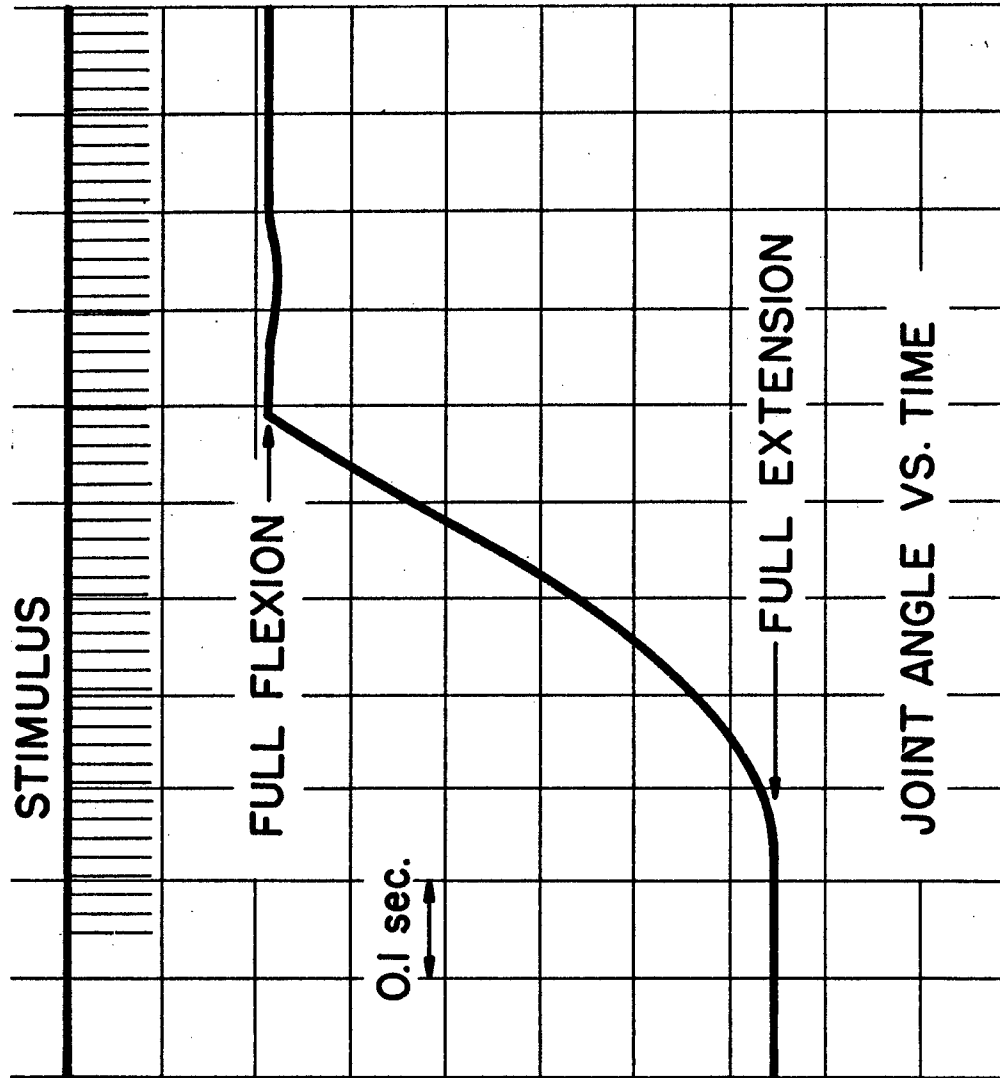
10-26-1966
SUBJECT: W.J.C.
LOAD 2 FT. LBS.
I = 15 ma.
D = 0.4 ms.
f = 50 cps.

FIG. IV - 14 TYPICAL RECORD OF ISOTONIC CONTRACTION OF BICEPS
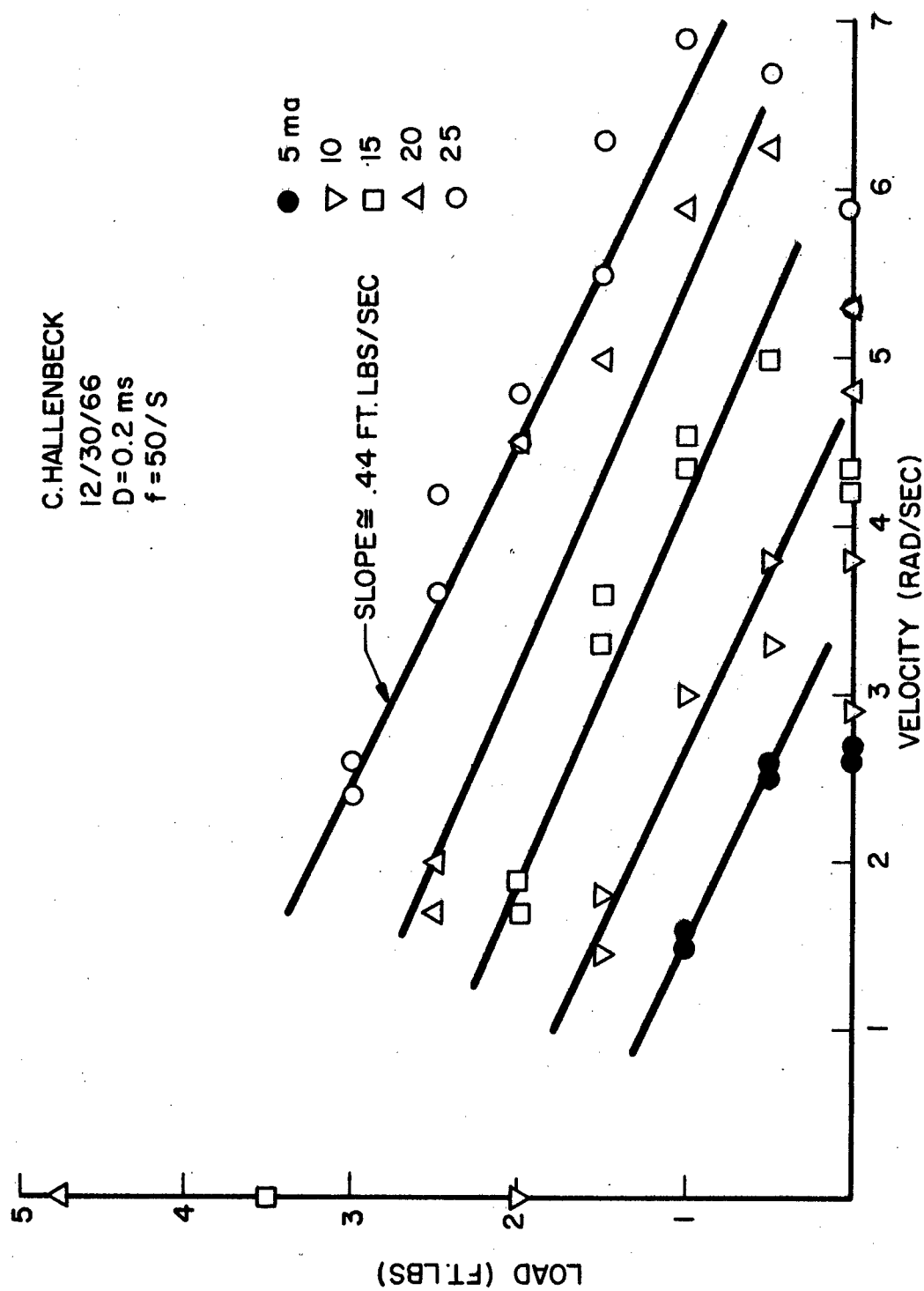
FIG. IV - 15 LOAD-VELOCITY CURVES OF STIMULATED MUSCLE

C. HALLENBECK
12/30/66
D = 0.2 ms
f = 50/S

SLOPE ≅ .44 FT. LBS/SEC

5 ma ●
10 ▽
15 □
20 △
25 ○

VELOCITY (RAD/SEC)

LOAD (FT.LBS)

current as the parameter. In five of ten experiments, the data points could be represented fairly well by straight lines. Furthermore, the average slope of these lines was found to be 0.49 ft-lb-sec with a range of 0.44 to 0.60 ft-lb-sec. As mentioned in Chapter II, this slope is actually a measure of the internal damping of the muscle. Some of the viscous drag must also be atrributed to the joint capsule and fascia.

4. Theoretical Determination of Delay plus Lag Time (t_o)

Thus far, this section has been concerned with the dynamic modeling of the steady state behavior of isotonically contracting muscle. Before a steady state velocity is assumed by the limb, however, there is a delay plus lag time. The delay we assume to be the same as for the isometric muscle. The lag is affected by the lag due to the isometric muscle and that due to viscous drag and the inertia of the limb. Assuming the lower arm to be a pure inertia:

$$T(t) = J \ddot{\phi} + C \dot{\phi} \qquad (IV.14)$$

$$T(s) = s(Js+C)\phi(s) \qquad (IV.15)$$

$$\therefore G_1(s) = \frac{\phi(s)}{T(s)} = \frac{1}{s(Js+C)} = \frac{1/C}{s(\frac{J}{C}s+1)} \qquad (IV.16)$$

where "C" is primarily the viscosity of the muscle which has been determined previously to be 0.49 ft-lb-sec (i.e., Figure IV-15). The inertia of the lower limb (J) can be calculated approximately. The weight of the forearm and hand is given by Corell[5] as 3.7 lbs. Assuming the lower arm to be a slender rod 16 inches long, the inertia is given by:

$$I = \frac{1}{3} mL^2 = \frac{1}{3} \left(\frac{3.7}{32.2} \right) \left(\frac{16}{9} \right) \tag{IV.17}$$

$$= .068 \text{ slug ft}^2$$

then IV-11 becomes

$$G_1(s) = \frac{2.04}{s(.136 s+1)} = \frac{K'}{s(Qs+1)} \tag{IV.18}$$

Any load torque acting on the limb also affects the elbow angle through this same transfer function. The situation is depicted in Figure IV-16. The application of a load torque (T_L) decreases the torque available to move the limb (T).

$$T = T_M - T_L \tag{IV.19}$$

$$\rightarrow \boxed{\dfrac{Ke^{-T_0 s}}{(Ps+1)^2}} \xrightarrow{T_M} \overset{+}{\underset{-}{\bigcirc}} \xrightarrow{T} \boxed{\dfrac{K'}{s(Qs+1)}} \xrightarrow{\phi}$$

T_L
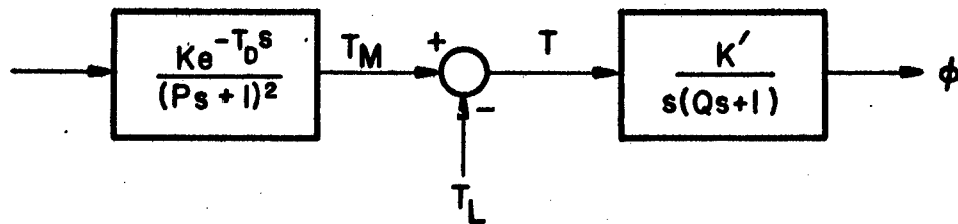
FIG. IV-16 ISOTONIC MODEL OF MUSCLE

where T_M is the torque produced by the stimulated muscle. The elbow angle therefore is given by:

$$\phi(s) = \frac{K K' I e^{-T_D s}}{s(Qs+1)(Ps+1)^2} - \frac{T_L K'}{s(Qs+1)} \qquad (IV.20)$$

The response of this transfer function to a step input was determined using the MIMIC language on the Univac 1107 computer. The response under various load conditions is plotted in Figure IV-17. Notice that in addition to the decreasing slope of the response due to increasing load, there is also a greater lag with increasing load. It is this latter characteristic of the response which will be used to evaluate this model. That is, there are several ways in which the response of the model can be matched to the obtained experimental data. Those methods are very time consuming even when the digital computer is used. A simple graphical method was devised which makes use of the asymptotes of the responses to determine the delay plus lag times.

None of the isotonic records were observed to be underdamped (oscillatory), therefore a transfer function for such records would contain only real poles. That is, the transfer function for the system under no-load conditions could be approximated as:

JAN 14, 1967

u(t)

$$\frac{3.0e^{-.02s}}{(.05s+1)^2}$$

ML

$$\frac{2.0}{s(.15s+1)}$$

RAD.

STEP RESPONSE OF

ANGLE (RADIANS)

2.0
1.8
1.6
1.4
1.2
1.0
.8
.6
.4
.2

ML=0

=0.5 FT.LBS.

1.0

1.5

2.0

0.1 0.2 0.3 0.4 0.5 0.6 0.7 0.8 0.9

TIME (SEC)

FIG.IV-17 STEP RESPONSE OF ISOTONIC MODEL UNDER VARIOUS LOAD CONDITIONS
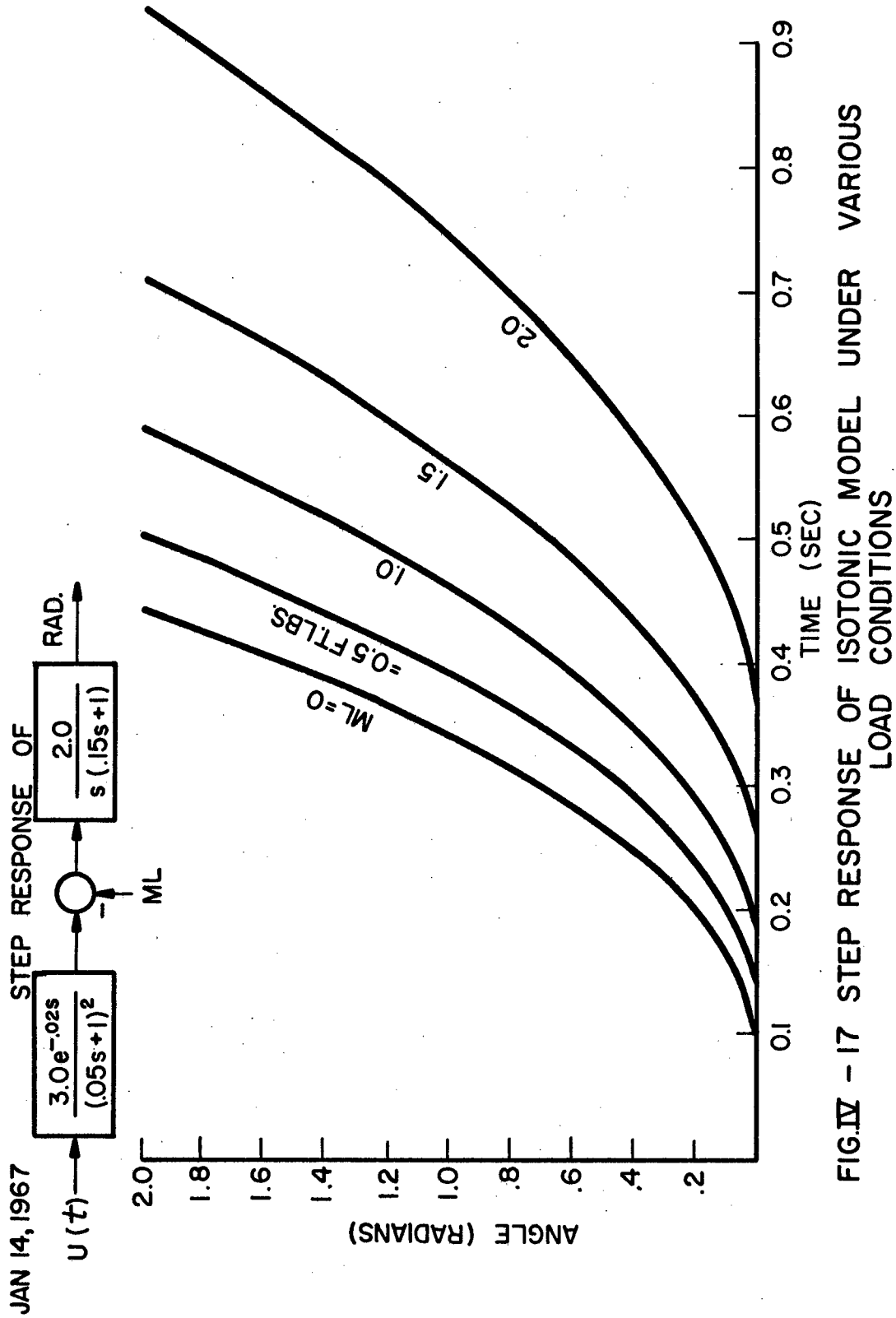
$$G(s) \ = \ \frac{Ke^{-T_D s} \sum_m A_m s^m}{s \, \pi_n (T_n s+1)} \qquad (IV.21)$$

the response of the system to a step change in stimulus is

$$\phi(s) \ = \ \frac{Ke^{-T_D s} \sum_m A_m s^m}{s^2 \, \pi_n (T_n s+1)} \qquad (IV.22)$$

$$= \ \frac{A}{s^2} + \frac{B}{s} + \text{transients} \qquad (IV.23)$$

$$A \ = \ \left[\frac{Ke^{-T_D s} \sum_m A_m s^m}{\pi_n (T_n s+1)} \right]_{s=0} = KA_0 \qquad (IV.24)$$

$$B \ = \ \frac{d}{ds} \left[\frac{Ke^{-T_D s} \sum_m A_m s^m}{\pi_n (T_n s+1)} \right]_{s=0} \qquad (IV.25)$$

$$= \left\{ \frac{\pi_n (T_n s+1) \frac{d}{ds} \left[Ke^{-T_D s} \sum_m A_m s^m \right]}{\left[\pi_n (T_n s+1) \right]^2} - \frac{\left[Ke^{-T_D s} \sum_m A_m s^m \right] \frac{d}{ds} \left[\pi_n (T_n s+1) \right]}{\left[\pi_n (T_n s+1) \right]^2} \right\}_{s=0} \qquad (IV.26)$$

$$= \left\{ \frac{\prod_n (T_n s+1) \left[-T_D K e^{-T_D s} \sum_m A_m s^m + K e^{-T_D s} \sum_m (m+1) A_{(m+1)} s^m \right]}{\left[\prod_n (T_n s+1) \right]^2} - \right.$$

$$\left. \frac{K e^{-T_D s} \sum_m A_m s^m \sum_{k=1}^n T_k \frac{\prod_n (T_n s+1)}{T_k s+1}}{\left[\prod_n (T_n a+1) \right]^2} \right\}_{s=0} \qquad (IV.27)$$

$$= -T_D K A_0 + K A_1 - K A_0 \sum_n T_n \qquad (IV.28)$$

$$= K(-A_0 T_D + A_1 - A_0 \sum_n T_n) \qquad (IV.29)$$

then

$$\phi_{(t)} = K A_0 t + K(-A_0 T_D + A_1 - A_0 \sum_n T_n) + \text{transients} \qquad (IV.30)$$

$$= K A_1 + K A_0 (t - T_D - \sum_n T_n) + \text{transients} \qquad (IV.31)$$

Since $\phi(t=0) = 0$, $A_1 = 0$, therefore

$$\phi(t) \sim t - T_D - \sum_n T_n \qquad (IV.32)$$

This is the equation of a straight line with t-intercept

$T_D + \sum_n T_n$. Therefore, to evaluate the sum of the delay plus lag

times of our muscle model, we can simply extend the linear part

of the angle response curve to the t-axis.

This is true, however, only from the no-load records.

Introducing a load also affects the t-intercept as we have seen in

Figure IV-17. Continuing with the straight line approximations,

the response of the model, under load, is given by:

$$\phi(s) = \frac{K'KIe^{-T_D s}}{s^2(Ps+1)^2(Qs+1)} - \frac{T_L K'}{s^2(Qs+1)} \qquad (IV.33)$$

$$= \frac{A}{s^2} + \frac{B}{s} + \ldots + \frac{C}{s^2} + \frac{D}{s} + \ldots \qquad (IV.34)$$

$$A = \left[\frac{K'KIe^{-T_D s}}{(Ps+1)^2 (Qs+1)} \right]_{s=0} = K'KI \qquad (IV.35)$$

$$B = \frac{d}{ds} \left[\frac{K'KIe^{-T_D s}}{(Ps+1)^2(Qs+1)} \right]_{s=0} \qquad (IV.36)$$

$$= \left\{ \frac{(Ps+1)^2(Qs+1)(K'KI)(-T_D)e^{-T_D s}}{\left[(Ps+1)^2(Qs+1)\right]^2} - \right. \tag{IV.37}$$

$$\left. \frac{K'KIe^{-T_D s}\left[2(Ps+1)(P)(Qs+1)+(Ps+1)^2(Q)\right]}{\left[(Ps+1)^2(Qs+1)\right]^2} \right\}_{s=0}$$

$$= K'KI(-T_D) - K'KI(2P+Q) \tag{IV.38}$$

$$B = -K'KI(T_D + 2P+Q) \tag{IV.39}$$

$$C = -\frac{T_L K'}{Qs+1}\bigg|_{s=0} = -T_L K' \tag{IV.40}$$

$$D = -\frac{d}{ds}\left[\frac{T_L K'}{Qs+1}\right]_{s=0} = \frac{T_L K'Q}{(Qs+1)^2}\bigg|_{s=0} = T_L K'Q \tag{IV.41}$$

then

$$\phi(t) = K'KIt - K'KI(T_D+2P+Q) - T_L K't + T_L K'Q + \ldots \tag{IV.42}$$

$$= K'KI(t-T_D-2P-Q) - T_L K'(t-Q) + \ldots \tag{IV.43}$$

This is the equation of two straight lines which when summed gives the steady state response of ϕ. Figure (IV-18) shows the graphical construction of this response. The t-intercept (t_0) of this asymptote can now be found. This point corresponds to the point where $\phi = 0$.

$$K'KI(t_0 - T_D - 2P - Q) = T_L K'(t_0 - Q) \tag{IV.44}$$

$$t_0(1 - \frac{T_L}{KI}) = T_D + 2P + Q - \frac{T_L Q}{KI} \tag{IV.45}$$

$$t_0 = \frac{KI(T_D + 2P + Q) - T_L Q}{KI - T_L} \tag{IV.46}$$

Substituting in the values found previously

$$t_0 = \frac{KI(.02 + .10 + .136) - .136 \, T_L}{KI - T_L} \tag{IV.47}$$

$$= \frac{.256 \, KI - .136 \, T_L}{KI - T_L} \tag{IV.48}$$

this function is plotted in Figure IV-19. This graph expresses the expected value of the t-intercept for our experimental data given the load and the torque that the muscle exerts (KI). Also plotted in this figure are experimentally obtained points for three different
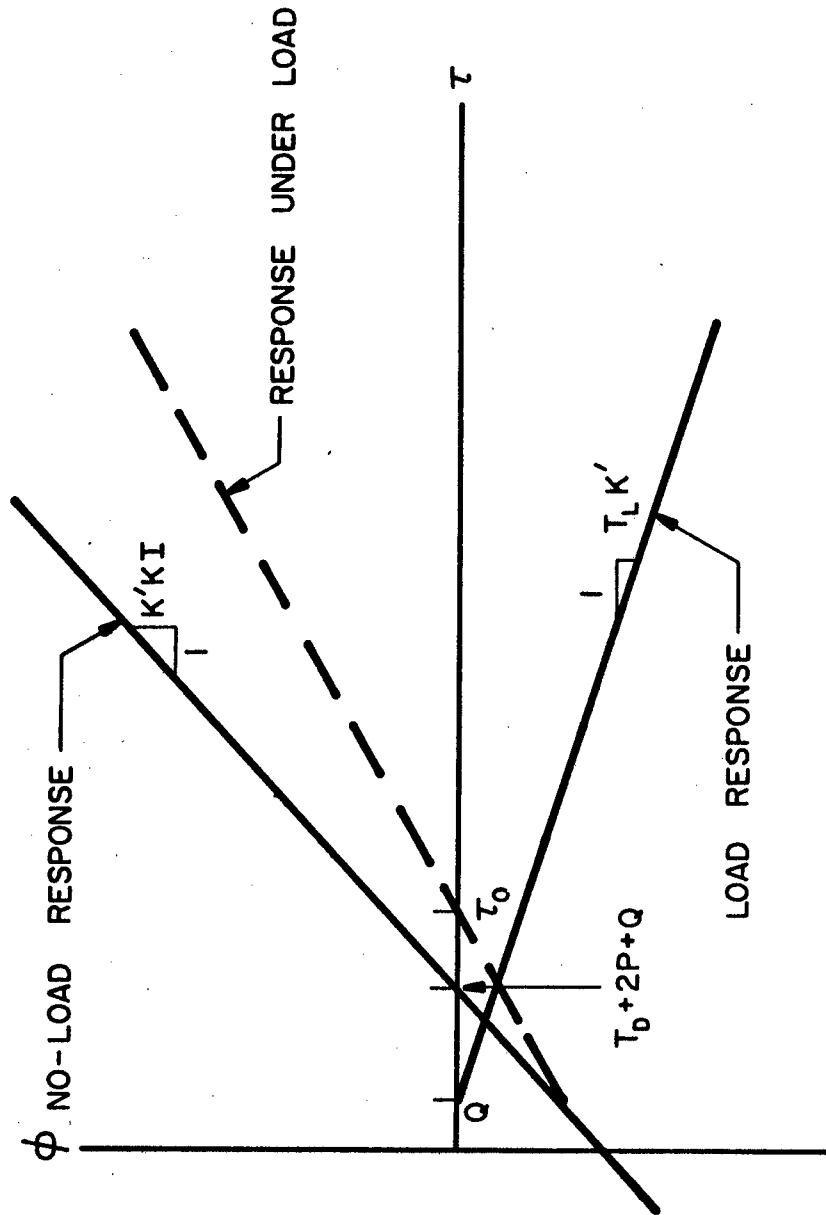
FIG. IV-18 EFFECT OF LOAD ON THE ASYMPTOTIC RESPONSE OF ISOTONIC MODEL

137
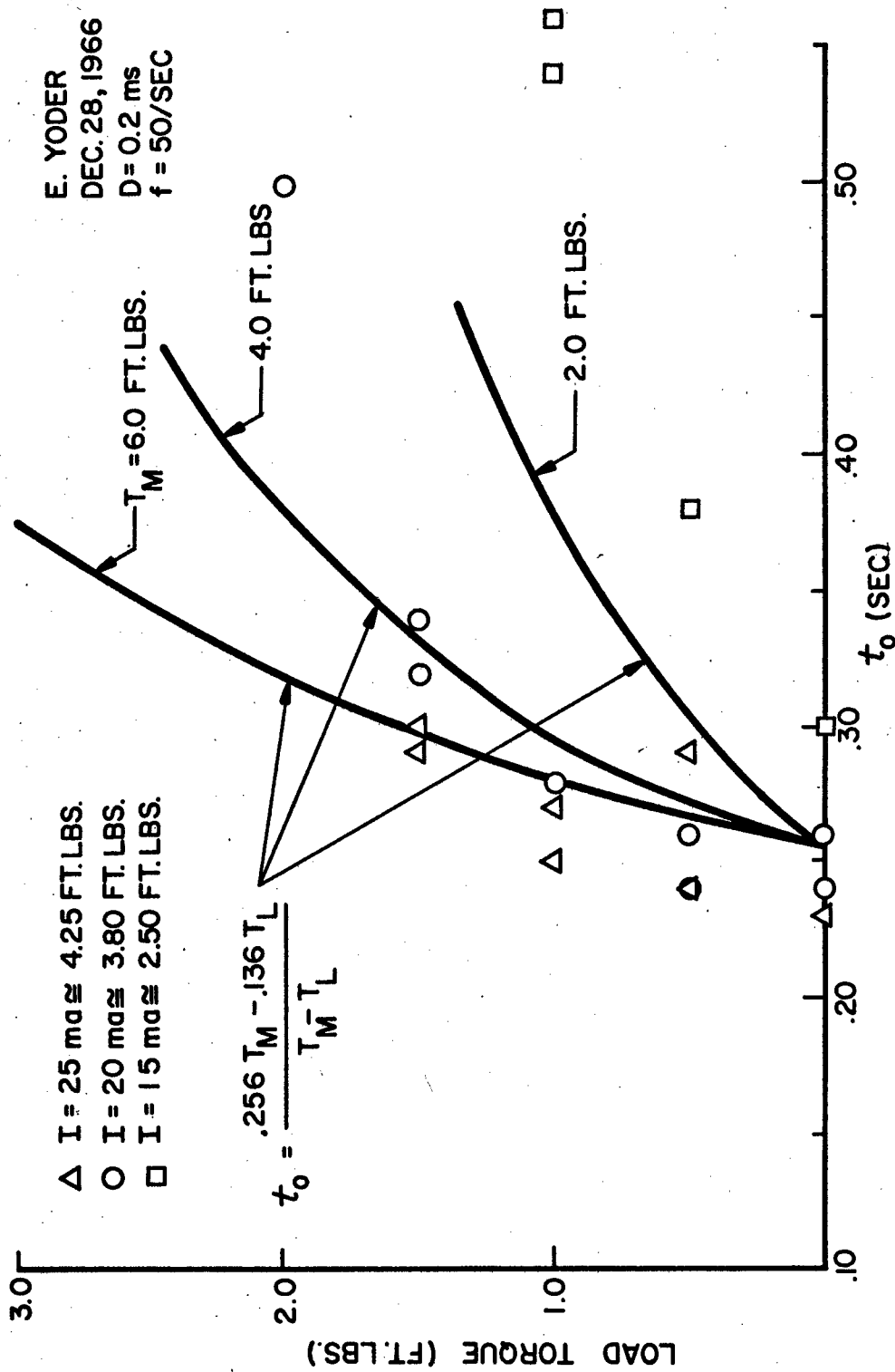
FIG. IV-19 t_o AS A FUNCTION OF LOAD TORQUE

stimulus currents. Corresponding values of muscle torque were obtained from the linearized load-velocity curves and are also indicated. The data points for $I = 20$ and 25 ma (3.80, 4.25 ft-lbs) are within 15% of the theoretical 4.0 ft-lb curve. The 15 ma (2.5 ft-lbs) data points on the other hand have larger values of t_0 than the theoretical curve has. No explanation of this discrepancy is given although this condition also prevailed in other experiments.

5. Muscle Lengthening Experiment

If a muscle is stimulated, allowed to shorten, and a heavy load is applied, the muscle will lengthen. The rate of lengthening, just as in the case of muscle shortening, is determined by the muscle viscosity. A. V. Hill[25] has shown, however, that the viscosity is about twice as large for the lengthening muscle. A series of experiments were performed to see if this could be observed. Steve Diamond, an undergraduate student, performed these experiments for a junior lab project under the author's direction. Three such experiments were conducted. The results of one of the experiments is shown in Figure IV-20. The slopes of the curves ranged from 0.90 to 1.16 with an average value of 1.0 ft-lb seconds. This viscous coefficient is about twice the value found in the muscle shortening experiments (0.49 ft-lb seconds) thus confirming Hill's prediction.
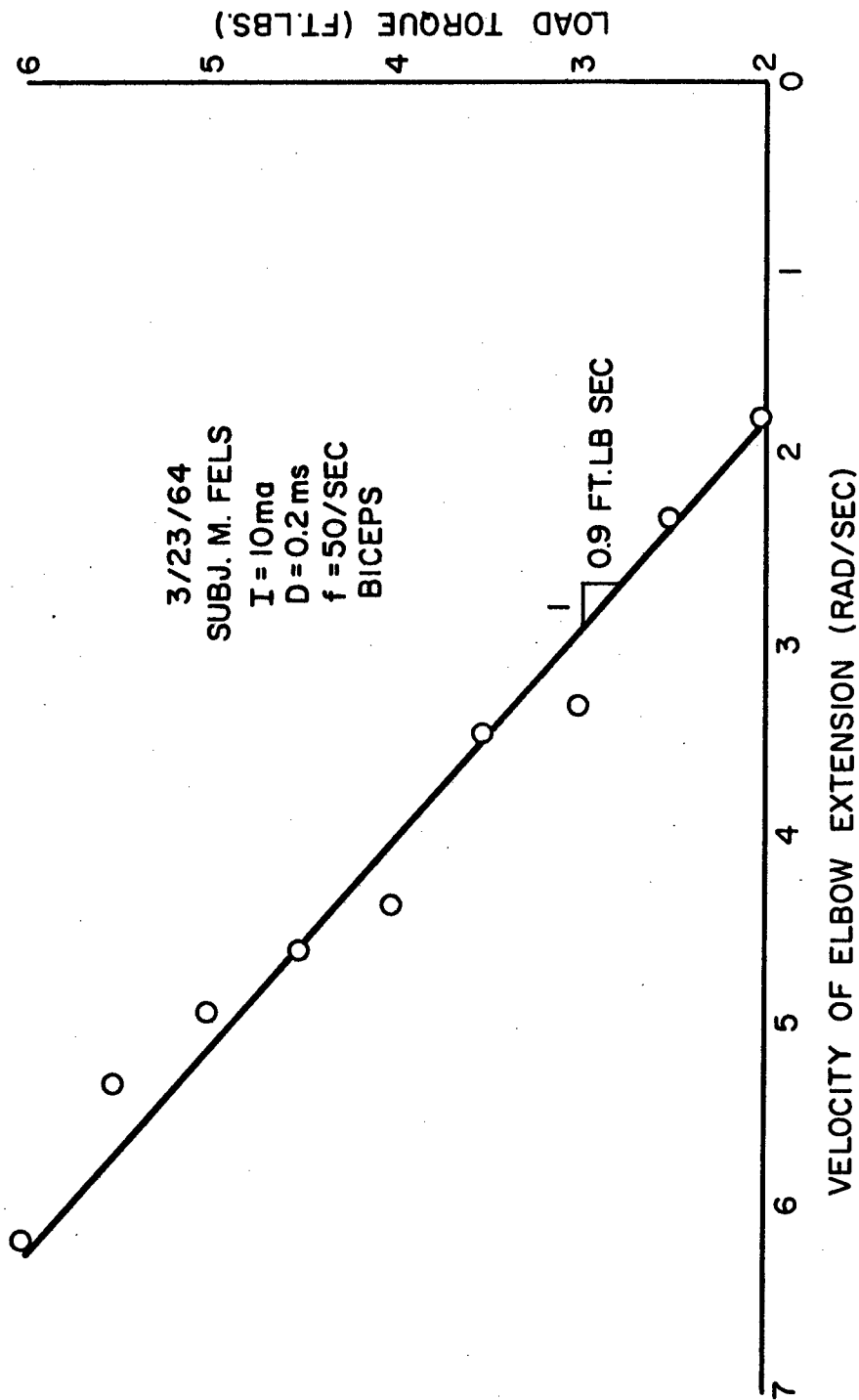
FIG. IV-20 LOAD-VELOCITY CURVES FOR LENGTHENING STIMULATED MUSCLE

CHAPTER V

CONTROL SCHEMES FOR STIMULATED MUSCLE

A. POSITION CONTROL WITH TWO ANTAGONISTIC MUSCLES

The first attempt to control the movement of a limb by electrical stimulation was aimed at duplicating, in a crude fashion, the normal physiologic control of movement. We have seen in Chapter II that normally innervated muscle has its own built-in control scheme which has at least position and velocity feedback. The first external control system was designed to be a closed-loop position-control with position-feedback. The elbow joint angle was to be controlled by alternately stimulating two antagonistic muscles in response to an error signal.

The principal flexor of the elbow joint is the brachialis muscle. Although this muscle possesses a motor point, the resulting contraction due to an external stimulus is less than the contraction of the biceps muscle stimulated with the same current. For this reason, the biceps was always used as the elbow flexor in our experiments. There is a complication, however, in that the action of the biceps during flexion also supinates the pronated forearm. This problem was controlled by fastening the forearm in a position which was mid-way between supination and pronation.

The principal extensor of the elbow joint is the triceps muscle which has three heads; the long head, the lateral head, and the medial head. There is a motor point associated with each of the heads; therefore, a choice had to be made among them. The long head is the least powerful in elbow extension and was discounted. In general, the lateral head produced the greatest contraction and was used in all the experiments. In the following discussion whenever the term flexor is used we will be referring to the biceps muscle and whenever the term extensor is used we will be referring to the lateral head of the triceps muscle.

1. The Controller

A controller was developed[73] to modulate the amplitude of stimulus voltage to the flexor and extensor muscles. The command signal (input position) can be generated by a potentiometer or any suitable voltage source. A block diagram of the over-all system is shown in Figure V-1.[*] Chronologically this system was developed by Dr. L. Vodovnik and the author in 1964. At this time the stimulus voltage-input, torque output characteristics of muscle were modeled as

$$K_4 e^{-\tau_0 s} \tag{V.1}$$

---

[*] Circuit diagram of controller is in Appendix.

142
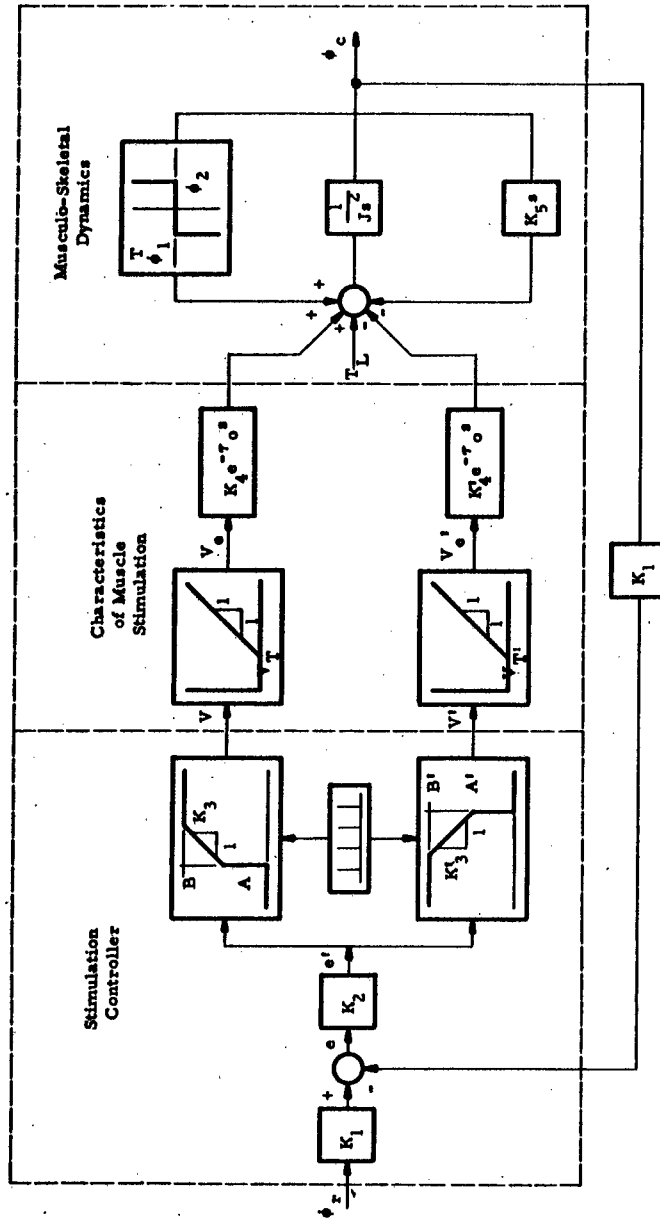
FIG. V-1. BLOCK DIAGRAM OF AGONIST–ANTAGONIST POSITION CONTROL.

which has since been improved to

$$\frac{Ke^{-\tau s}}{(s+a)^2} \qquad (V.2)$$

The two are grossly equivalent, however, if we consider the second order lag to produce a delay of $t = \frac{1}{a}$. That is, the impulse response of the second order lag is

$$te^{-at} \qquad (V.3)$$

which reaches a maximum at

$$\frac{d}{dt}\left[te^{-at}\right] = 0 \qquad (V.4)$$

$$e^{-at} - ate^{-at} = 0 \qquad (V.5)$$

or $\qquad t = \frac{1}{a} \qquad (V.6)$

Therefore the analysis should not be greatly in error if we let

$$\tau_0 = \tau + \frac{1}{a} \qquad (V.7)$$

Notice that the controller portion of Figure V-1 contains a discontinuity at e' = 0. This has been provided to ensure that the stimulus, when on, is always above threshold (V_T). Otherwise, an unwanted dead zone due to subthreshold stimuli would be included. The saturation level (B) is included to limit the current applied to the muscle. The musculo-skeletal dynamics are characterized by the extremes of flexion and extension, ϕ_1 and ϕ_2, an inertia and a viscosity. The elasticity about the joint, being quite small within ϕ_1 and ϕ_2 (Figure IV-4) was neglected. A theoretical analysis of the dynamics of the system may now be performed. If all the controller components are adjusted so that the system operates in a linear mode, the open loop transfer function for a positive e' can be approximated as

$$GH(S) = \frac{K_1 K_2 K_3 K_4 \, e^{-\tau_o S}}{S(JS + K_5)} \qquad (V.8)$$

using the mean values of the coefficients this becomes

$$GH(S) = \frac{70 \, e^{-0.05s}}{s(0.075s+1)} \qquad (V.9)$$

A Nyquist plot of this transfer function is shown in Figure V-2. From control theory the closed loop system will be unstable since

$$GH(s) = \frac{70 \, e^{-0.05 \, s}}{s \, (0.075 \, s + 1)}$$
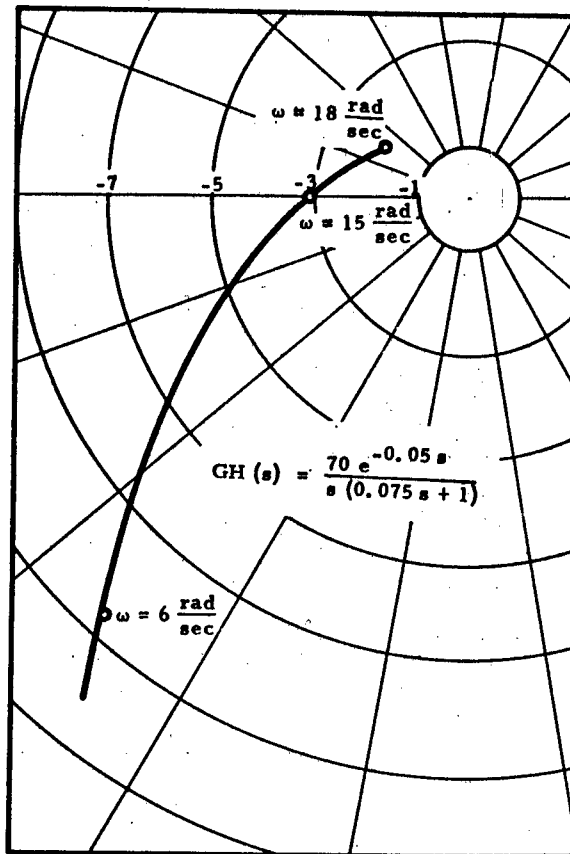
FIG. V-2. THEORETICAL NYQUIST DIAGRAM.

the curve encircles the singular point at -1. A means of compensation, therefore, is required for the closed loop operation of the system.

A twin-T network was built to perform this function. Placed in the closed loop it decreased the gain of the system at the critical frequency. From the theoretical curve of Figure V-2 this frequency is 15 rad/sec or 2.4 cps.

2. Experimental Findings

The open loop tests were conducted using a low frequency sinusoidal oscillator (Hewlett Packard Model 202A) as the input signal. Continuous recordings of the input signal voltage and the angle of the elbow joint (output) were made on a Visicorder recorder. The experimental setup is shown in Figure V-3. During an experiment, the frequency was varied in steps from 0.1 cps to 2 cps for specific values of input amplitude.

The results of the four such experiments conducted were quite similar. For frequencies below 0.6 cps the records were characteristically as shown in Figure V-4. That is, the elbow moves at a speed of about 2 rad/sec in this case to its extremes of flexion and extension (saturates) independent of the input frequency. When the frequency approaches 0.6 cps, however, the output follows an approximately sinusoidal oscillation. Figure V-5 shows a
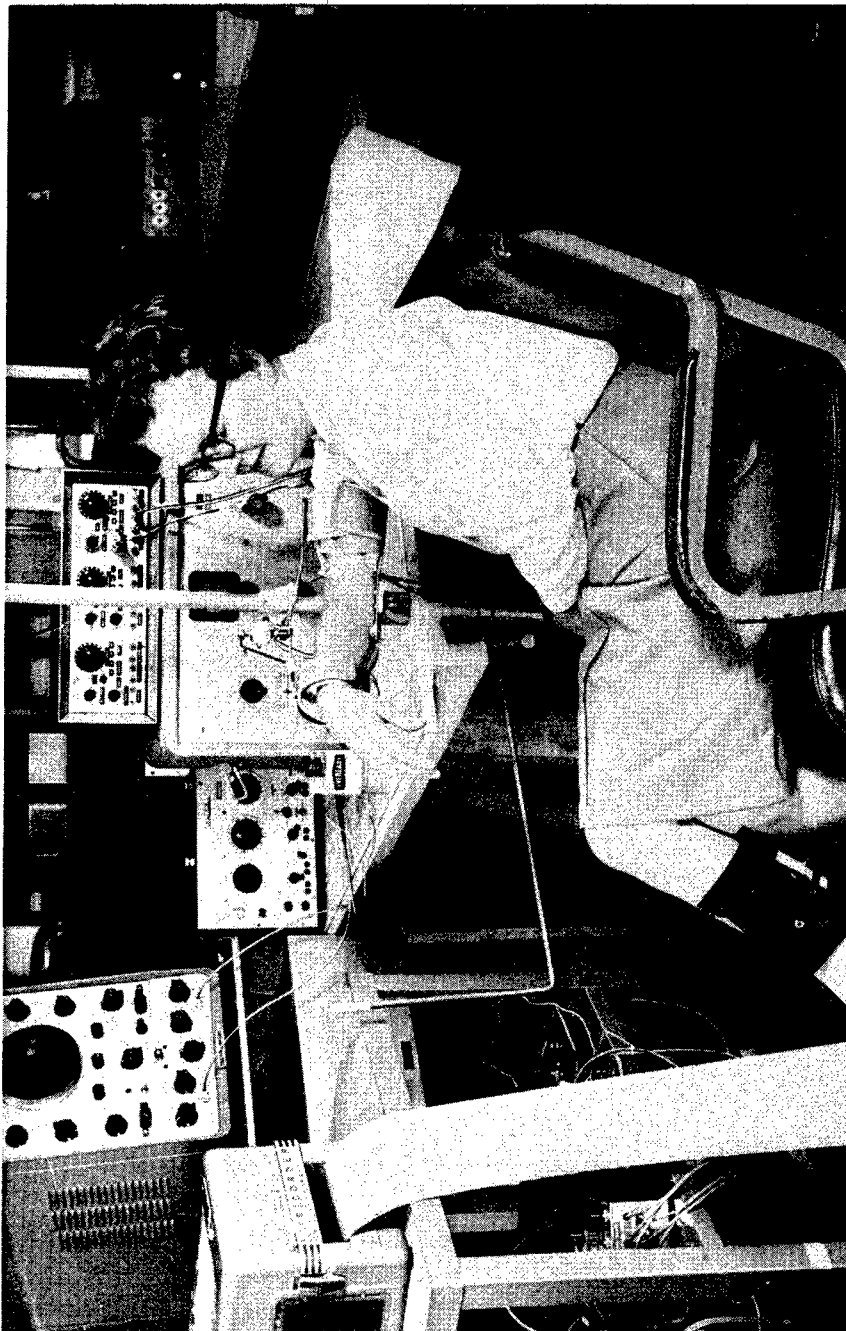
FIG. V-3. EXPERIMENTAL SETUP.

148
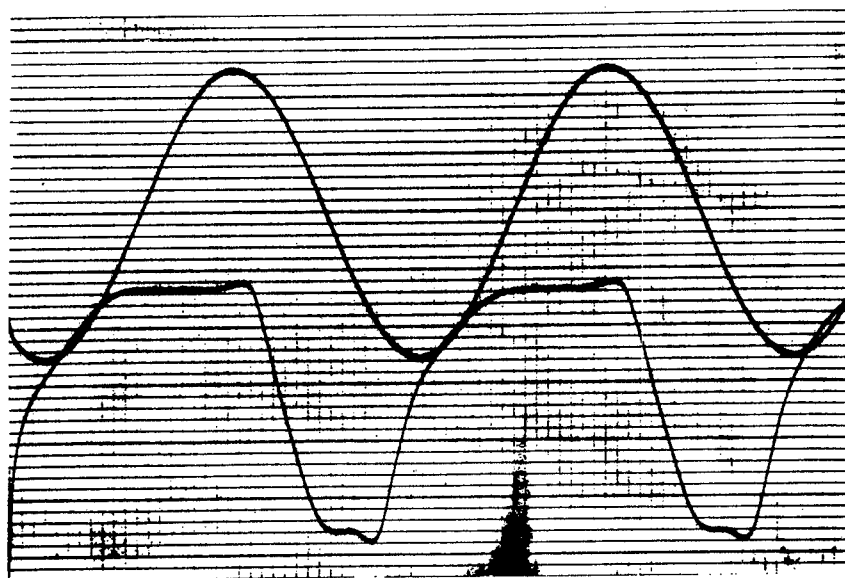
FIG. V-4 INPUT VOLTAGE AND OUTPUT ELBOW ANGLE VS.
TIME, f-0.3cps.
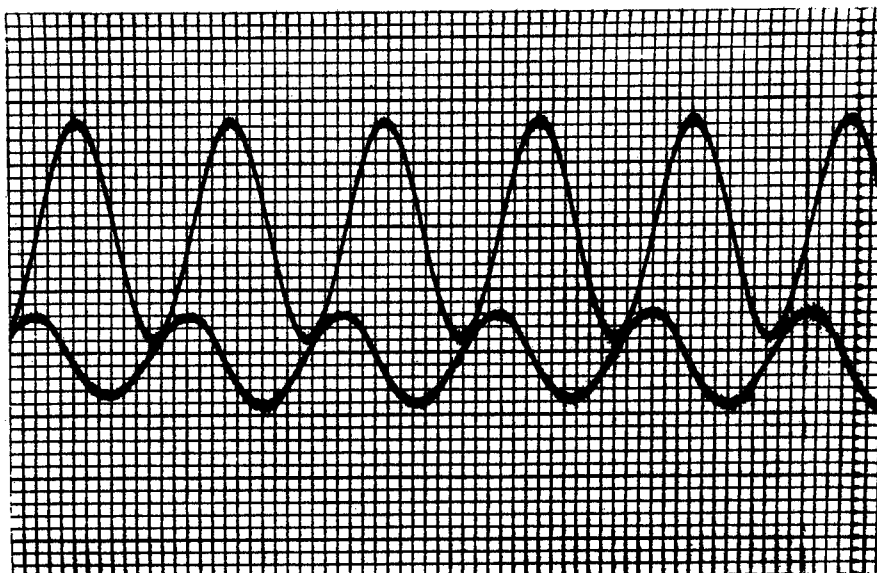
FIG. V-5. INPUT VOLTAGE AND OUTPUT ELBOW ANGLE VS.
TIME, f-0.8 cps.

typical record obtained at a frequency of 0.8 cps.

It was found that for each of the four experiments conducted that the output lagged the input by 180° at a frequency which was invariably between 0.8 and 1.0 cps. · Also the open loop gain at this frequency was greater than 1 indicating, as suspected from the theoretical analysis, that the closed loop system will be unstable unless some means of compensation is provided.

For frequencies of about 1.3 cps the output followed an erratic variation of low amplitide which at times followed a sub-harmonic of the input frequency.

As a further confirmation that compensation was necessary, the loop was closed and the compensator was omitted. An input signal was then applied to the controller and the arm began to oscillate violently at about 1 cps. The twin-T network was then inserted and the oscillations ceased. The compensator introduced a disadvantage, however, in that the dynamic response of the closed loop system was affected. Because of the attenuation of the filter, the frequency response on either side of 0.87 cps was also affected. In the static case the angular position of the elbow joint was con-trollable to within about $\pm 5^{\circ}$.

As a concluding experiment, the amplifier of the electronic bypass[69] was used to provide an external signal to the controller.

EMG pickup electrodes were placed over the extensor digitorum communis (EDC) of the left arm; then they were connected through the amplifier to the external (EXT) input jack of the controller. When the wrist was relaxed, the flexor received the maximum stimulus, whereas when the EDC was contracted maximally the extensor received the maximum stimulus. The subject was then able to control the position of his elbow joint by varying the contraction of the EDC of his left arm. No quantitative measurements were made at this time but the subject was asked to point to the experimenter's finger as the experimenter moved his finger in a random fashion in the plane of rotation of the arm. With very little training the subject was able to perform this function quite well for speeds within the normal range of movement.

B. BIDIRECTIONAL CONTROL WITH A SINGLE MUSCLE AND A FATIGUE-PREVENTING LOCK

A large class of limb movements are performed against gravity. These movements may be performed by the action of a single muscle acting against the gravitational load. A consequence of this scheme is that effort must be expended to maintain a constant joint angle. Since the muscle is subject to fatigue it would not be practical to expect the stimulated muscle to maintain a constant joint angle for any length of time. A proposed solution to this fatigue problem is to install a joint lock and stimulate the muscle

only when a <u>change</u> of joint angle is desired. Use of a joint lock requires that the control system is stable. For this reason the first past of this section will be concerned with determining the necessary parameters for stable, acceptable control system operation irrespective of the application of a lock. The lock and the locking criteria will then be discussed followed by the experimental evaluation of certain of the control systems.

1. Control Modes

The use of a counteracting load torque in the control system requires that the muscle be operated about a biased operating point. That is, the muscle must produce a torque equal to the load torque to maintain a joint angle; and fluctuations of the muscle torque about the operating point cause the limb to change position. If the load is variable an added complication arises in that the operating point must shift to compensate for the varying load. Such a varying load torque would be produced, for example, when the limb rotates about a horizontal axis. The moment arm of the load is then related by the cosine of the joint angle. We will here consider the case where the load is constant.

The first control mode considered was the closed loop position control with a switching element (Figure V-6). The characteristics of electrically stimulated muscle contain
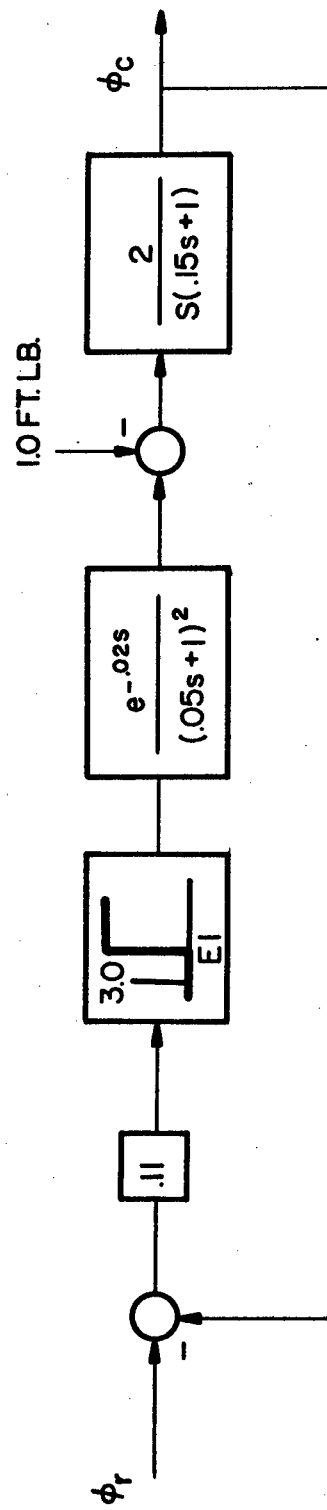
FIG. Ⅴ-6 DISCONTINUOUS CLOSED LOOP POSITION CONTROLLER

nonlinearities, i.e., dead zone, migrating motor point, angle

dependence of muscle torque, nonlinear gain and fatigue. The

switching element gates the stimulus either on or off and bypasses

the dead zone and nonlinear gain. That is, the stimulus is either

zero or some level above the threshold. This system was modeled

on the Univac 1107 digital computer using the MIMIC simulation

language. Figure V-7 shows the step response of this system for

two different values of dead zone (E_1) of the switching element.

The loop gain and dead zone of the system were varied in an

attempt to obtain acceptable performance. In each case the

response contained a limit cycle of about 1.0 cps. Increasing the

size of the dead zone decreases the amplitude of the limit cycle but

in so doing the controller becomes insensitive to small changes in

the input signal. Also, the load imposes a steady state error on the

joint angle. For these three reasons then: a limit cycle, dead

zone for the input signal, and high load sensitivity, the closed loop

position control with a switching element was judged to be un-

acceptable. If such a discontinuous controller was poor, perhaps

a continuous closed loop position system would be better.

The switching element was replaced by the discontinuous

plus proportional element shown in Figure V-8. This is the same

type of element as used in the controller of Section V A. Any error
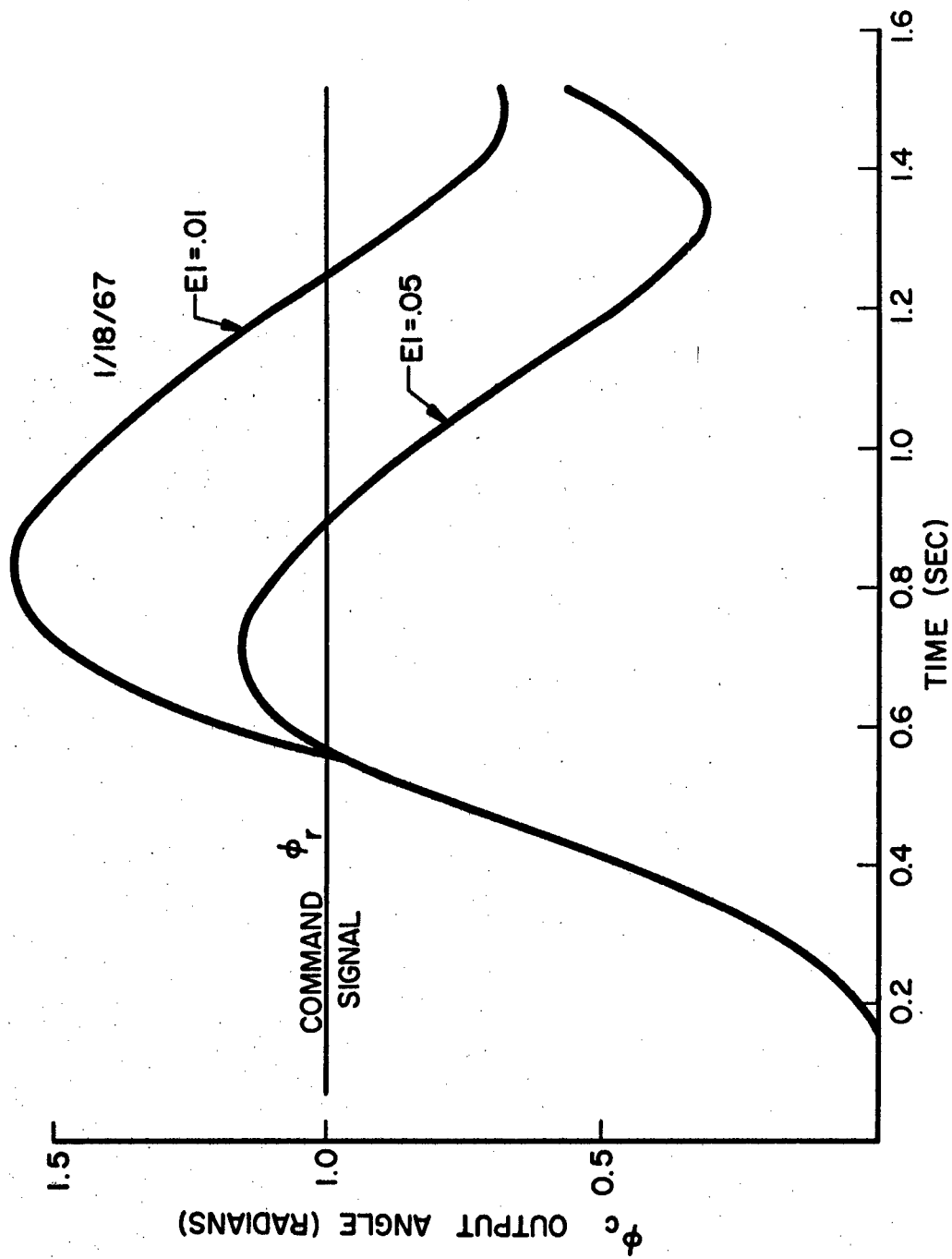
FIG. $\underline{\text{V}}$ -7 THEORETICAL STEP RESPONSE OF DISCONTINUOUS CLOSED LOOP POSITION CONTROLLER
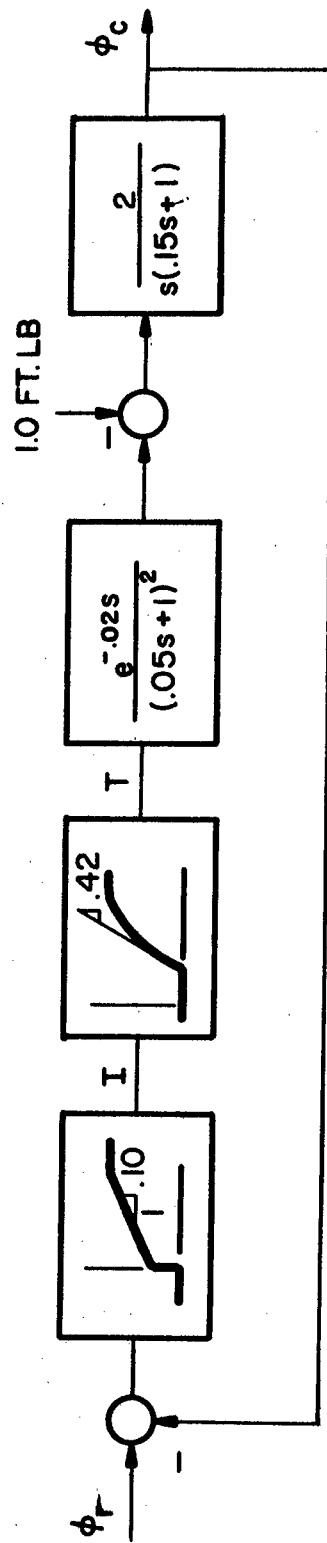
FIG. Ⅴ - 8 PROPORTIONAL CLOSED LOOP POSITION CONTROLLER

signal produces a stimulus which is above the threshold value of the muscle. This system was also modeled on the Univac 1107 and the step response is shown in Figure V-9. The loop gain (.084) was calculated to give stable operation. The critical gain was found to be .114 at a frequency of 6.2 rad/sec. The response of the system, though stable, is also very load sensitive. The load sensitivity may be calculated,

$$\frac{\phi_c}{T_L} = - \frac{\dfrac{2}{s(.15s+1)}}{1 + \left[\dfrac{2}{s(.15s+1)}\right]\left[\dfrac{.042\ e^{-.02s}}{(.05s+1)^2}\right]} \qquad (V.10)$$

$$= \frac{-2\ (.05s+1)^2}{s(.15s+1)(.05s+1)^2 + .084\ e^{-.02s}} \qquad (V.11)$$

Applying a unit step change in load and using the final value theorem:

$$\phi_c \bigg|_{t=\infty} = \lim_{s \to 0} \left[\frac{-2\ (.05s+1)^2}{s(.15s+1)(.05s+1)^2 + .084\ e^{-.02s}}\right]$$

$$(V.12)$$

$$= -23.8\ \text{rad/ft-lb}$$
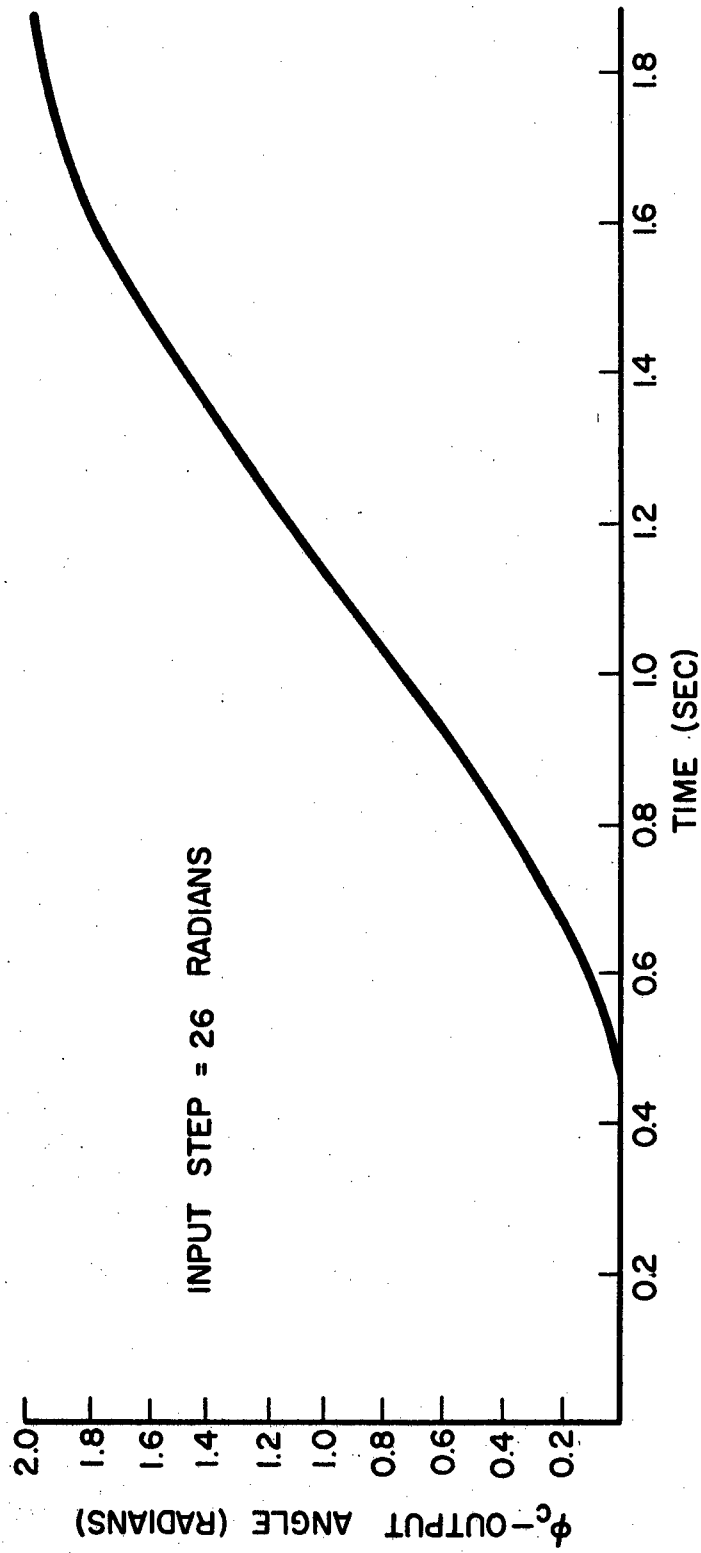
FIG. $\overline{\text{V}}$-9 THEORETICAL STEP RESPONSE OF PROPORTIONAL CLOSED LOOP POSITION CONTROLLER

The closed loop position controller would therefore have a static

transfer function

$$\phi_c = \phi_r - 23.8 \, T_L \qquad\qquad (V.13)$$

The load sensitivity is very high. Compensation schemes, however,

could theoretically be applied which would allow a higher loop gain

and therefore better regulation.

The next type of control considered was a velocity control.

Since the limb is to be controlled by a human, he can guide the

limb to a desired position by controlling its velocity. The simplest

form of this control is the open loop velocity control as shown in

Figure V-10. This system, of course, is stable but just as the

position control, it is quite load sensitive. That is, the greater

the load the slower the limb moves for a given input signal. This

error in output velocity due to the load is given by

$$\frac{\dot{\phi}_c}{T_L} = \frac{-2}{.15s+1} \qquad\qquad (V.14)$$

Applying a unit step change in load and using the final value

theorem

$$\dot{\phi}_c \Big|_{t=\infty} = -2 \text{ rad/sec/ft-lb}$$
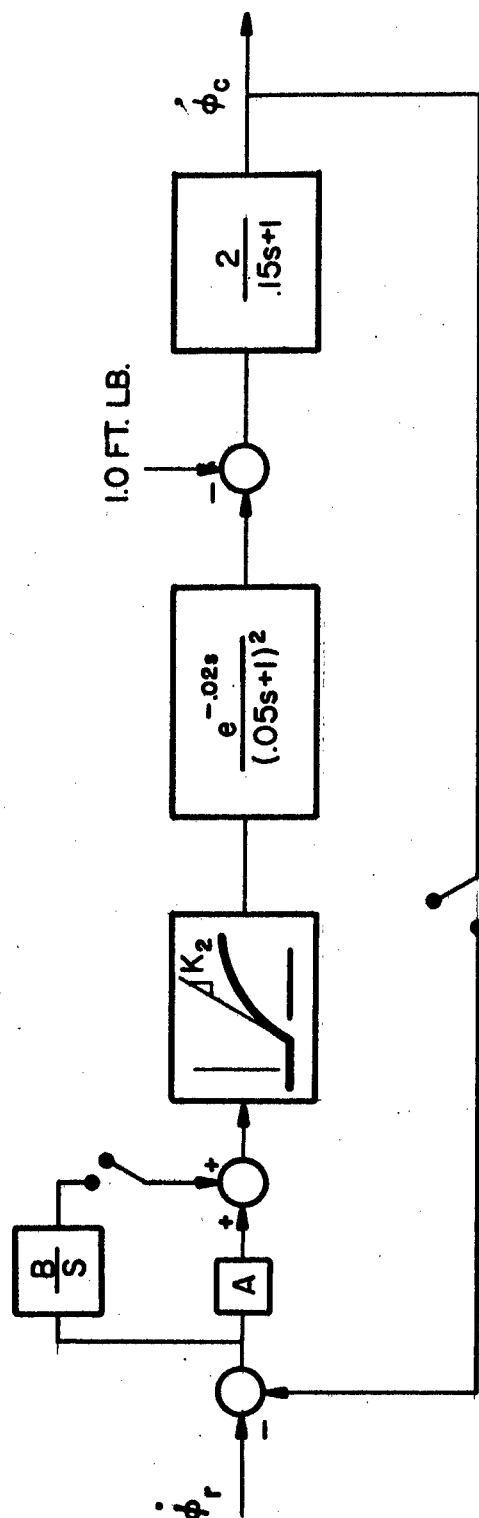
FIG. V-10   VELOCITY CONTROLLERS

Closing the velocity loop (Figure V-10) has the effect of decreasing this load sensitivity, i.e.,

$$\frac{\dot{\phi}_c}{T_L} = \frac{-\dfrac{2}{.15s+1}}{1 + \left[\dfrac{2}{(.15s+1)}\right]\left[\dfrac{AK_2 e^{-.02s}}{(.05s+1)^2}\right]} \qquad (V.15)$$

$$= \frac{-2(.05s+1)^2}{(.15s+1)(.05x+1)^2 + 2AK_2 e^{-.02s}} \qquad (V.16)$$

A unit step change in load gives the final value

$$\dot{\phi}_c \bigg|_{t=\infty} = -\frac{2}{1+2AK_2} \qquad (V.17)$$

The critical loop gain for stability was found to be $2AK_2 = 3.15$ at a frequency of 20 rad/sec. The error in velocity is then equal to

$$\dot{\phi}_c \bigg|_{t=\infty} = -.482 \text{ rad/sec/ft-lb}$$

Even greater load insensitivity can be achieved by using a proportional plus integral controller (Figure V-10). The velocity error due to the load then is given by:

$$\frac{\dot{\phi}_c}{T_L} = - \frac{\dfrac{2}{.15s+1}}{1 + \left[A + \dfrac{B}{s}\right]\left[\dfrac{K_2 e^{-.02s}}{(.05s+1)^2}\right]\left[\dfrac{2}{.15s+1}\right]} \qquad (V.18)$$

$$= \frac{2(.05s+1)^2(s)}{s(.05s+1)^2(.15s+1) + (As+B)(2K_2 e^{-.02s})} \qquad (V.19)$$

$$\dot{\phi}_c \bigg|_{t=\infty} = 0 \quad \text{rad/sec/ft-lb}$$

The critical gains for stability were calculated. For the proportional part a gain of 1.65 was critical; for the integral part it was 11.6. The frequency at the critical point was 15 rad/sec.

These three velocity control systems were simulated on the Univac 1107 computer using the MIMIC simulation language. The velocity outputs of each system to a step input of 1.5 rad/sec are shown superimposed in Figure V-11. The load sensitivity of the open loop and closed loop proportional systems is quite obvious. Both the closed loop systems, however, are oscillatory, which may, at first glance, seem unacceptable. Remember, however, that although these are velocity controls, what we are

162
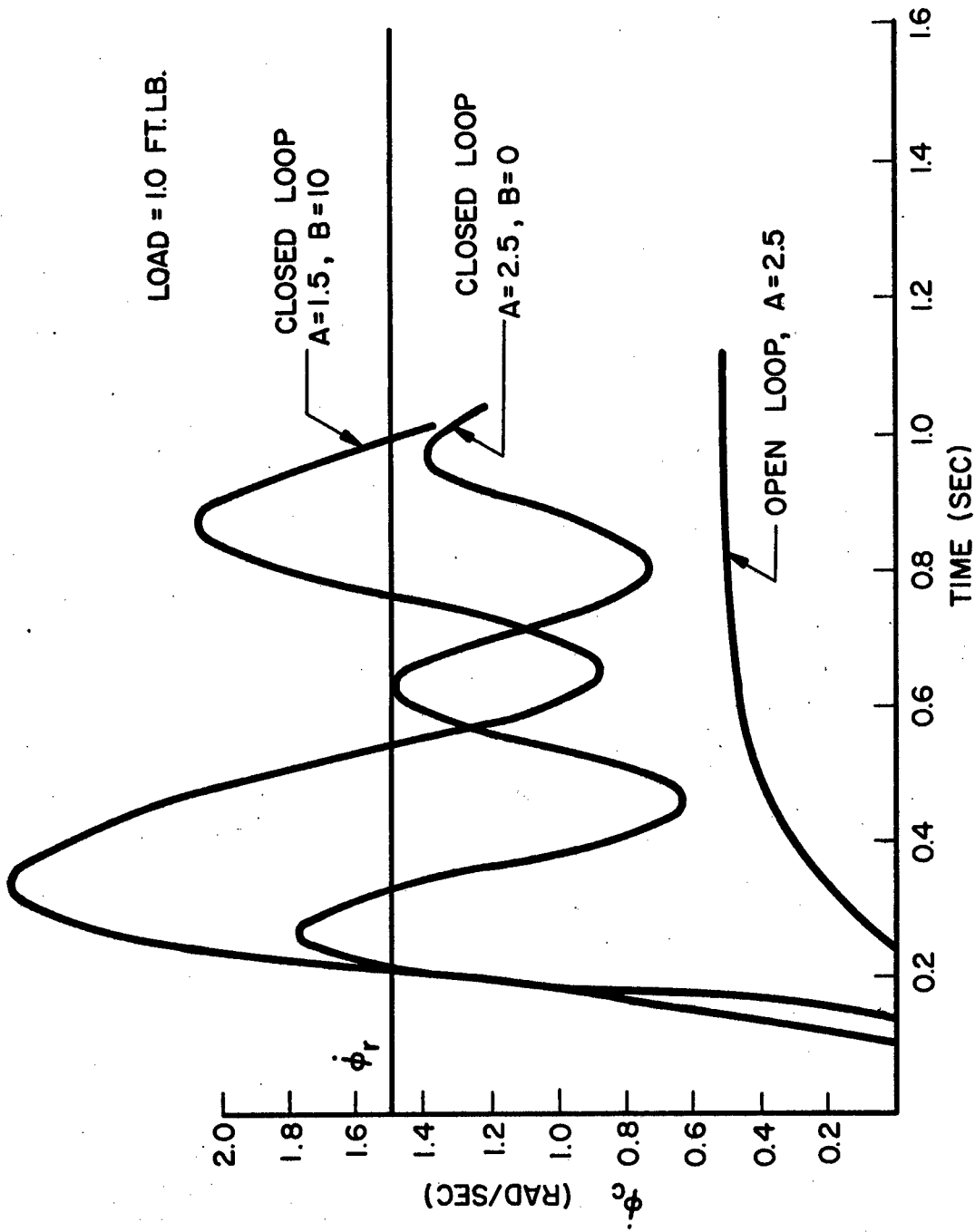
FIG. Ⅴ-11 RESPONSE OF VELOCITY CONTROLLERS TO STEP INPUT

really trying to control is the position. The integral of the velocity curves, the position curves, are shown in Figure V-12. Notice that although there are slight oscillations, the curves closely approximate ramps.

2. Joint Lock

One of the biggest problems encountered in this project was finding a small, lightweight joint lock which had the necessary torque capacity. The lock should be capable of maintaining the weight of the lower arm plus a light load in the hand. An average forearm and hand weighs 3.7 lbs. and has a moment arm of 6.7 in. (5) Adding a 2 lb. weight in the hand increases the load to about 4.2 ft-lbs. The commercially obtainable clutches and brakes with this torque capacity were all about 4 inches in diameter by about 2 inches high and weighed about 10 lbs. It was obvious that such a brake could not be used on an orthosis so work was begun to design and build one. Clearly any type of friction lock would be too large. A ratcheting mechanism would support the load and be lightweight but it could only by indexed at discrete angles which are separated by at least 5 degrees. This corresponds to positioning the finger-tips in increments of about 1.5 inches.

A bidirectional lock which would theoretically have infinite resolution was designed and built. This lock shown in Figure V-13

164
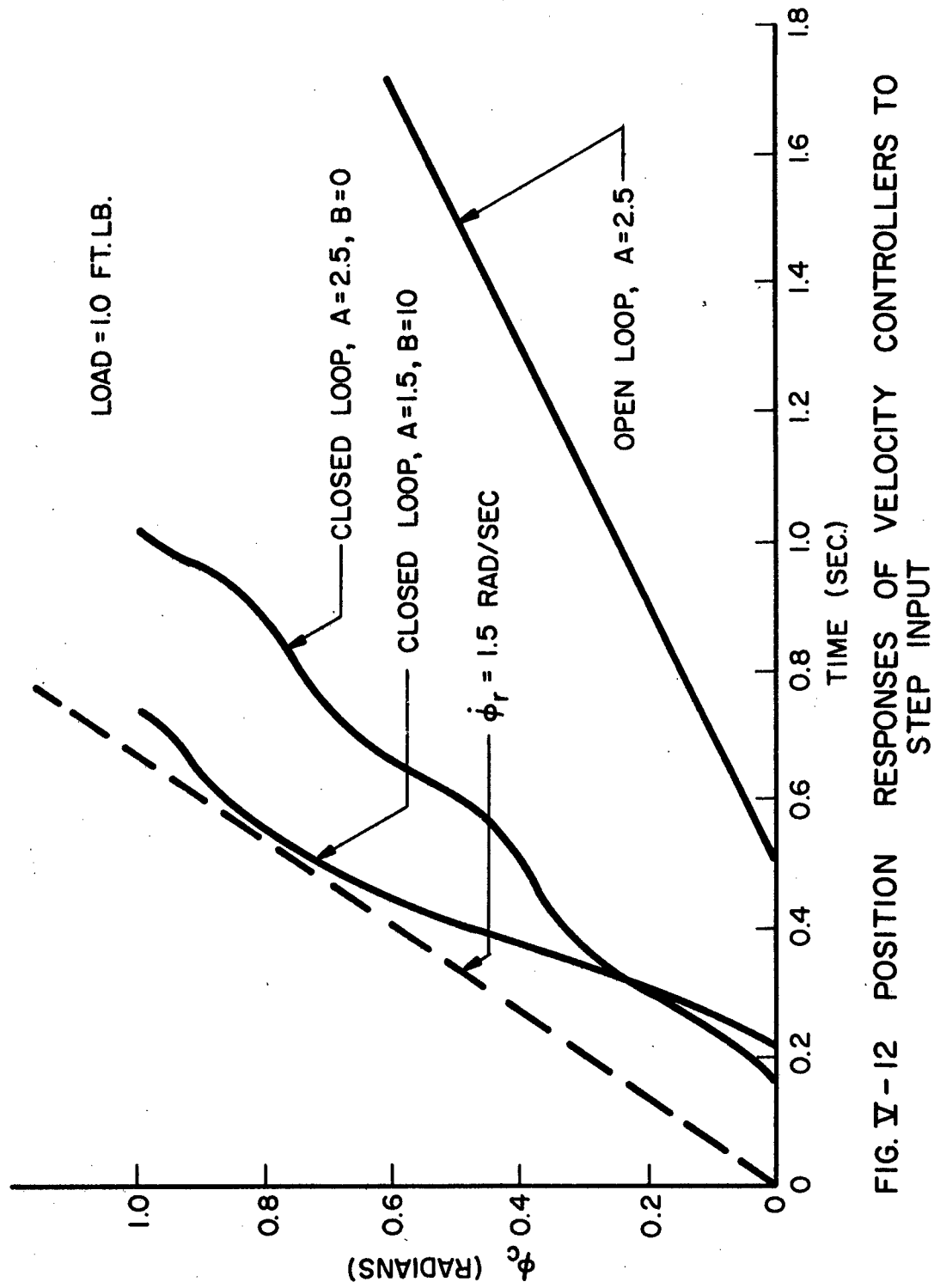
FIG. Ⅴ-12 POSITION RESPONSES OF VELOCITY CONTROLLERS TO
STEP INPUT
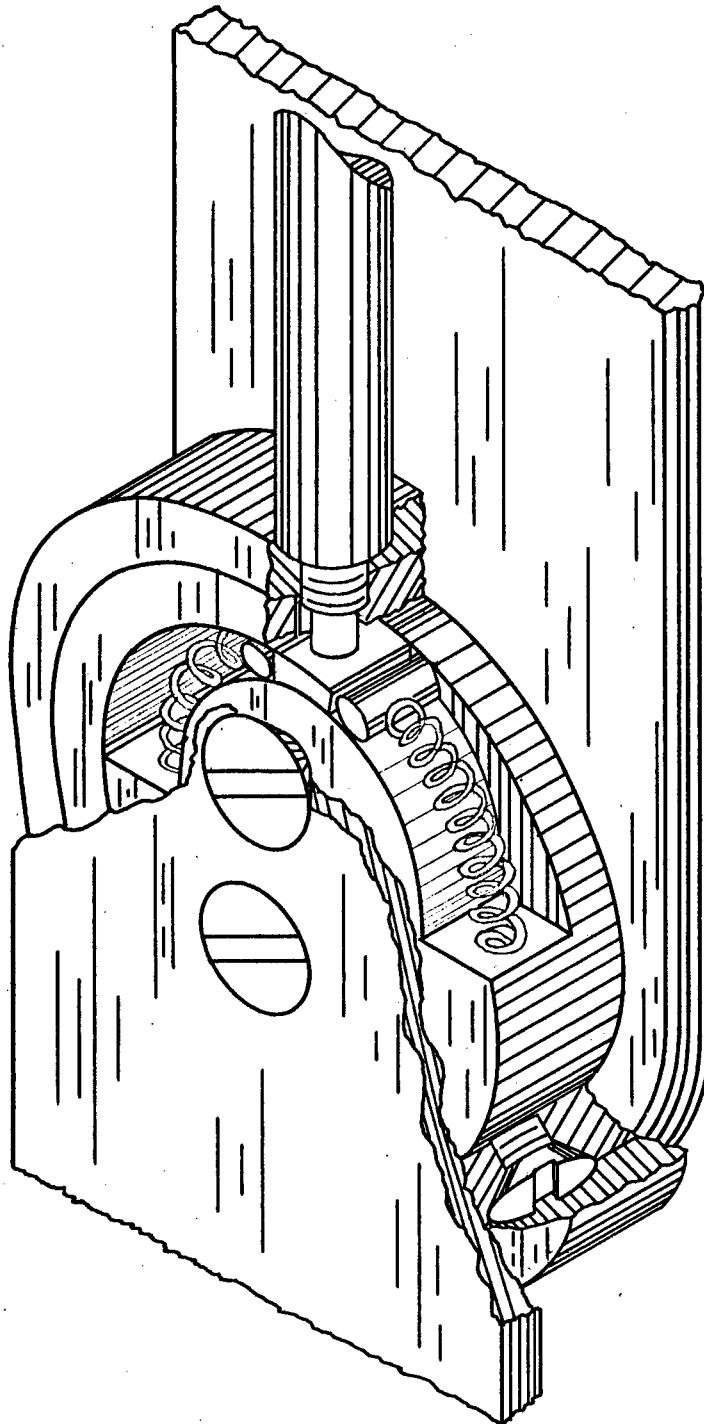
FIG. V - 13 BIDIRECTIONAL, ROLLER WEDGE,
JOINT LOCK

works on the roller wedge principle. In the lock state both pins are forced into the narrowing annular space between the rotating shaft and the stationary outer race. If the shaft moves in either direction the pin wedges tighter. If movement is desired in one direction the lever pushes the pin into the larger annular space and allows movement only in this direction. This type of a lock requires that the contact surfaces be hardened, otherwise the very large forces* at the contact points will cause the surfaces to dimple and the lock will be ineffective. The major shortcoming of this lock is that only two pins are used. This produces radial forces on the shaft which must be balanced by the bearing surfaces. Under these high forces the bearing surfaces wore and created much "slop" in the operation of the lock. A series of wedge pins spaced circumferentially around the shaft would take the load off the bearings and probably work better. A device of this configuration was found to be commercially available. It is a Torrington drawn cup roller clutch. A model RCB-081214 roller clutch was supplied by the manufacturer. This unit which has a 73 in-lb. capacity weighs only .043 lbs. Including two roller bearings, the over-all dimensions are 3/4 in. diameter by 7/8 in. long and it fits a hardened 1/2 in. diameter shaft.

---

* See Appendix.

In its purchased state the roller clutch may not be released. It was therefore modified as indicated in Figure V-14. In its normal operation, the cage is kept from rotating with respect to the outer race by means of small protrusions on the cage which fit into grooves in the outer race. These protrusions on the cage were machined off, thereby allowing the cage to be rotated with respect to the outer race. To disengage the lock then, the cage is rotated clockwise, forcing the pins into the larger annular space. This prevents the pins from wedging and allows the shaft to rotate in either direction. Bidirectional locking can be obtained by mounting another unit on the shaft which locks in the opposite direction. The cage itself could not be manipulated externally so a bushing was expoxied to the cage and provided an external connection for a solenoid actuator. This lock was mounted on the elbow shaft of the experimental apparatus and was found to work very well. The lock has supported 7.5 ft-lbs and can be released by turning the bushing a few degrees. A small solenoid is used to produce this rotation. This is possible because, in use, the lock is only released when it is unloaded. That is, the lock is only released when the muscle is fully supporting the load. The criteria for turning the lock on or off will now be discussed.
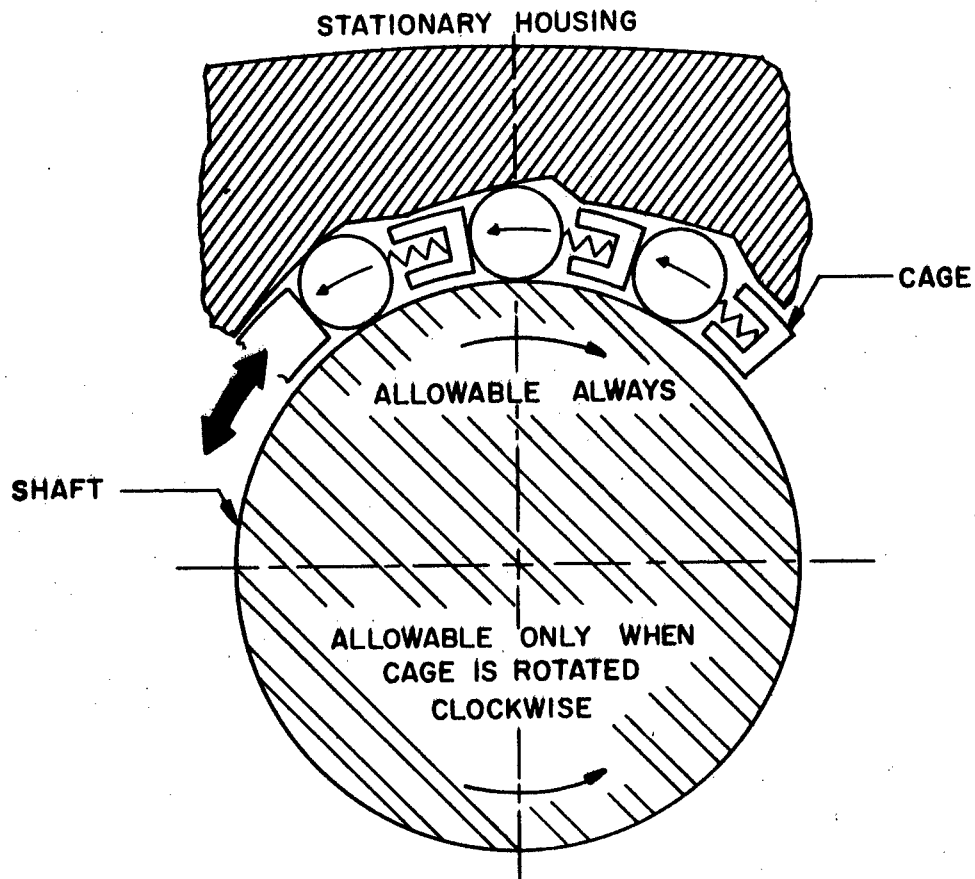
FIG. Ⅴ-14 RELEASE PRINCIPLE OF ROLLER CLUTCH

The easiest way to control the lock, in terms of hardware at least, is an on-off switch. The patient would then be required to control the position of his limb and the state of the lock. This may be acceptable if he were expected to control only a single joint but it would place a large burden on the patient if he were to control a multi-joint orthosis. The decision was made therefore to control the actuation and de-actuation of the lock automatically. Different schemes would be necessary, of course, depending upon whether the position or velocity system were used. A lock control system was first of all synthesized for the position system. This system is shown schematically in Figure V-15. In principle there are actually three control systems contained within this system: a position control, a zero torque control, and a lock actuation control. The function of the zero torque loop is to reduce the torque on the brake to zero by stimulating the muscle sufficiently to support the load. The lock is then released and simultaneously the control mode is changed to position control.

More specifically, the switches (A, B, C) are controlled by the variables e(error), T_B (torque on the brake) and $\dot{\phi}_c$ (velocity of the output angle). Relays (1, 2, 3, 4), "and" gates, and flip flops F_1, F_2, are used to perform the switching logic. The table in Figure V-16 shows the switching operations at times t_0 to t_4

170
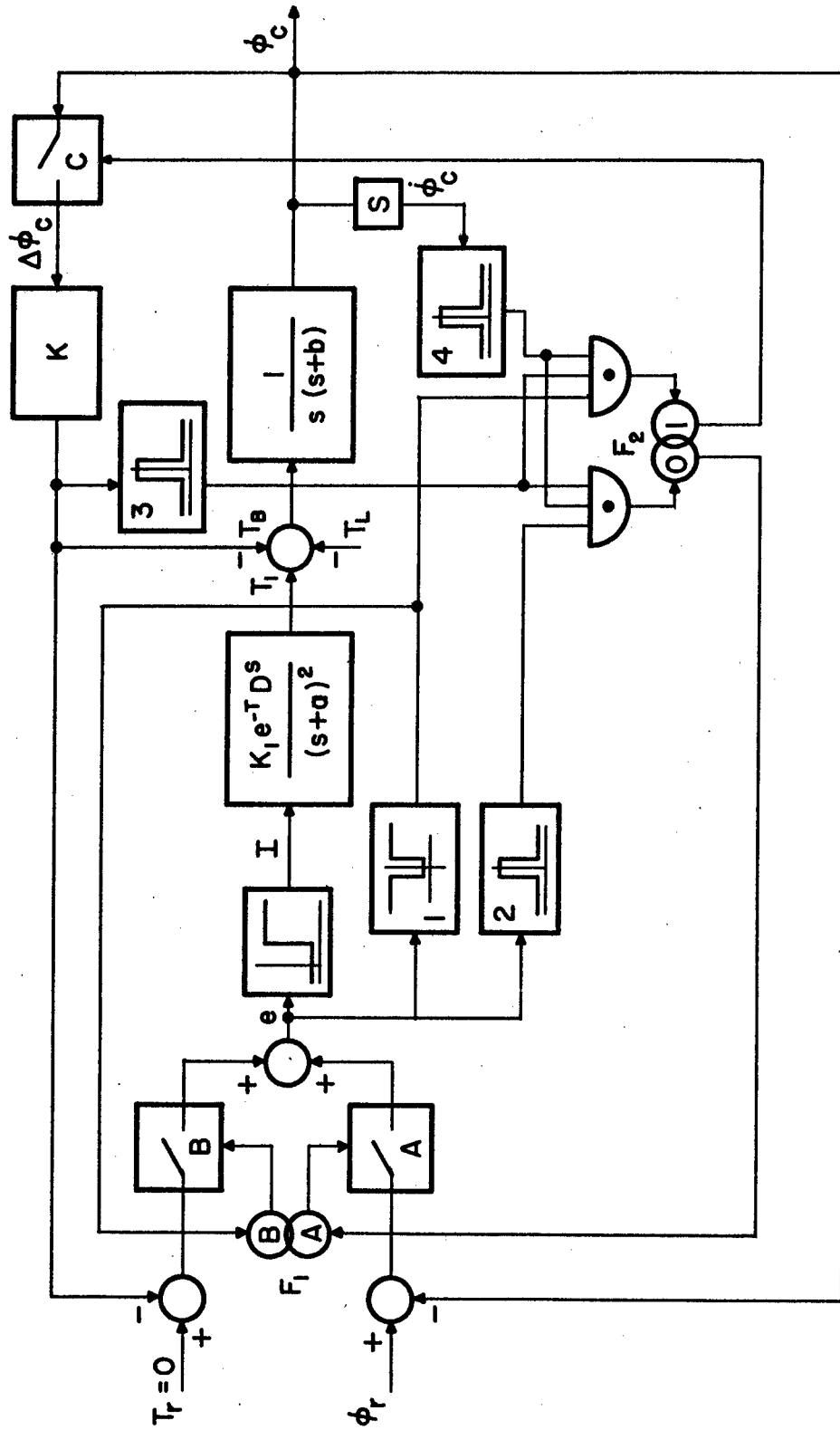
FIG. Ⅴ-15 POSITION CONTROL UTILIZING A JOINT LOCK

	e	T_B	$\dot{\phi}_C$	A	B	C	
t_0	0	1	0	1	0	1	REST
t_1	1	1	0	0	1	1	$\Delta\phi_r$ INPUT TORQUE LOOP CONTROL
t_2	0/1	0	0	1	0	0	LOCK RELEASE, POSITION LOOP CONTROL
	1	0	1	1	0	0	MOVEMENT
t_3	0	0	1	1	0	0	e IN DEAD ZONE
t_4	0	0	0	1	0	1	LOCK ACTUATION
	0	1	0	1	0	1	REST
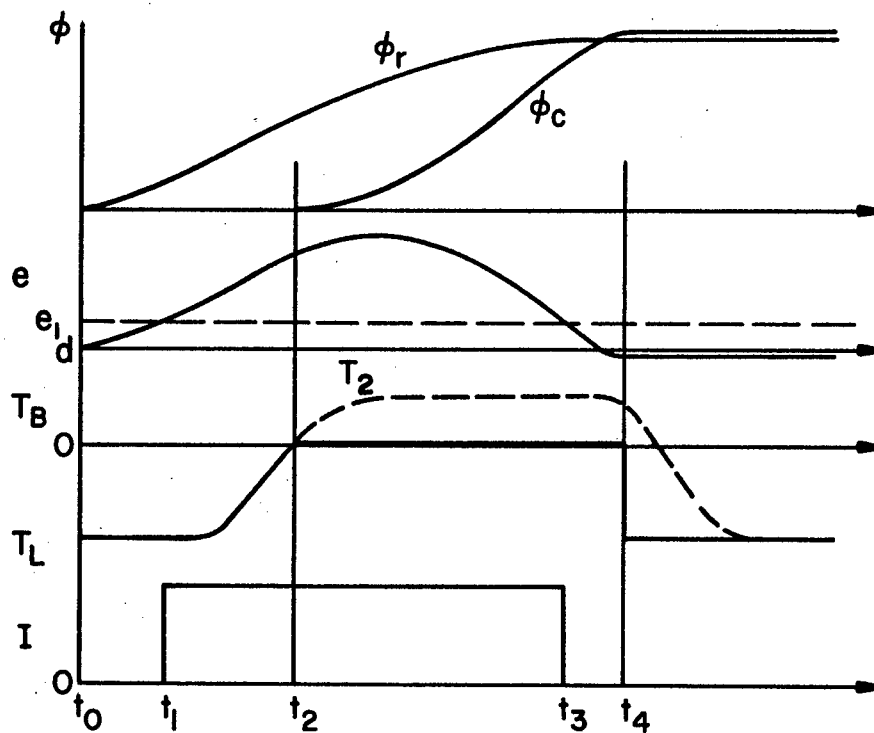
FIG. V-16 STEP RESPONSE OF POSITION CONTROLLER UTILIZING A JOINT LOCK

during the response to a positive command signal ($\Delta\phi_r$). In the table logical "1" implies a signal of sufficient magnitude to activate the relays, or in the case of switches, a switch closure.

At t_0 the system is at rest. Switch A is closed making it a closed loop position system. Switch C is also closed so that the lock is actuated and imposes a high stiffness (K) to the joint. At t_1, $e > e_1$, and a stimulus I is applied to the muscle. This value of e also passes through relay 1 then back to flip flop F_1, and causes switch B to close and A to open. The system is now a closed loop torque system with zero input. The stimulated muscle causes T_1 to increase thereby relieving the joint lock of the load torque (T_L). When the brake torque (T_B) is "0" this signal passes through 3 and is "anded" with $e > e_1$ and $\dot{\phi}_c = 0$ and causes F_2 to switch to "0". When this happens (t_2) two things occur simultaneously: switch C opens releasing the brake and F_1 is switched causing B to open and A to close. The system is once again a closed loop position control and ϕ_c increases. The value of e reaches e_1, at t_3 and the stimulus I goes to zero. When e, T_B, and $\dot{\phi}_c = 0$, F_2 switches to 1 closing C which actuates the lock (t_4). The system is now at rest in the new position. In a similar manner the response to a negative command signal can be described.

The closed loop position system as we have previously seen is very load sensitive, and a complex compensation scheme would be necessary to make it at all feasible.

A simpler solution was therefore sought using the velocity type of controller. The system to be discussed was developed jointly by the author and Barry Romich, undergraduate student, for his senior lab project. After many modifications of the original design, the system shown in Figure V-17 was finally implemented. This system also contains three different control systems: an open loop torque control, velocity control, and a digital control for the lock. At rest the lock is actuated and supports the load. To begin any movement the input signal must be raised until the muscle supports the load. This is the open loop torque system. As the input increases to support the load it triggers the flip flop which energizes a solenoid to release the lock. Because of the character-istics of the lock it may not release until the torque on the lock is zero. The lock therefore releases only when the muscle fully supports the load. At this stage the limb may be moved in a posi-tive or negative direction. The lock is then actuated by a slight positive velocity (against the load), or in the case of a movement in the negative direction (with the load), when the limb comes to rest. The lock always allows movement in the positive direction.

FIG. $\underline{\text{V}}$-17 VELOCITY CONTROLLER UTILIZING A JOINT LOCK

This complete system was implemented as shown in the schematic

diagram of Figure V-18. More complete circuit diagrams may be

found in the Appendix. Notice that the three types of velocity con-

trollers may be used: open loop, proportional closed loop, and

proportional plus integral closed loop.

3. Evaluation of Velocity Controllers

Experiments were conducted using the above described

control systems. In each case a permanent record was made on a

Visicorder recorder of the command signal ($\dot{\phi}_r$), the stimulus (I),

the angular velocity of the elbow ($\dot{\phi}_c$) and the elbow angle itself

(ϕ_c). (See Figure V-19). The first point of interest was the

stability of the proportional closed loop velocity system. The loop

gain was increased until the velocity oscillated considerably when

an input signal was applied. Figure V-20 shows this underdamped

response. Notice that the frequency of oscillation is approximately

3.0 cps. This value is very close to the frequency predicted by the

MIMIC simulation ($\sim$2.94 cps) and the value calculated in Section

VB1 (20 rad/sec = 3.18 cps). The critical value of loop gain was

also found in this section to be 3.15. The gains of the electronic

components in the loop are easily available from Figure V-18. The

operational amplifier M-2 was set at a gain of 3.5 volts/volt; the

modulator had a gain of 1.7 ma/volt, and the tachometer had a

FIG. V-18 SCHEMATIC DIAGRAM OF VELOCITY CONTROLLER UTILIZING JOINT LOCK
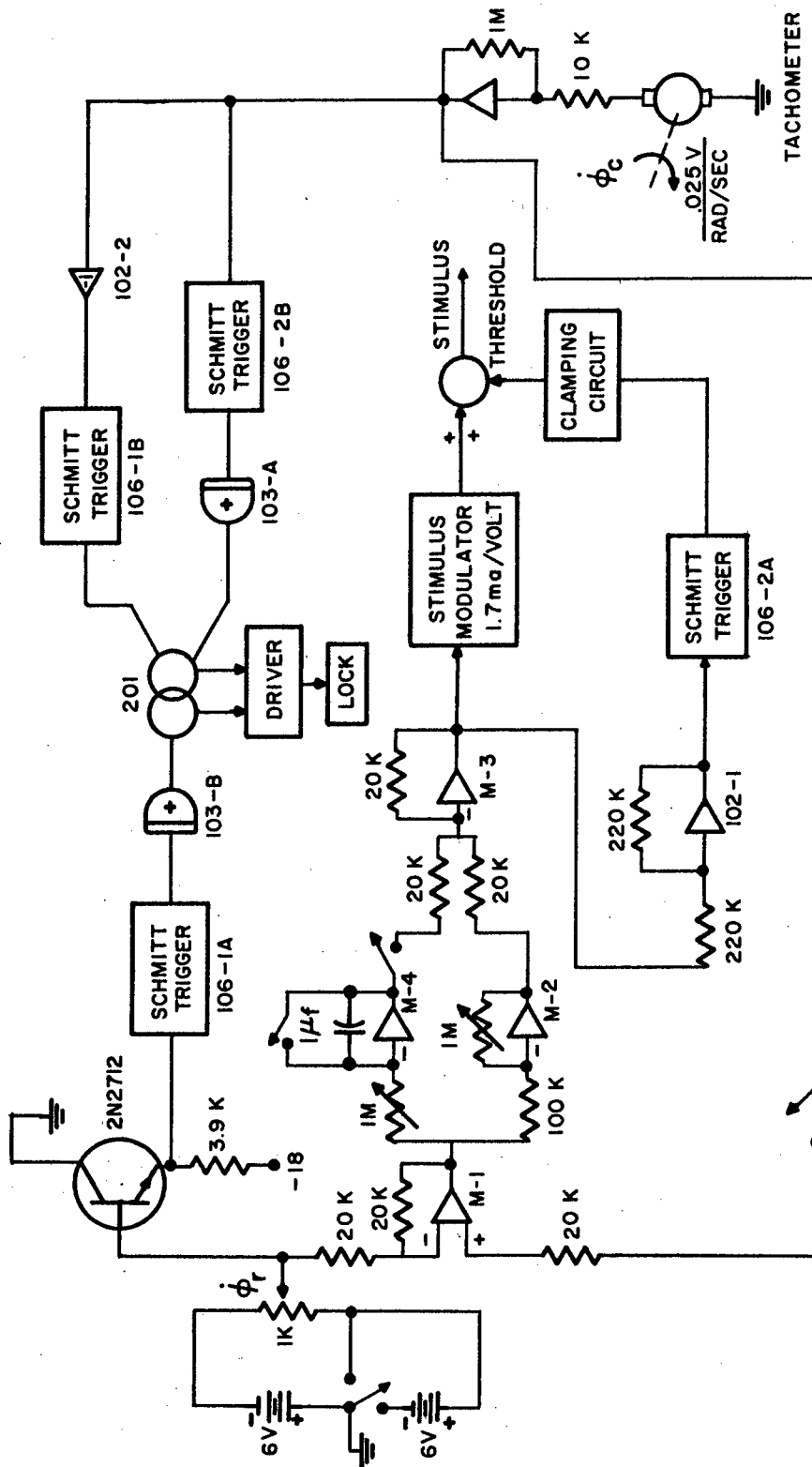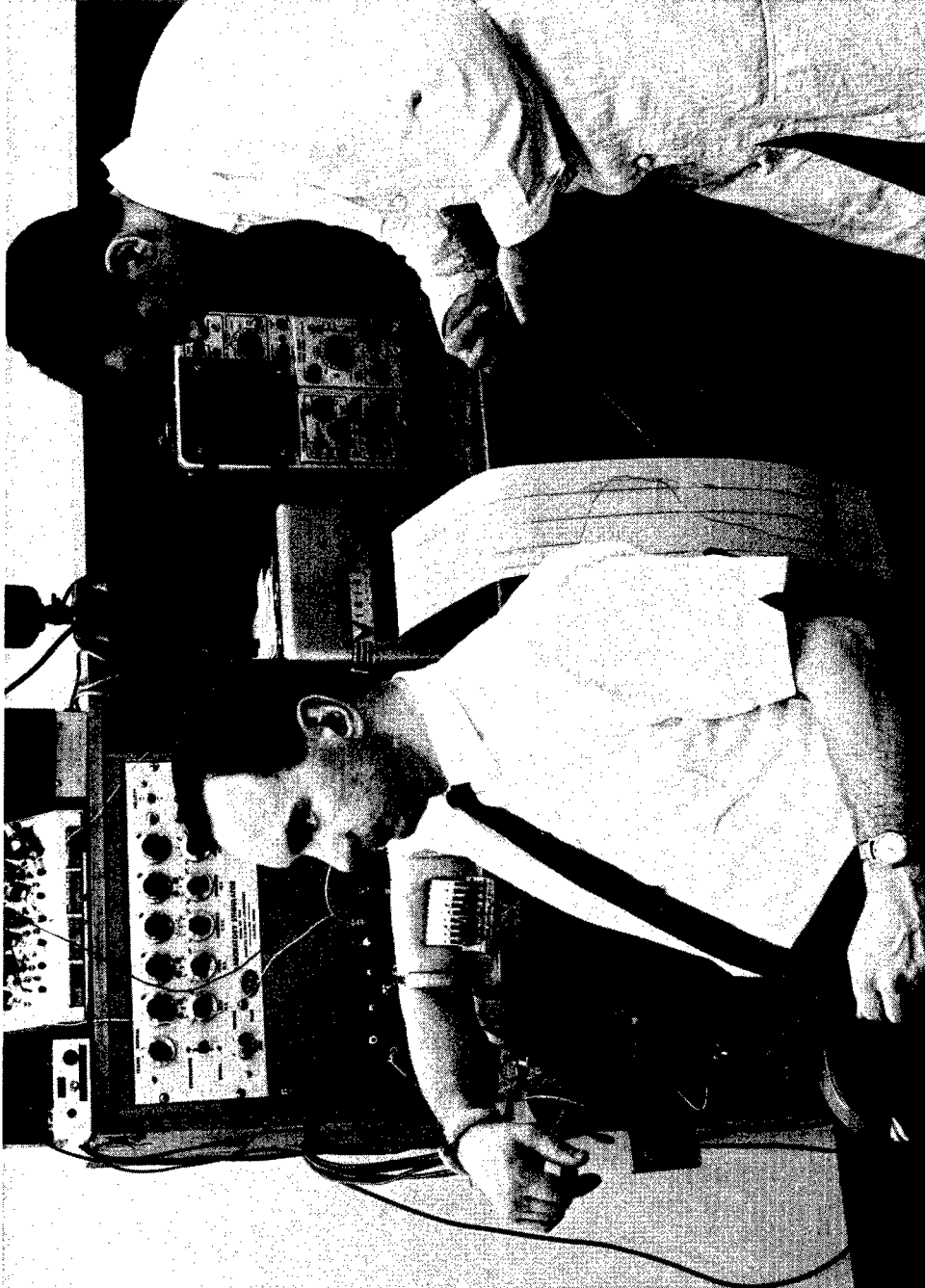
FIG. V-19. SETUP FOR CONTROL SYSTEM EVALUATION.
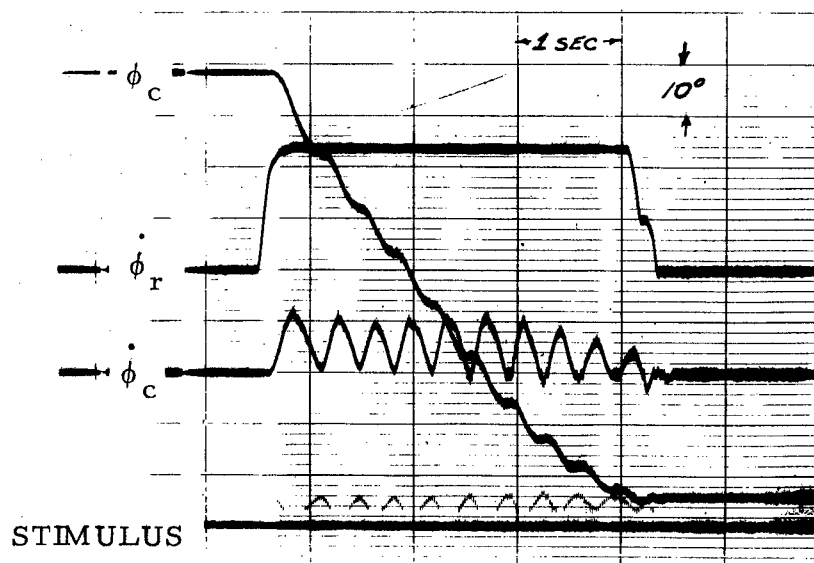
FIG. V-20. UNDERDAMPED RESPONSE OF PROPORTIONAL
CLOSED LOOP VELOCITY CONTROL.
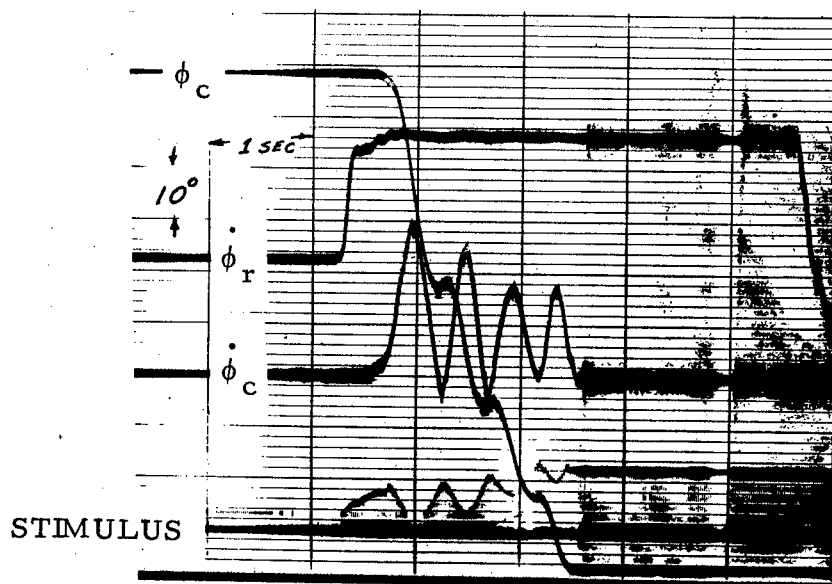
FIG. V-21. UNDERDAMPED RESPONSE OF PROPORTIONAL
PLUS INTEGRAL CLOSED LOOP VELOCITY CON-
TROL.

sensitivity of .025 volts/rad/sec which was amplified by a factor
of 100. The loop gain was then

$$3.5 \times 1.7 \times K_2 \times K_3 \times 2.5 = 3.15 \qquad (V.20)$$

where K_2 and K_3 are the muscle constants

$$K_2 = ? \text{ ft-lbs/ma}$$

$$K_3 = 2 \text{ rad/sec/ft-lb}$$

then

$$K_2 K_3 = \frac{3.15}{3.5 \times 1.7 \times 2.5} = .222 \frac{\text{rad/sec}}{\text{ma}} \qquad (V.21)$$

and

$$K_2 = \frac{.222}{2} = .111 \frac{\text{ft-lbs}}{\text{ma}} \qquad (V.22)$$

which is a reasonable value for K_2 as determined from the curve
of Figure III-27.

The same procedure was repeated for the proportional plus
integral controller. The underdamped response is shown in
Figure V-21. The frequency of oscillation is 2.08 cps. The value
predicted by the MIMIC simulation is 2.27 and the value calculated

in Section VB1 is 15 rad/sec = 2.38 cps.

The gains of the closed loop systems were then set to give a slightly oscillatory response. The three systems were then subjected to step changes in input ($\dot{\phi}_r$). The average value of the output velocity ($\dot{\phi}_c$) was then recorded. The data is plotted in Figure V-22. Notice that the straight line representing the open loop operation does not go through the origin. This is due to the biasing of the operating point by the load. Increasing the load causes this line to shift down but remain at the same inclination. Before a movement can be performed the input must be raised to a value of 1 volt (in this case) before the load torque is balanced. Closing the proportional velocity loop has no effect on this bias level since the system is actually running open loop until this value is exceeded. The proportional plus integral controller on the other hand does not have a biased operating point. Any positive nonzero input will cause the limb to move at a controlled velocity.

Knowing the open loop response, the closed loop response can be predicted. That is, using the known values of gain and the muscle model the system equations can be written. For example, the open loop response for a gain of 8.50 ma./volt can be fitted by the straight line,

$$\dot{\phi}_c = 1.70 \, \dot{\phi}_r - 1.8 \qquad\qquad (V.23)$$

GAIN ma/VOLT	LOOP	
	CLOSED	OPEN
8.50	□	○
$1.7 + \dfrac{10.2}{S}$	△	

DAVIDOVAC
3/30/67
LOAD = 1.0 FT. LB.

$\dot{\phi}_c = 1.70\,\dot{\phi}_r - 1.8\,T_L$

$\dot{\phi}_c = .55\,\dot{\phi}_r$

$\dot{\phi}_c = .324\,\dot{\phi}_r - .343\,T_L$

$\dot{\phi}_c$ — OUTPUT — (RAD/SEC)

$\dot{\phi}_r$ — INPUT — (VOLTS)
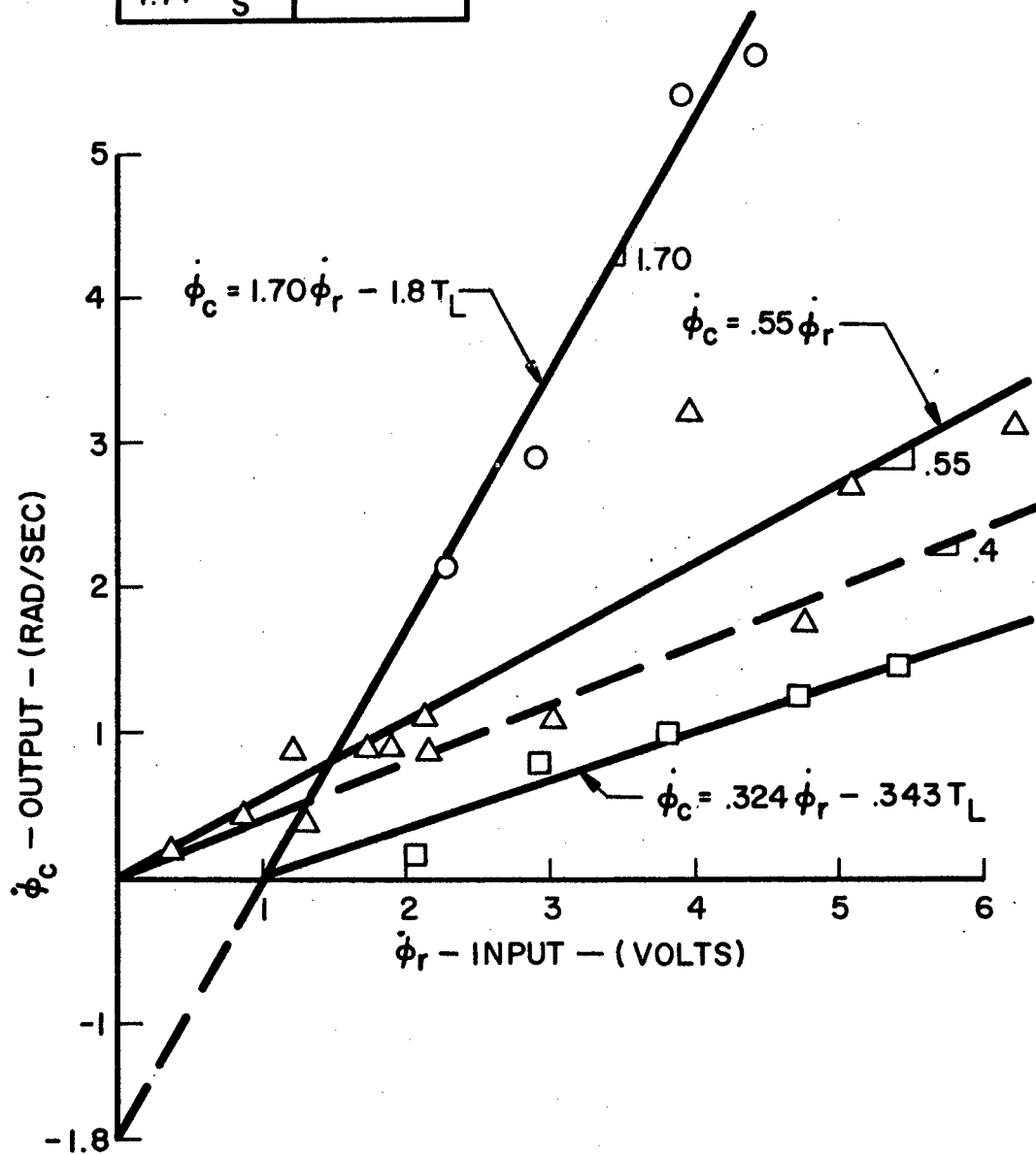
FIG. V – 22. INPUT – OUTPUT RELATIONS OF OPEN AND CLOSED LOOP SYSTEMS

The theoretical equation is,

$$\phi_c = A \left(\frac{ma}{volt}\right) \times K_2 \left(\frac{ft\text{-}lbs}{ma}\right) \times K_3 \left(\frac{rad/sec}{ft\text{-}lb}\right) \times \dot{\phi}_r - K_3 T_L \qquad (V.24)$$

Since T_L = 1.0 ft-lb, K_3 = 1.8 which agrees fairly closely with the value of $\frac{1}{.49}$ = 2.04 determined in Chapter IV. Then

$$K_2 = \frac{1.70}{8.50 \times 1.8} = .11 \frac{ft\text{-}lbs}{ma} \qquad (V.25)$$

Closing the loop with velocity feedback from the tachometer ($H = .025 \frac{volts}{rad/sec} \times 100$) yields the equation

$$\dot{\phi}_c = \frac{AK_2K_3}{1+AK_2K_3H} \dot{\phi}_r - \frac{K_3}{1+AK_2K_3H} T_L \qquad (V.26)$$

Substituting in the experimentally obtained values,

$$\dot{\phi}_c = \frac{1.70}{1+1.70(2.50)} \dot{\phi}_r - \frac{1.80}{1+1.70(2.50)} T_L \qquad (V.27)$$

$$= .324 \dot{\phi}_r - .343 T_L \qquad (V.28)$$

This line is drawn in Figure V-22. It is seen to represent the data points very well.

Similarly, for the proportional plus integral controller; assuming the muscle dynamics to be the same, the steady state response is given by

$$\frac{\dot{\phi}_c}{\dot{\phi}_r} = \lim_{s \to 0} \left[\frac{2(1.7s + 10.2)(.11e^{-.02s})}{s(.05s+1)^2(.15s+1) + 2(1.7s+10.2)(.11e^{.02s})2.5} \right]$$

(V.29)

$$= \frac{(2)(10.2)(.11)}{(2)(10.2)(.11)(2.5)} = 0.4 \frac{rad/sec}{volt}$$

(V.30)

The slope of the line through the experimentally obtained points of Figure V-22 is 0.55 rad/sec/volt. A dotted line of slope 0.4 rad/sec/volt is also drawn on the figure for comparison.

The preceding discussion has shown that, from the point of view of control theory, the controllers perform pretty much as expected. What needs to be evaluated next is whether the lock and its associated logic circuitry works and if so can a human use the controller. Practice sessions were held to see how well the position of the arm could be positioned using each of the controllers. The lock actuation control was found to work quite well except for lock actuation when the limb has a negative velocity. In this condition the lock should then actuate when the velocity of the limb

approaches zero. This mechanism was found to be unreliable and would cause the lock to actuate prematurely. In any case the lock may still be actuated by a positive velocity of the limb. That is, movements in the negative direction must be followed by a slight positive velocity to actuate the lock. With the lock control system performing satisfactorily then the velocity controllers were appraised. The desired response independent of the type of controller was the same. Figures V-23 and 24 show successful attempts to position the limb in both the positive and negative directions. Notice in Figure V-23 that the input $(\dot{\phi}_r)$ is brought up to a value, the arm flexes at a constant rate, and when the desired position is reached the input is reduced rapidly and the limb stays locked in this position. In Figure V-24 the arm extends to a position. This is brought about by first of all increasing the input until the muscle overcomes the load. At this point the lock releases and the input signal may decrease causing the limb to extend with the load. The desired angle is overshot a slight amount then the input signal is once again increased to overcome the load and cause the lock to actuate, then decreased to zero. The relative difficulty with which these operations can be performed with each of the three velocity controllers is discussed below.
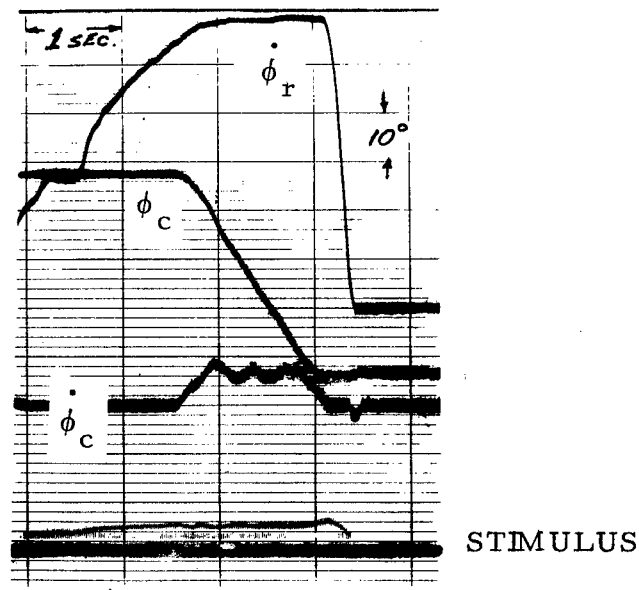
FIG. V-23. CONTROLLED FLEXION USING PROPORTIONAL
CLOSED LOOP SYSTEM.
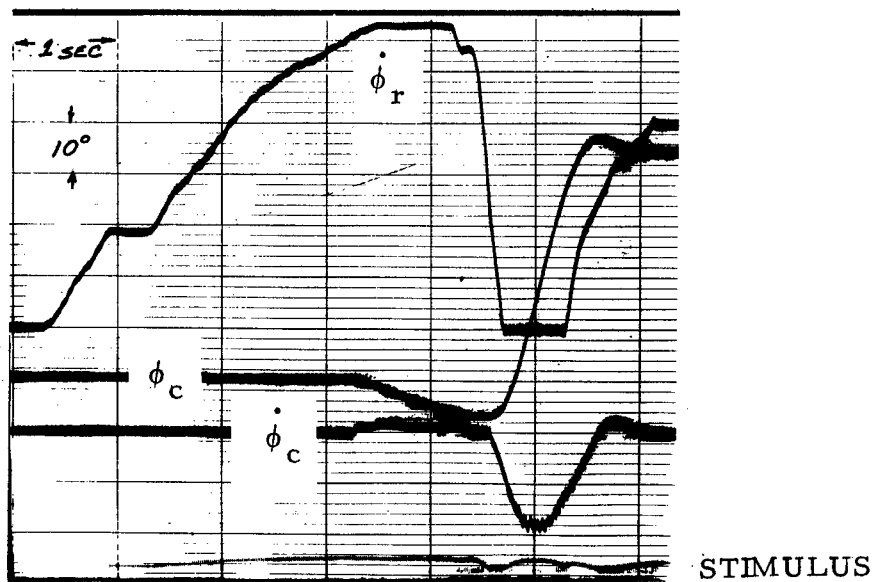
FIG. V-24. CONTROLLED EXTENSION USING PROPORTIONAL
CLOSED LOOP SYSTEM.

Open loop velocity controller. - This system, as we have seen, is very load sensitive. This, however, may not be as large a drawback as thought earlier since the human controlling the limb is quite adaptive. If a patient were to control a single muscle he may be able to do this with no feedback fairly well. In the experiments the open loop gain was fairly high which means that inputs that were slightly above the equilibrium point caused the limb to move fairly rapidly. Even so, a fair degree of control was achieved.

Closed loop proportional velocity controller. - Feeding back the velocity does not affect the amount of input signal needed to reach the equilibrium point before movement takes place. This means that, as in the open loop case, the human must "hunt" for this value of input before he can perform a movement. Above this value the velocity is more easily controlled than the open loop since there is some regulation. Again the adaptive behavior of the human must be exploited for this system to perform properly.

Closed loop proportional plus integral velocity controller. - This controller proved to be superior to the other two in that there was no "dead zone" for the input signal. There is no hunting for the operating point and any positive signal causes the muscle to contract. There is a lag, however, due to the integrator in the

forward loop.   After some training, however, the adaptive human

is able to use this controller as well or better than the other two.

CHAPTER VI

CONCLUSIONS AND RECOMMENDATIONS

The conclusion is drawn that controlled stimulation of muscle is indeed feasible for the actuation of limb movement. As mentioned previously, however, all experiments were performed on normal relaxed individuals, simulating muscle with an upper motor neuron lesion. As far as the stimulated unparalyzed biceps muscle is concerned, it produces enough torque (about 4 ft-lbs) to power the limb and a modest load against the force of gravity. Further, these movements can be performed at speeds within the range for normal movements (up to 6 rad/sec). The controllability of these movements using either of the velocity controllers discussed and a joint lock is also quite good. The proportional plus integral controller, though, seems to be superior.

It seems that there is no functional difference, in terms of stimulated response, between normal relaxed muscle and muscle with an upper motor neuron lesion (UMNL). The dynamic modeling and control schemes therefore should be directly applicable to non-atrophied muscle with an UMNL. The parameter values of the muscle model will change from one muscle to the next, but the

form of the model should be directly applicable to all of the muscles of the body. It is very unlikely, however, that a paralyzed person can be found whose paralyzed muscles all have an UMNL. Paralyzed persons generally have both UMNL and LMNL's. The electrical excitability of muscle with a LMNL has not been dealt with in this thesis other than to indicate the form of its strength duration curve. If we consider the optimal pulse width to be the chronaxie value (shown by Vodovnik in ref. 67), then the optimal pulse width for muscle with a LMNL is about 2 msec. This means that the duty cycle of the DC pulsed stimulus must be increased by a factor of 10 (0.2 msec = chronaxie for UMNL). This increase in the energy level of the stimulus will, of course, be more painful as indicated in Figure III-8. Perhaps a different waveform would be a better stimulus.

In any event, any comprehensive orthotic aid powered by stimulated muscle would involve two different types of electrical stimuli to actuate the differently involved muscles. It is therefore recommended that the mechanical response of electrically stimulated muscle with a LMNL also be modeled and evaluated as to its feasibility as a controlled actuator.

The solutions to controlling a stimulated limb described in this thesis, though workable and quite effective, require considerable

instrumentation both on the orthosis and off. Since this system was built and tested, however, new insights into the problem have emerged and it now seems possible that a much simpler controller could be built which may work as well or better. This system is the closed loop torque control shown in Figure VI-1 . The torque under control (T_c) is the resultant of the muscle torque minus the load torque. This is the actual torque available to move the limb which has a fixed gain of about 2 rad/sec/ft-lb, depending upon the viscous damping. This torque can be transduced by placing strain gages on the splint structure. Controlling this torque, therefore, controls the output velocity of the limb. The control can be effected by varying the amount of torque feedback (H). At rest $H = 0$ and the stimulus is off. To begin a movement H is set to 1. 0 and the muscle produces a torque equal to the load $(T_c = 0)$. This eliminates "hunting" for the zero torque. The lock is then released using the same switching logic as the velocity controllers. Varying H about the 1. 0 value then controls the velocity of the limb.

Implementation of this scheme requires no bulky potentio-meters or tachometer to be mounted on the splint structure. All that is required is a joint lock at the bearing and the application of strain gages. The electronic hardware necessary is a high gain
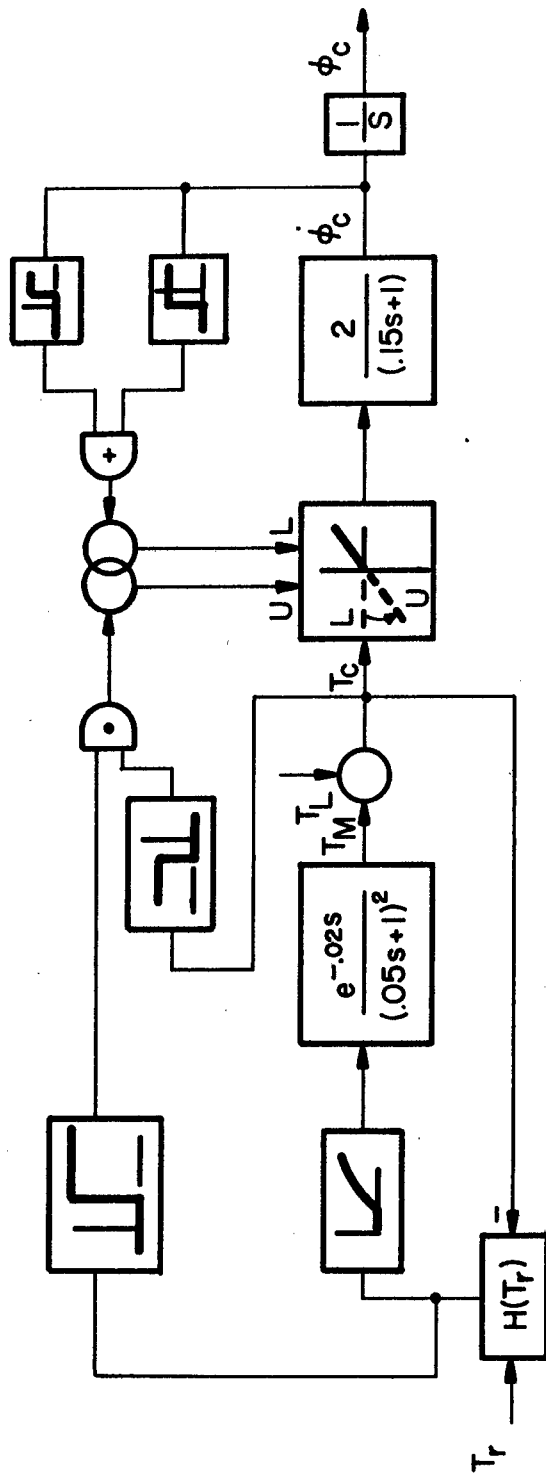
FIG. $\underline{\text{VI}}$-1 PROPOSED CLOSED LOOP TORQUE CONTROLLER

amplifier with variable gain, a modulated stimulator and a compensation scheme to allow the necessarily high loop gain. It is recommended, therefore, that this controller also be implemented and evaluated along with the velocity controllers. A lightweight orthosis should be developed which includes the joint lock and control schemes. Then by a carefully conducted evaluation with patients this device could be directly compared with existing orthoses powered by motors and cross-weave actuators.

It may be found that tracking a motor point with a surface electrode is not a practical solution. In this case, then implant stimulation, where the stimulating electrode is placed on the muscle or nerve, may be the answer. Work is being carried out in this area by members of the Cybernetic Systems for the Disabled group. Dr. Vodovnik and graduate students, R. Lorig and H. Peckham, are investigating the use of radio frequency telemetry as a control signal for an implanted stimulator.

APPENDIX

GRAPHICAL DECONVOLUTION

Problem statement - Given the transfer function and output of a

black box, determine the input.

Method of Solution - The input will be approximated by a sequence

of impulses of various magnitude such that the sequence of impulse

responses at the output add to give the measured output curve.

Once the input impulses are determined, a smooth input function

can be synthesized.

Procedure -

1. On transparent graph paper, construct a set of
   impulse response curves for the black box with
   different magnitudes. (Figure A-1.)

2. Plot the output curve on similar graph paper
   using the same time scale. (Figure A-2.)

3. Now place the graph paper with the output curve
   over the impulse response curves so that the time
   axes coincide. Slide the output curve to the right
   or left until the output curve most closely matches
   an impulse response curve.

4. Now subtract the impulse response curve from the
   output curve. Record the magnitude of the impulse
   on the output plot at time t= 0 of the impulse response
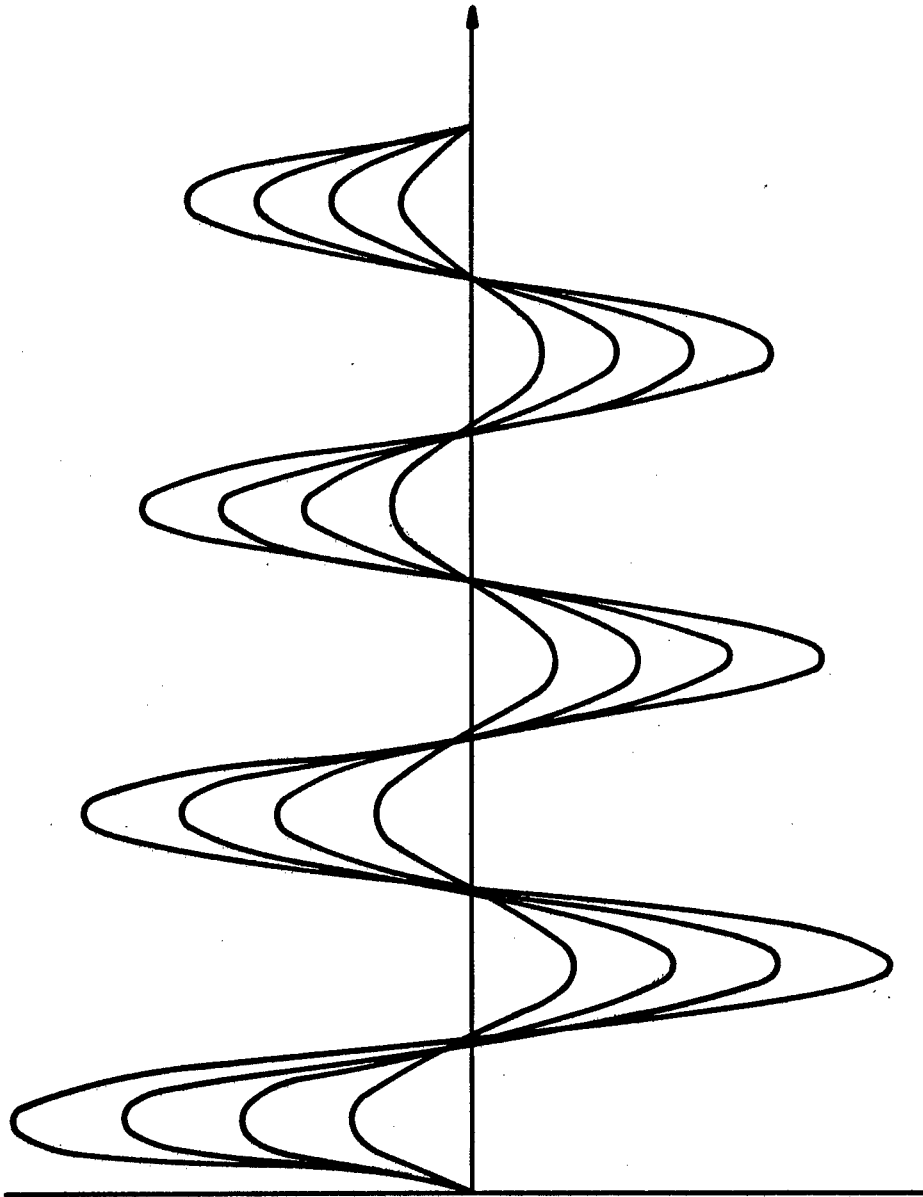   curve. (Figure A-3.)

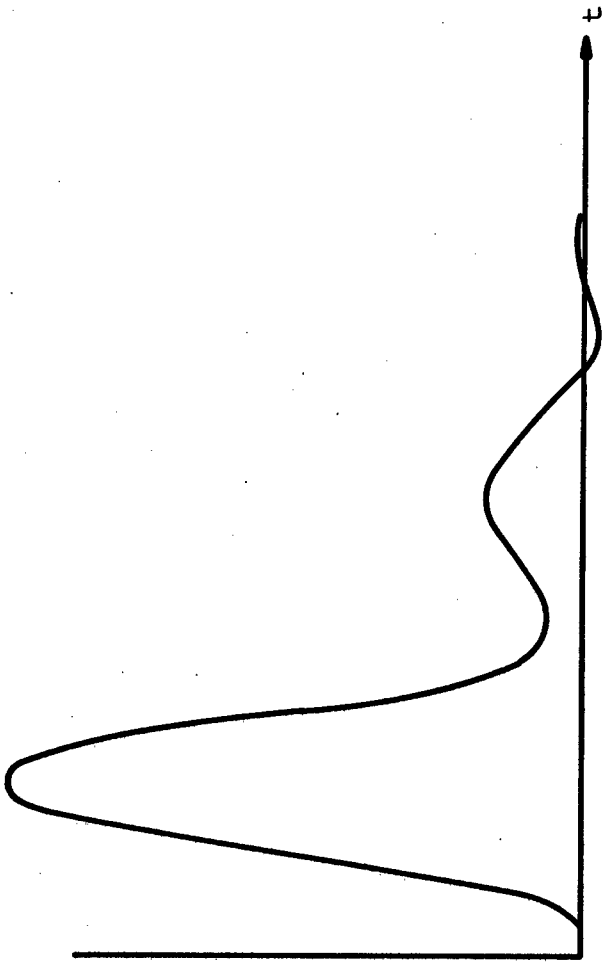Figure A-1. IMPULSE RESPONSE CURVES OF BLACK BOX

Figure A-2. OUTPUT CURVE OF BLACK BOX
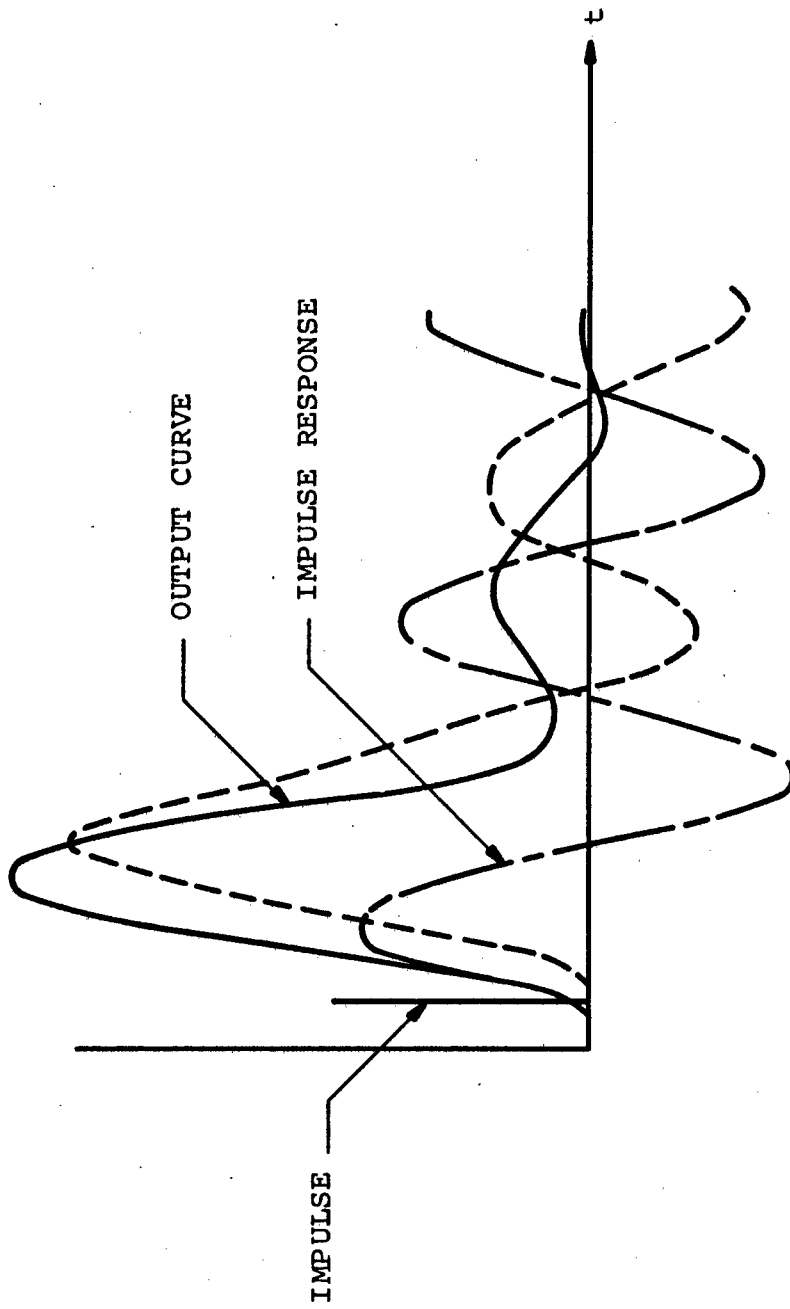
Figure A-3. OUTPUT CURVE MINUS IMPULSE RESPONSE

5. Repeat this procedure on the reduced output curve
   until this curve has a near zero value for all time.
   The resulting sequence of impulses then represents
   an approximation to the input curve. If these
   impulses are evenly spaced, then a smooth curve
   may be drawn through the peaks of the impulses.

   If the impulses are not evenly spaced, an equivalent
   set of evenly spaced impulses may be obtained.
   Integrate the pulses, then fit the resulting stepwise
   curve with a smooth line. Now divide the time axis
   into equal increments to obtain the set of evenly
   spaced impulses.

The procedure is quite rapid and allows a person to guess at

a solution and try it immediately.

STIFFNESS OF TORQUE TRANSDUCER

Referring to Figure A-4.

$h = 0.15$ inch.

$b = 0.50$ inch

$I = \dfrac{bh^3}{12} = .00014$ in lb sec^2

$\delta = \dfrac{F\, l^3}{3EI} =$ deflection of cantilever beam

$\quad\;\; = r\,\theta$

$K = \dfrac{T}{\theta} = \dfrac{Fr}{\theta} = \dfrac{r^2\, 3\,EI}{l^3}$

$r = 1.5$ inch

$l = 2$ inch

$K = \dfrac{(1.5)^2\, 3 \times 30 \times 10^6 \times .00014}{(2)^3}$

$\quad = 3538$ in lbs/rad

$\quad = 294$ ft-lbs/rad

The torque, however, is being transmitted to the gear at a pressure angle of $14\,1/2^\circ$.

$K_{actual} = K \tan 14\,1/2^\circ = 294\,(.968)$

$\qquad\quad\; = 285$ ft-lbs/rad
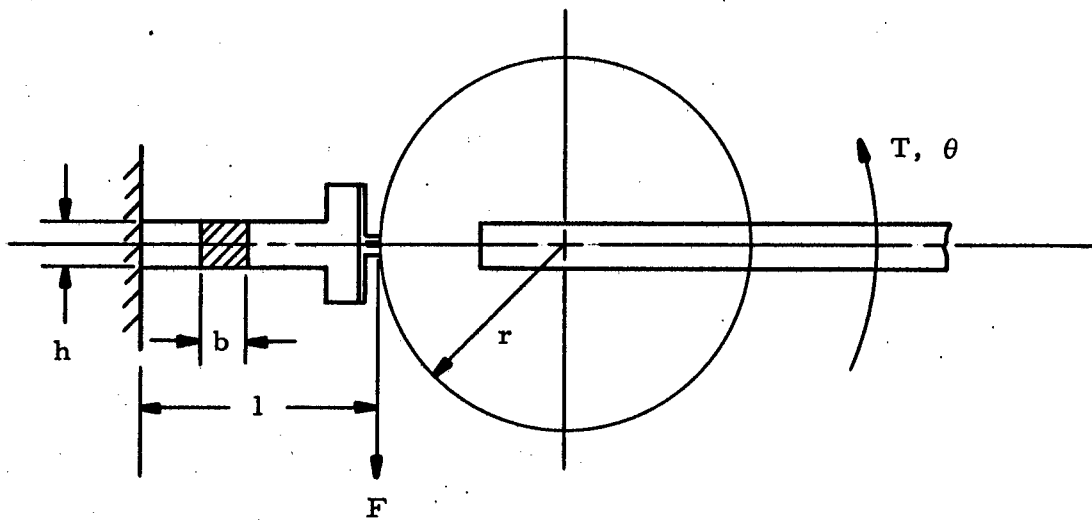
Figure A-4. TORQUE TRANSDUCER
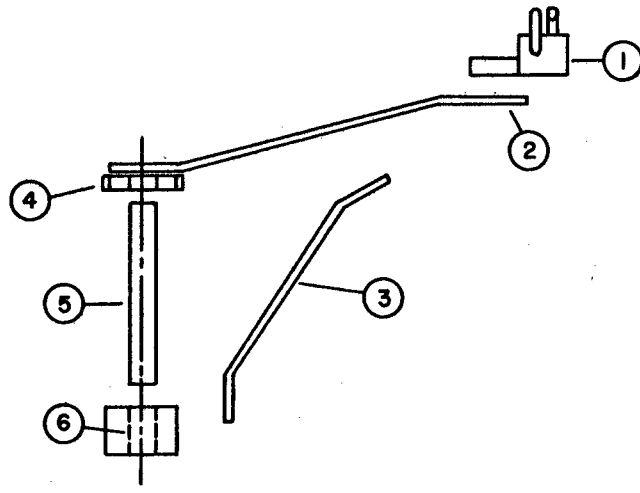
Part	Weight (lbs)	Inertia (Ft lb sec^2)
1	.88	.02090
2	.44	.00096
3	.67	.00087
4	.46	.00012
5	3.52	.00009
6	1.00	.00013

$$I_{Total} = .02307 \text{ Ft lb sec}^2$$

Figure A-5. INERTIA OF ARM SUPPORT
STRUCTURE
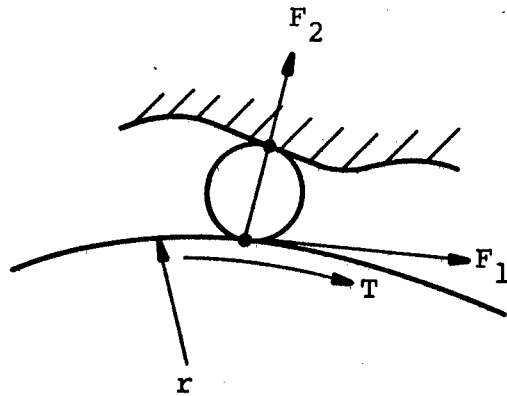
Assuming a coefficient of friction $\mu = 0.2$,

$$F_1 \cong \mu F_2 = 0.2 F_2$$

For a torque of $T = 5$ ft-lbs, and a shaft radius $r = .25$ inch,

$$F_1 = \frac{T}{r} = \frac{60}{.25} = 240 \text{ lbs}$$

$$\therefore \quad F_2 = 1200 \text{ lbs}$$

In the multi-pin lock, this force is distributed among the pins and reduces the dimpling effect of the pins on the shaft and outer race.

Figure A-6. FORCES IN ORTHOTIC LOCK

THIS CIRCUIT
CLAMPS THE
STIMULATING
CURRENT TO
ZERO UNTIL
THE SCHMITT
TRIGGER FIRES

6AQ5 OF CURRENT DRIVER
(FIG. III-10)

100 Ω

2.5 K

CURRENT
ADJ.

240 K

100 K

18 K

+18

82 K

SCHMITT
TRIGGER
INPUT

STIMULUS
OUT

Figure A-7. CURRENT CLAMPING CIRCUIT

Figure A-8.   SOLENOID DRIVER

Figure A-9.   INVERTER

Figure A-10.   AND GATE
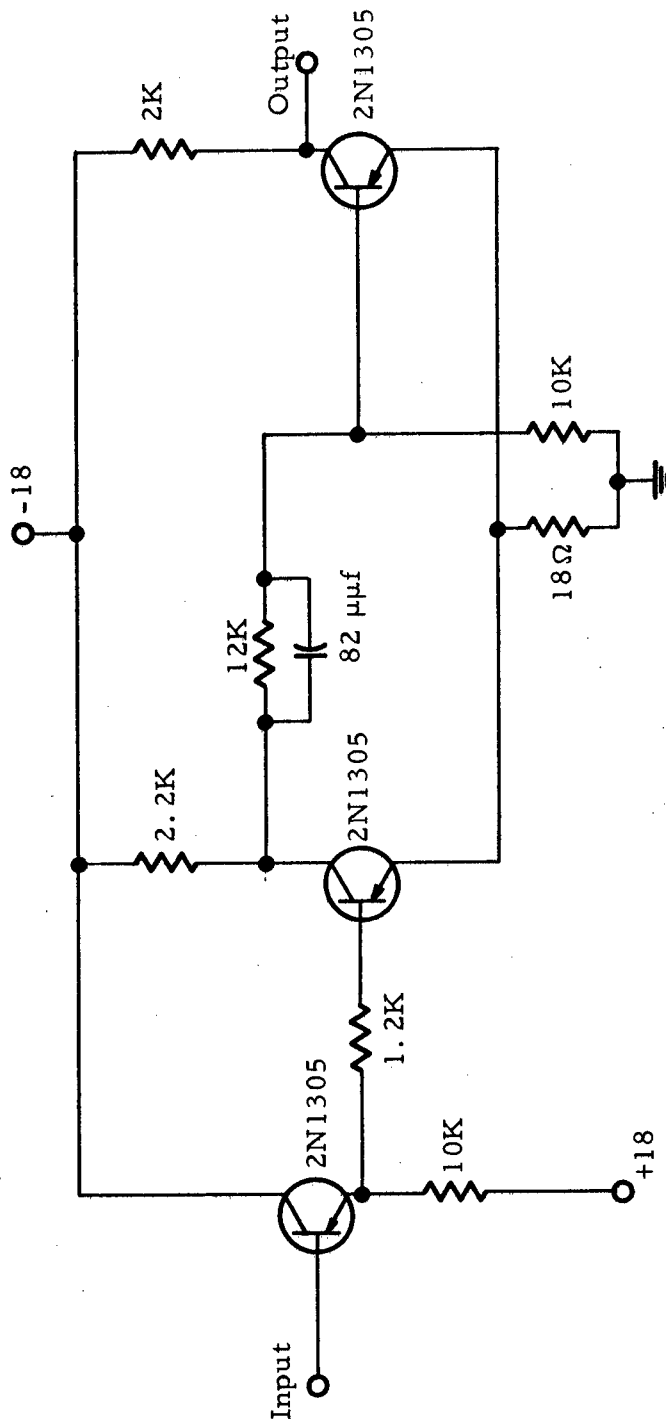
Figure A-11. SCHMITT TRIGGER WITH INPUT DRIVER

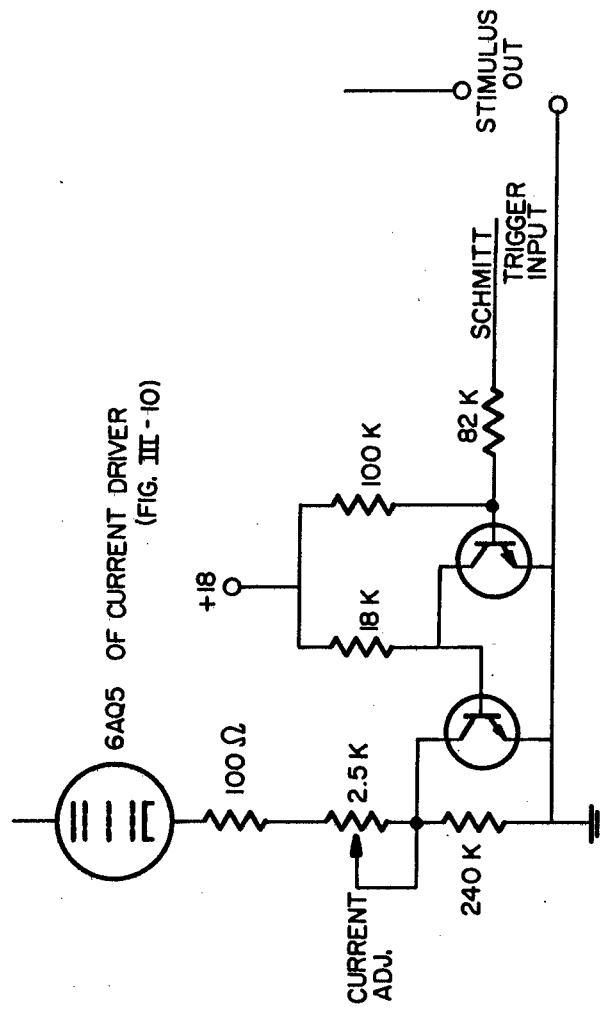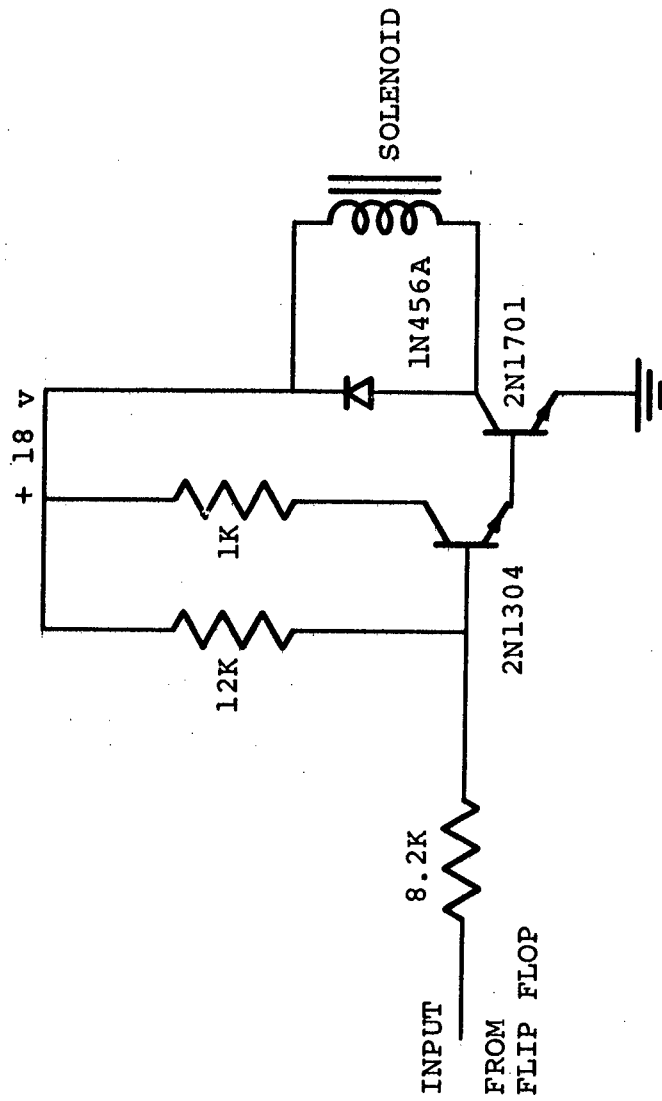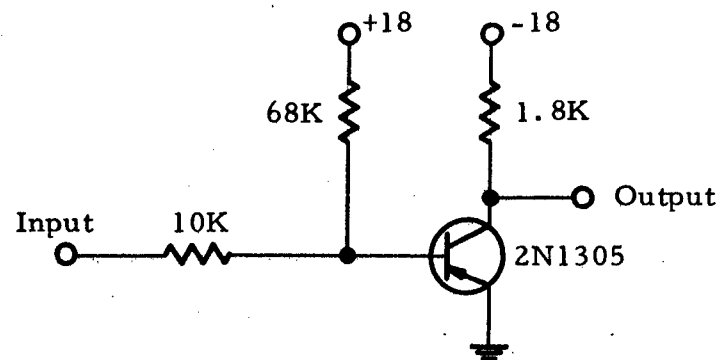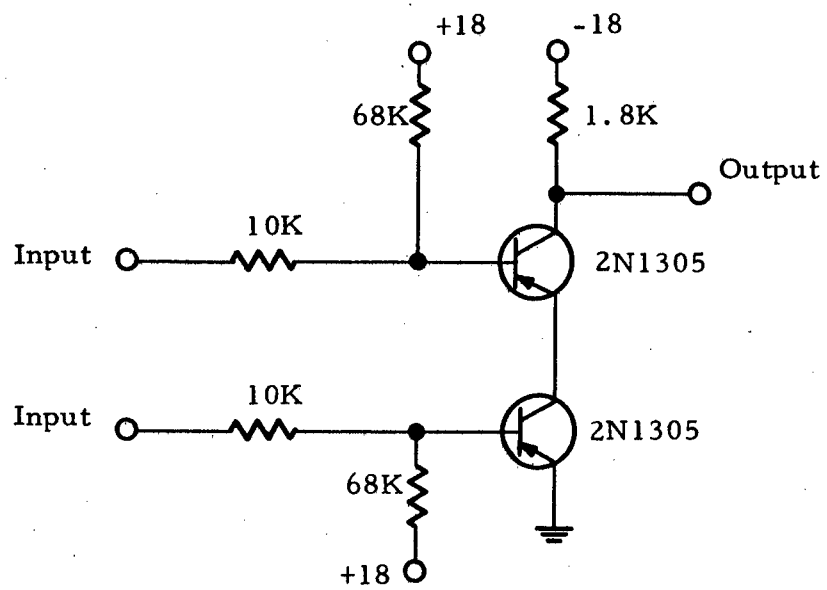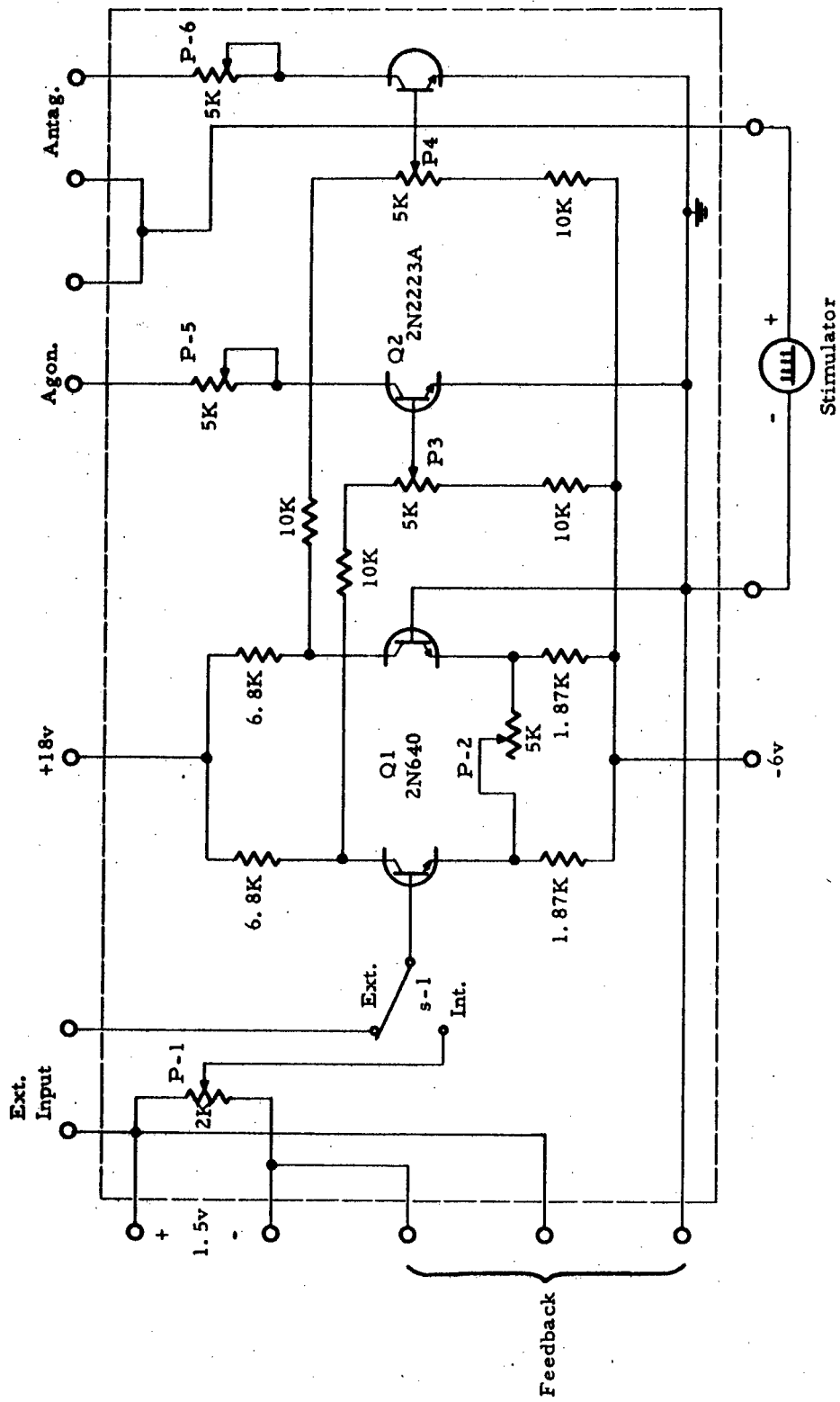Figure A-12. CIRCUIT DIAGRAM OF AGONIST-ANTAGONIST CONTROLLER

REFERENCES

1. Antomonoy, Y. G., "Mathematical Models of Excitation", U.S.S.R., translated from the Russian. NASA Publication N66 15003.

2. Basmajian, J. V., Latif, A., "Integrated Actions and Functions of the Chief Flexors of the Elbow", Journal of Bone and Joint Surgery, 39-A/5: 1106-1118, Oct. 1957.

3. Burke, J. F., Pocock, G. S., Wallis, W. D., "Electrophysiological Bracing in Peripheral Nerve Lesions", Journal of the APTA, Vol. 43, No. 7.

4. Caldwell, C., "Recent Experiments concerning Direct Muscle Stimulation", unpublished project report.

5. Corell, R. W., "Design Studies of the Development of the Case Research Arm-Aid", Ph.D. thesis, Case Institute of Technology, 1964.

6. Crochetiere, W. J., "A Preliminary Analysis of the Dynamics of the Human Finger", M.S. thesis, Case Institute of Technology, 1964.

7. Crochetiere, W., Vodovnik, L., Reswick, J. B., "The Design of Control Systems for Electronic Activation of Human Limb Movements", to be presented at the JOINT AUTOMATIC CONTROL CONFERENCE, Philadelphia, June 1967.

8. Crochetiere, W. J., "Stimulation of Skeletal Muscle by Wire Electrode", Highland View Hospital, 1964.

9. Crochetiere, W. J., Vodovnik, L., Reswick, J. B., "Electrical Stimulation of Skeletal Muscle - A Study of Muscle as an Actuator", Medical and Biological Engineering, in print.

10. Crochetiere, W. J., Reswick, J. B., "Towards a Functional Model for Electrically Stimulated Skeletal Muscle", in Proceedings of the 19th Annual Conference, Engineering in Medicine and Biology, 1966.

11. Dalziel, C. F., "Deleterious Effects of Electrical Shock", Meeting of experts on electrical accidents and related matters, Geneva, 1961.

12. Dalziel, C. F., Massoglia, F. P., "Let-Go Currents and Voltages", Applications and Industry, published by AIEE, May 1956.

13. Dimitrijevic, M. R., "Use of Physiological Mechanisms in the Electrical Control of Paralyzed Extremities", International Symposium on External Control of Human Extremities, Dubrovnik, Yugoslavia, Aug. 29 - Sept. 2, 1966.

14. Echternach, J. L., "Electrophysiological Bracing in Radial Nerve Compression Injury", Journal of the American Phys. Therapy Association, Jan. 1964, Vol. 44, No. 1, pp. 26-27.

15. Feinstein, B., Lindegard, B., Nyman, E., Wolfhart, G., "Morphologic Studies of Motor Units in Normal Human Muscles", Acta Anatomica, 23, 127-142, 1955.

16. Furman, G. G., "Neuro Muscular Control: Possible Subject for Bionic Study", report - Electronics Research Laboratory, University of California, Berkeley, California, Series No. 60, Issue No. 393, August 1961.

17. Fleming, D. G., "A Constant Current Apparatus for the Production of Electrolytic Lesions", Electroencephalography and Clinical Neurophysiology Journal, Vol. 9, No. 3, August 1957.

18. Gilson, A. S., Schoepfle, G. M., Walker, S. M., "The Time Course of Tension Development in the Muscle Response" "Muscular Contraction", Annals of N.Y. Academy of Sciences, Vol. 47, 1947, pp. 697-715.

19. Gracanin, F., Dimitrijevic, M. R., "Application of Functional Electrical Stimulation in Rehabilitation of Neurologic Patients", Symposium Internationale Ad Rehabilitationem in Neurologia Praga 20.-23. IX, 1966.

20. Granit, R., "Systems for Control of Movement", Premier Congres International Des Sciences Neurologiques, 63-99.

21. Grant, J. C. B., Grant's Atlas of Anatomy, Williams and Wilkins Co., 1962.

22. Hammond, B. H., Merton, P. A., Sutton, G. G., "Nervous Gradation of Muscular Contraction", British Medical Bulletin, Vol. 12, 1956, pp. 214-218.

23. Henneman, E., Olson, C. B., "Relations between Structure and Function in the Design of Skeletal Muscles", Journal of Neurophys., Vol. 28, 1965, pp. 581-598.

24. Hill, A. V., "The Heat of Shortening and the Dynamic Constants of Muscle", Proc. Roy. Soc. (London) B, Vol. 126, pp. 136-195, Oct. 1938.

25. Hill, A. V., "The Series Elastic Component of Muscle", Proc. Royal Soc. (London) B, Vol 137, pp. 273-280, July 1950.

26. Hill, A. V., "The Mechanics of Active Muscle", Proc. Royal Soc. (London) B, Vol. 141, pp. 104-117, 1953.

27. Hinchliffe, H., Pierce, D. S., "A Variable-Function Biological Stimulator for use in the Study of Neuromuscular Phisiology", in Proceedings of the San Diego Symposium for Biomedical Engineering, 1964.

28. Hoeft, L. O., Mundie, J. R., "Servoanalysis of the Leg Muscles of the Cat", Bionics Symposium, 1963, AF Systems Command, Wright-Patterson Air Force Base, Ohio.

29. Houk, J. C., "A Mathematical Model of the Stretch Reflex in Human Muscle Systems", M.S. thesis, Massachusetts Institute of Technology, 1963.

30. Inman, V. T., Saunders, M., Abbott, L. C., "Observations on the Functions of the Shoulder Joint", The Journal of Bone and Joint Surgery, Vol. XXVI, No. 1, Jan. 1944.

31. Introduction to the Practice of Electrodiagnosis, published by Siemens-Reiniger-Werke Ag, Erlangen, Germany.

32. Johnson, A. R., "The Servo-analysis of Postural Reflexes", Ph. D. thesis, Massachusetts Institute of Technology, June 1960.

33. Kantrowitz, A., "Electronic Physiologic Aids", Report of the Maimonides Hospital, Brooklyn, N. Y., 1963.

34. Katz, B., "The Relation Between Force and Speed in Muscular Contraction", Jour. Physiol., London, 96, 45-64.

35. Lane, J., Zebo, T., Highland View Hospital, personal communication.

36. Levin, A., Wyman, J., "The Viscous Elastic Properties of Muscle", Proc. Roy. Soc. (London) B, Vol. 101, pp. 218-243, April, 1927.

37. Liberson, W. T., Holmquist, H. J., Scot, D., Dow, M., "Functional Electrotherapy: Stimulation of the Peroneal Nerve Synchronized with the Swing Phase of the Gait of Hemiplegic Patients", Archives of Physical Medicine and Rehabilitation, Feb. 1961, pp. 101-105.

38. Licht, S., Electrodiagnosis and Electromyography, Waverly Press, Baltimore, Maryland, 1961.

39. Livingston, R. B., Paillard, J., et al, "Plasticite d'une synergie musculaire dans l'execution d'un mouvement volontaire chez l'homme", J. Physyologie, 1951, 43, 605-619.

40. Long, C. II, Lawton, E. B., "Functional Significance of Spinal Cord Lesion Level", Arch. Phys. Med. Rehab., April 1955.

41. Long, C. II, Masciarelli, V. D., "An Electrophysiologic
     Splint for the Hand", Archives of Phys. Med. and Rehab.,
     Sept. 1963, pp. 499-503.

42. Lubin, M., "Measurement of Mechanical Properties of
     Muscle under Servo Control", Proc. IRE, Nov. 1959,
     pp. 1880-1888.

43. Matthews, P. B. C., "Muscle Spindles and Their Motor
     Control", Physiol. Reviews, Vol. 44, No. 2, 219-288.

44. Morecki, A., Ekiel, J., Fidelus, K., "Mechanoelectrical
     and Biomechanical Principles of Control of the Human
     Upper Limb Muscles", Archiwum Budowy Maseyn, Tom XI,
     1964, Zeszyt 4, pp. 727-754.

45. Morecki, A., Ekiel, J., Fidelus, K., "The Peripheral
     Organization of Externally Controlled Natural and Artificial
     Limbs", IX Automation and Instrumentation Conference and
     Exhibition, Milano, 19-25 Nov. 1966.

46. Partridge, L., "Motor Control and the Myotatic Reflex",
     Amer. Jour. Phys.Med., Vol. 40, No. 3, 96-103, 1961.

47. Partridge, Lloyd, "Stretch Reflex Interactions Studied with
     the Aid of Simulation", Amer. Jour. of Phys. Med., Vol. 42,
     No. 2, 78-100, 1964.

48. Plonsey, R., "Bioelectric Phenomena", course notes, 1963.

49. Ralston, M. J., "Recent Advances in Neuromuscular
     Physiology", Amer. Jour. Phys. Med., 36, 94-120.

50. Rashevsky, N., Mathematical Biophysics, Vol. 1, Dover
     Publications, New York, N. Y., 1960.

51. Reswick, J. B., "A Simple Graphical Method for
     Deconvolution", Beihefte zur Regelungstechnik: Anwendung
     von Rechenmaschinen bei der Berechnung von Regelvolgangen,
     R. O. Wenberg, 1958 Muenchen.

52. Reswick, J. B., Vodovnik, L., Long, C. II, Lippay, A.,
     Starbuck, D., "An Electronic Bypass for Motor Neuron
     Lesions", 17th Annual Conference on Engineering in
     Medicine and Biology Proceedings; p. 15, Cleveland, 1964.

53. Reswick, J. B., Ko, W., Vodovnik, L., McLeod, W., Crochetiere, W., "On the Cybernetic Restoration of Human Function in Paralysis", presented at External Control of Human Extremities Conference, Dubrovnik, Yugoslavia, Sept. 1966.

54. Ritchie, J. M., Wilkie, D. R., "The Dynamics of Muscular Contraction", J. Physiol., Vol. 143, pp. 104-113, Aug. 1958.

55. Roberts, T. D. M., "Rhythmic Excitation of a Stretch Reflex, Revealing (a) Hysteresis and (b) A Difference Between the Responses to Pulling and to Stretching", Quarterly Jour. of Physiology, Vol. XLVIII, 1963, pp. 328-345.

56. Ruch-Patton in Physiology and Biophysics, pp. 113-133, W. B. Saunders, Phila., London, 1965.

57. Schwartz, E. F., "A Newer Concept in the Treatment of Peripheral Nerve Injuries and Paralysis", Southern Medical Journal, Journal of the Southern Medical Association, Vol. 53, No. 6, June 1960, pp. 712-715.

58. Smith, E., Barnett, J., "Study on Incidence of Quadriplegia, Polio and Peripheral Nerve Injuries", UMORP, Nov. 30, 1959.

59. Stark, L., "Neurological Feedback Control Systems" in Advances in Bioengineering and Instrumentation, Plenum Press, N. Y., 1966, Vol. 1.

60. Steckler, L., "To Walk Again", Radio Electronics, pp. 42-43, Aug. 1961.

61. Steinberger, W. W., Amon, R., Sweet, R., "Maintaining Denervated Skeletal Muscle by Direct Stimulation", read at the meeting of Federation of American Societies of Experimental Biology, 1963.

62. Stephens, W. G. S., "The Current Voltage Relationships in Human Skin", Med. Electron. Biol. Engng., Vol. 1, pp. 389-399, 1963.

63. Taft, C. K., Course notes, "Discontinuous Control", Spring 1963.

64. Thomas, D. H., "The Physical Properties of the Human Finger", Ph. D. thesis, Case Institute of Technology, 1965.

65. Truxal, J. G., Control System Synthesis, McGraw-Hill, 1955.

66. Van der Meulen, J. P., "The Gamma Loop in the Mediation of Muscle Tone", read at Hypertonia Symposium, 1964.

67. Vodovnik, L., Reswick, J. B., "Control Theory Concepts in Functional Electrical Stimulation of Extremities", Automatika, Theoretical Supplement, T. 1, No. 2, Zagreb, 1965, pp. 33-38.

68. Vodovnik, L., Kralj, A., Kelsin, D., Borovsak, M., "Simulation of Purposeful Movements by Electrical Stimulation of Muscles", presented at External Control of Human Extremities Conference, Dubrovnik, Yugoslavia, Sept. 1966.

69. Vodovnik, L., Long, C. II, Reswick, J. B., Lippay, A., Starbuck, D., "Myo-Electric Control of Paralyzed Muscles", Trans. of IEEE, BME-12, July - Oct. 1965, pp. 169-172.

70. Vodovnik, L., Dimintrijevic, M., Prevec, T., Logar, M., "Electronic Walking Aids for Patients with Peroneal Palsy", World Medical Electronics, February 1966, p. 58-61.

71. Vodovnik, L., "The Dynamic Response of a Musculo-Skeletal System due to Electrical Stimulation", EDC Report 4-64-10, Case Institute of Technology, 1964.

72. Vodovnik, L. et al, "Pain Response to Different Tetanizing Currents", Archives of Phys. Med. and Rehab., Vol. 46, 187-192, 1965.

73. Vodovnik, L., Crochetiere, W. J., Reswick, J. B., "Control of a Skeletal Joint by Electrical Stimulation of Antagonists", Medical and Biological Engineering, in print.

74. Vodovnik, L., McLeod, W. D., "Electronic Detours for Broken Nerve Paths", Medical Electronics, Sept. 20, 1965 pp. 110-116.

75. Vossius, G., "Der Sogenannte 'Innere' Regelkreis der Willkurbewegung", Kybernetic, Vol. 1, pp. 29-32, Jan. 1961.

76. Wakim, K., Krusen, F., "The Influence of Electrical Stimulation on the Work Putput and Endurance of Denervated Muscle", Arch. Phys. Med., 36:370, 1955.

77. Wilkie, D. R., "Mechanical Properties of Muscle", British Medical Bulletin, Vol. 12, 1956, pp. 177-182.